A STUDY ON PILE GROUP WITH ADJUSTABLE RIGIDITY SUBJECTED TO LARGE HORIZONTAL DISPLACEMENT

by

Sercan Akbaşak

B.S., Civil Engineering, Yildiz Technical University, 2017

Submitted to the Institute for Graduate Studies in
Science and Engineering in partial fulfillment of
the requirements for the degree of
Master of Science

Graduate Program in Civil Engineering

Boğaziçi University

2021

ACKNOWLEDGEMENTS

This project would not have been possible without the support of many people. Many thanks to my adviser, Prof. Gökhan Baykal, who read my numerous revisions and helped make some sense of the confusion. Also, thanks to my committee members, Prof. Ayşe Edinçliler and Assoc. Prof. Mustafa Kubilay Keleşoğlu, who offered guidance and support. I would also like to thank research assistant Uğur Can Erginağ and laboratory technicians for their help and kind attitudes.

Thanks to the Boğaziçi University Scientific Research Fund (Project No: BAP 18A04P2) for providing me with the financial means to complete this study. And finally, thanks to my parents, numerous friends, and my laboratory partner Suad Mert Gümüşalan who endured this long process with me, always offering support and love.

ABSTRACT

A STUDY ON PILE GROUP WITH ADJUSTABLE RIGIDITY SUBJECTED TO LARGE HORIZONTAL DISPLACEMENT

The segmental pile system, which is composed of alternating concrete blocks and rubber sheets, connected with anchor cable is a non-continuous system. The rigidity of the pile system may be adjusted by tensioning the anchor cable. There is a question of whether it can be treated as a beam which is a continuous system. The working mechanism is through the friction developed at the joints. The primary objective of this study is to compare this behavior of the non-continuous pile system with the continuous pile system with adjustable rigidity. To be able to adjust the rigidity of the continuous pile system, water pressure in a confined rubber cylinder is used. Three-point bending, oedometer, and large displacement model pile tests are conducted to investigate the behavior of the model piles subjected to horizontal displacement. Model pile tests on a continuous single and 3 x 3 pile groups with 2.4D spacing are conducted. Various pile-soil modulus ratios are studied with the help of the piles with adjustable rigidity and embedded in poorly graded sand compacted to different relative densities. The experiments are conducted on fixed-head piles at large displacements of up to 50 mm (pile diameter, D is equal to 35 mm). The model pile group system can withstand large displacements without failure. Limited to the test and boundary conditions applied, the lateral capacity of the pile group is related to pile-soil modulus ratios. In conclusion, the non-continuous pile system and the continuous pile system showed similar load-displacement behavior. Although, the mechanisms leading to horizontal capacity development for both pile systems are completely different.

ÖZET

YÜKSEK YATAY DEPLASMANDA RİJİTLİĞİ AYARLANABİLİR KAZIK GRUPLARI ÜZERİNE BİR ÇALIŞMA

Sürekli olmayan kazık sistemlerinde, bu sistemlerin kiriş olarak ele alınıp alınamayacağı sorusu vardır. Bu çalışmanın amacı, bu davranışı ayarlanabilir rijitliğe sahip sürekli bir kazık sistemi ile karşılaştırmaktır. Ayrıca rüzgar, deprem, dalga gibi yanal kuvvetler de kazıkların tasarımında büyük öneme sahiptir. Bu nedenle, çalışmanın dikkati yanal yüklü kazıkların kazık-zemin rijitliğine odaklanmıştır. Bu çalışmada, yanal yüklü kazıkların incelenmesi için üç nokta eğilme, konsolidasyon ve yüksek deplasman kesme deneyleri gerçekleştirilmiştir. Yüksek deplasman kesme deneyleri sürekli tekli kazıklar ve 3 x 3 kazık grupları (kazıklar arası mesafe 2.4D) üzerinde gerçekleştirilmiştir. Çeşitli kazık-zemin rijitliği oranları rijitliği ayarlanabilir kazıklar yardımıyla farklı sıkılık derecelerinde kompakte edilip kötü derecelenmiş kum içerisine yerleştirilmesiyle incelenmiştir. Deneyler, kazıkların plakalarına sabit (ankastre) bir şekilde yerleştirilip, 50 mm'ye kadar yüksek deplasman (kazık çapı, D 35 mm'dir.) uygulanarak gerçekleştirilmiştir. Model kazık grubu yüksek deplasmanda uygun bir şekilde çalışmıştır. Yanal yüklü kazık deneylerinin sonuçları sunulmuş ve tartışılmıştır. Deney sonuçları göstermiştir ki, kazık gruplarının yanal kapasiteleri büyük oranda kazık ve zemin arasındaki rijitliğe bağlıdır. Sonuç olarak, sürekli olmayan kazık sistemi ve sürekli kazık sistemi için, her iki kazık sistemi için yatay kapasite oluşumuna yol açan mekanizmalar farklı olmasına rağmen, benzer yük-deplasman davranışı gözlemlenmiştir.

TABLE OF CONTENTS

ACKNOWLEDGEMENTS iii
ABSTRACT iv
ÖZET v
LIST OF FIGURES viii
LIST OF TABLES xv
LIST OF SYMBOLS xvii
LIST OF ACRONYMS/ABBREVIATIONS xix
1. INTRODUCTION 1
2. LITERATURE REVIEW 4
2.1. Piles 4
2.1.1. Group of Piles 4
2.1.2. Pile Properties 6
2.1.3. Analytical Models for Laterally Loaded Piles 9
2.1.3.1. Subgrade-Reaction Analysis 11
2.1.3.2. Broms' Model (1964) 12
2.1.3.3. Elastic Analysis 14
2.1.3.4. Blum's Model (1932) 16
2.1.3.5. P-y Curves 18
2.1.3.6. Strain Wedge Model 21
2.1.3.7. Analysis of Pile Groups 23
2.2. Elastic Modulus of Soil and Pile Rigidity 26
2.3. Review of Laterally Loaded Pile Group Studies in Literature 30
2.4. Review of Related Studies Done at Boğaziçi University Karl Terzaghi Soil Mechanics and Geotechnical Engineering Laboratory 51
3. METHODOLOGY 61
3.1. Soil Material and Soil Placement 61
3.2. Pile Material 62
3.3. Test Setup and Instrumentations 70

3.4. Testing Program and Conditions 75
3.4.1. Three-Point Bending Test 75
3.4.2. Oedometer Test 76
3.4.3. Laterally Loaded Pile Group Test at Large Displacement 77
4. TEST RESULTS AND DISCUSSION 81
4.1. Test Results 81
4.1.1. Three-Point Bending Tests 81
4.1.2. Oedometer Tests 87
4.1.3. Laterally Loaded Pile Group Tests at Large Displacement . . . 88
4.2. Discussion 96
4.2.1. Three-Point Bending Tests 96
4.2.2. Oedometer Tests 98
4.2.3. Laterally Loaded Pile Group Tests at Large Displacement . . . 102
5. CONCLUSION 109
REFERENCES 111
APPENDIX A: ADDITIONAL TEST RESULTS 118

LIST OF FIGURES

Figure 2.1. Stress Conditions Under Piles (a) Single Pile (b) A Group of Piles [10]. 5

Figure 2.2. Group Effect. 5

Figure 2.3. Shadowing and Edge Effects in a Laterally Loaded Group of Piles [13]. 6

Figure 2.4. Passive Piles [16]. 7

Figure 2.5. An Active Pile [18]. 8

Figure 2.6. (a) Free-Head Long Piles, (b) Free-Head Short Piles, (c) Fixed-Head Long Piles, and (d) Fixed-Head Short Piles [20]. 9

Figure 2.7. Soil Resistance Against Laterally Loaded Piles [22]. 10

Figure 2.8. Soil Reaction and Failure Mechanisms for Short (a) and Long Piles (b) [25]. 13

Figure 2.9. A Floating Pile [4]. 15

Figure 2.10. A Socketed Pile [5]. 17

Figure 2.11. The Soil Wedge (a) and The Pile Scheme (b) [28]. 18

Figure 2.12. An Analysis of P-y Soil-Pile Model [22]. 19

Figure 2.13. Examples of P-y Curves in Ductile (A) and Brittle (B) Soils [29]. . 20

Figure 2.14. Strain Wedge Developed in Soil [31]. 22

Figure 2.15. Geometry of Wedges in Soil [31]. 22

Figure 2.16. Interaction Between Soil and Pile within Multiple Soil Layers [31]. 23

Figure 2.17. Illustration of a Pile Group [33]. 23

Figure 2.18. Concept of P-multiplier for Pile Groups [22]. 24

Figure 2.19. Shape Dimensions for Pipe Pile [34]. 29

Figure 2.20. Lateral Load - Deflection Curves (Single Pile) [1]. 33

Figure 2.21. Lateral Load - Deflection Curves for Two-Pile Group [1]. 34

Figure 2.22. Soil Apparatus [37]. 37

Figure 2.23. Derived p-y Curves at Depths [37]. 38

Figure 2.24. Pile Array Types (PAT's) [38]. 39

Figure 2.25. The Correlation Between The Average Load on The Piles in Each Three-row [38]. 40

Figure 2.26. The Load-Deflection Response (3x3 Pile Group, 3d Pile Spacing) [38]. 41

Figure 2.27. Piles and Boreholes [40]. 43

Figure 2.28. Total Pile Head Forces at Target Deflections [11]. 45

Figure 2.29. Single Pile and Free-Head Pile Group (3 x 3 Configuration) [42]. . 47

Figure 2.30. Lateral Load and Displacement for Loose and Dense State Soils [45]. 50

Figure 2.31. Distribution of the Lateral Effective Stresses with Depth [45]. . . . 50

Figure 2.32. Segmental Pile with Variable Flexural Rigidity. 51

Figure 2.33. Segmental Pile System Prepared for Winkler Tests [46]. 53

Figure 2.34. P-y Curves of the Segmental Pile System Placed on Elastic Springs 1K-2K-3K-Static Load [46]. 55

Figure 2.35. Displacement Values for the Piles Placed in Loose Soil [47]. 56

Figure 2.36. Displacement Values for the Pile Placed in Medium Dense Soil [47]. 56

Figure 2.37. Displacement Values for the Pile Placed in Dense Soil [47]. 57

Figure 2.38. Load-Displacement Curves for Segmental Pile Model [48]. 58

Figure 2.39. 750N Pile in a) Loose Sand b) Medium Dense Sand (x-axis displacement, y-axis depth) [48]. 58

Figure 2.40. 2250N Pile in a) Loose Sand b) Medium Dense Sand (x-axis displacement, y-axis depth) [48]. 59

Figure 2.41. Estimation of Deflection in Blocks [49]. 60

Figure 3.1. Grain Size Distribution. 61

Figure 3.2. a) Shear Stress - Horizontal Displacement b) Vertical Displacement - Horizontal Displacement Curves For Loose Soil. 63

Figure 3.3. a) Shear Stress - Horizontal Displacement b) Vertical Displacement - Horizontal Displacement Curves For Medium Dense Soil. 64

Figure 3.4. a) Shear Stress - Horizontal Displacement b) Vertical Displacement - Horizontal Displacement Curves For Dense Soil. 65

Figure 3.5. Fire Hoses as Piles. 66

Figure 3.6. Water Pump. 67

Figure 3.7. Water Distribution Hoses. 67

Figure 3.8. Pile Cap Plate. 68

Figure 3.9. Additional Wearing Layer. 69

Figure 3.10. Clamps. 69

Figure 3.11. Pile Group System. 70

Figure 3.12. Large-Size Model Pile Test Device. 71

Figure 3.13. Embedded Piles into the Lower Box. 73

Figure 3.14. Portable Jib Crane and Pile Group System. 74

Figure 3.15. Three-Point Bending Test Device. 76

Figure 3.16. Pile Group and Loading Direction ($S_1 = S_2 = 2.4$D, $S_3 = 1.9$D). . 78

Figure 3.17. Laterally Loaded Pile Group Test System. 79

Figure 4.1. Flexural Rigidity-Displacement Curves for Piles Without a Wearing Layer. 82

Figure 4.2. Flexural Rigidity-Displacement Curves for Piles With a Single Wearing Layer. 82

Figure 4.3. Flexural Rigidity-Displacement Curves for Piles With a Double Wearing Layer. 83

Figure 4.4. Flexural Rigidity-Displacement Curves for Piles Pressurized to 500 kPa. 83

Figure 4.5. Flexural Rigidity-Displacement Curves for Piles Pressurized to 1000 kPa. 84

Figure 4.6. Flexural Rigidity-Displacement Curves for Piles Pressurized to 1500 kPa. 84

Figure 4.7. The Pile Without a Wearing Layer (Test #1). 85

Figure 4.8. The Pile With a Wearing Layer (Test #4). 86

Figure 4.9. Oedometer Test Equipment. 87

Figure 4.10. Elastic Modulus-Vertical Stress Curves for Soil. 88

Figure 4.11. Vertical Stress - Vertical Strain Curves. 89

Figure 4.12. Void Ratio - Vertical Stress Curves. 90

Figure 4.13. Load-Lateral Deflection Curves for Pile Group in Loose Soil. . . . 91

Figure 4.14. Load-Lateral Deflection Curves for Pile Group in Medium Dense Soil. 92

Figure 4.15. Load-Lateral Deflection Curves for Pile Group in Dense Soil. . . . 92

Figure 4.16. Load-Lateral Deflection Curves for Pile Group Pressurized to 500 kPa. 93

Figure 4.17. Load-Lateral Deflection Curves for Pile Group Pressurized to 1000 kPa. 93

Figure 4.18. Load-Lateral Deflection Curves for Pile Group Pressurized to 1500 kPa. 94

Figure 4.19. Load-Lateral Deflection Curves for both Pile Group and Single Pile. 95

Figure 4.20. Load-Lateral Deflection Curves for Single Piles (1000 kPa). 95

Figure 4.21. Load-Lateral Deflection Curves for Single Piles (1500 kPa). 96

Figure 4.22. Comparison of Load-Displacement Curves (x-axis: displacement (mm), y-axis: load (N)). 106

Figure 4.23. Comparison of Load and Lateral Displacement Curves [48]. 106

Figure 4.24. Pile-Soil Modulus Ratios and Load Values at Displacement of 35 mm. 108

Figure A.1. Flexural Rigidity and Displacement Curves for the Piles (500 kPa without a Wearing Layer). 118

Figure A.2. Flexural Rigidity and Displacement Curves for the Piles (1000 kPa without a Wearing Layer). 119

Figure A.3. Flexural Rigidity and Displacement Curves for the Piles (1500 kPa without a Wearing Layer). 120

Figure A.4. Flexural Rigidity and Displacement Curves for the Piles (500 kPa with a Single Wearing Layer). 121

Figure A.5. Flexural Rigidity and Displacement Curves for the Piles (1000 kPa with a Single Wearing Layer). 122

Figure A.6. Flexural Rigidity and Displacement Curves for the Piles (1500 kPa with a Single Wearing Layer). 123

Figure A.7. Flexural Rigidity and Displacement Curves for the Piles (500 kPa with a Double Wearing Layer). 124

Figure A.8. Flexural Rigidity and Displacement Curves for the Piles (1000 kPa with a Double Wearing Layer). 125

Figure A.9. Flexural Rigidity and Displacement Curves for the Piles (1500 kPa with a Double Wearing Layer). 126

LIST OF TABLES

Table 2.1. Pile P-Multipliers, P_m, for Multiple Row Shading 25

Table 2.2. Range of Soil Modulus Values, E_s Based on Soil Type (AASHTO 2012). 27

Table 2.3. Soil Modulus Values, E_s From SPT N value (AASHTO 2012). . . . 27

Table 2.4. Soil Modulus Values, E_s From Cone Resistance, q_c (AASHTO 2012). 28

Table 2.5. Test Types and Notes for the Reviewed Studies in Literature. . . . 31

Table 2.6. Test Conditions for the Reviewed Studies in Literature. 32

Table 2.7. Relative Stiffness Factors, K_{rc} of Piles Tested. 33

Table 2.8. Soil Properties (Field Load Test). 35

Table 2.9. Pile Properties (Laboratory Load Test). 36

Table 2.10. The Main Characteristics of The Soil. 39

Table 2.11. The Main Characteristics of The Soil. 41

Table 2.12. Soil Properties. 44

Table 2.13. Soil Properties. 46

Table 2.14. Soil Properties. 48

Table 2.15. Soil Properties. 49

Table 2.16. Pile Properties. 49

Table 2.17. Test Conditions and Notes for the Previous Studies. 52

Table 3.1. Soil Properties. 62

Table 3.2. Peak and Residual Internal Friction Angles for Sand. 62

Table 3.3. Three-Point Bending Test Program. 76

Table 3.4. Laterally Loaded Pile Test Program. 80

Table 4.1. Flexural Rigidity Values for Piles. 85

Table 4.2. Elastic Modulus Values for Soil. 89

Table 4.3. Load Values (N) for Continuous and Non-Continupus Piles Obtained from Three-Point Bending Tests. 99

Table 4.4. Elastic Modulus Values for Sand. 100

Table 4.5. Pile-Soil Modulus Ratios, E_{pile}/E_{soil} (Piles without a Wearing Layer). 101

Table 4.6. Pile-Soil Modulus Ratios, E_{pile}/E_{soil} (Piles with a Single Wearing Layer). 101

Table 4.7. Pile-Soil Modulus Ratios, E_{pile}/E_{soil} (Piles with a Double Wearing Layer). 102

LIST OF SYMBOLS

b	Width of Square
B	Pile with Diameter
c_u	Undrained Shear Strength
C_c	Curvature Coefficient
C_u	Uniformity Coefficient
d_{10}	Effective Particle Size
d_{50}	Mean Particle Size
D	Outer Pile Diameter
D_r	Relative Density
D_1	Inner Pile Diameter
e	Distance
e_{max}	Maximum Void Ratio
e_{min}	Minimum Void Ratio
E	Elastic Modulus of Material (Young's Modulus)
E_c	Elastic Modulus of Concrete
E_p	Elastic Modulus of a Pile
E_pI_p	Flexural Rigidity of a Pile
E_s	Elastic Modulus of Soil
E_{st}	Elastic Modulus of Steel
EI	Flexural Rigidity
f'_c	Concrete Compressive Strength at 28 Days
G	Shear Modulus
G_s	Specific Gravity
I	Moment of Inertia
I_p	Moment of Inertia of a Pile
K	Modulus of Subgrade Reaction
L	Pile with Length
m	Meters

min	Minute
mm	Milimeters
M	Pile Bending Moment
N	Newton
p	Soil Resistance Per Unit Length
p_m	Group Efficiency
P	Load
Pa	Pascal
q_c	Cone Penetration Resistance
Q	Structural Loads
Q_s	Side Friction Resistance
Q_p	End Bearing Resistance
S	Pile Spacing
T	Characteristic Length of a Pile
y	Horizontal Displacement
z	Depth
β	Pile Characteristics
δ	Displacement
ϵ	Strain
η_h	Unit Subgrade Modulus
σ	Stress
ϕ	Internal Friction Angle
ϕ_{peak}	Peak Friction Angle

LIST OF ACRONYMS/ABBREVIATIONS

AASHTO	American Association of State Highway and Transportation Officials
ASTM	American Society for Testing and Materials
CPT	Cone Penetration Test
FEM	Finite Element Method
FHWA	Federal Highway Administration
GWL	Groundwater Level
LL	Liquid Limit
LVDT	Linear Variable Differential Transducer
ML	Low Plasticity Silt
OCR	Over Consolidation Ratio
PL	Plastic Limit
SP	Poorly Graded Sand
SPT	Standard Penetration Test
SPVFR	Segmental Piles with Variable Flexural Rigidity
USCS	Unified Soil Classification System

1. INTRODUCTION

Pile foundations have always been in use to transmit structural loads to deeper layers of soil for years. They are generally used in situations that the soil is inclined to settle extremely or has a low capacity. When piles are used under offshore and coastal structures, skyscrapers, and bridges, besides vertical loads, they are also subjected to lateral loads such as wind, earthquake (Rayleigh waves especially cause lateral ground motion at large displacement), and wave forces. Therefore, an attention must be devoted to lateral loads; they can comprise 30% of the total loads in some cases, for instance, offshore structures [1]. In most cases, the piles are used as a group. Even though using piles as a group decreases their individual capacities, the total capacity of the group is much higher. Thus, understanding the pile-soil interaction, which includes the interactive relation between two different substances, is very important in studying piles and soils under complex loading conditions.

A great number of empirical and theoretical study considering the behavior of piles and pile groups under lateral loading have been conducted in the literature. One of the first studies that focus on the behavior of laterally loaded piles belongs to Matlock and Reese (1960) [2]. The study includes bending moments, the subgrade reaction model, and solutions for long and short piles. Afterward, Broms (1964) [3] developed the ultimate lateral load model to determine the lateral capacities of free-headed short piles. Then, the model is developed to be used for fixed-head and long piles. Another milestone is accomplished by Poulos (1971) [4, 5]. His study includes the fixed-headed and free-headed conditions for both single piles and pile groups; and elastic analysis considering the relationship between load and displacement. The p-y method is the most extensively used analysis model for laterally loaded piles. Reese [6, 7] presents some solutions for the behavior of the soil surrounding the piles. In his studies, the factors of groundwater level, pile diameter, pile length, and type of loading on the p-y curves have been analyzed. Another significant study, including full-scale experiments on laterally loaded piles and pile groups, is conducted by Kim and Brungraber

(1976) [8]. The study reports that an increment in the lateral capacity of laterally loaded piles is observed when the pile spacing increases. Lastly, Poulos and Davis (1980) [9] mentioned the effect of the pile-soil rigidity ratio on the behavior of laterally loaded piles.

The piles preferred in engineering projects are mostly made of steel or concrete. However, this makes the piles much more rigid than that of the soil that the piles are embedded. Due to the rigidity difference between piles and soils, the piles cannot be displaced sufficiently under the lateral loads. Hence, this results in the damage or complete collapse of the piles. Within the scope of this study, the behavior of a pile group consisting of continuous piles is studied at large displacement in order to avoid such problems. The piles are designed to have adjustable rigidities. In this study, the lateral capacity of the piles subjected to lateral displacement is observed.

Through large displacement, large size model pile experiments, the continuous pile group with adjustable rigidity is tested, and the lateral displacement of up to 50 mm (143% of pile diameter) is conducted with strain control. The piles are made of fire hoses which can be pressurized to different rigidities by controlling the water pressure inside the piles. The piles are embedded into the sand, which is compacted at different relative densities, which are loose, medium dense, and dense. Consequently, the results are obtained for the lateral capacity of the pile group by studying three different flexural rigidities of the pile group and three different soil rigidities.

In the previous studies done at Bogazici University Karl Terzaghi Soil Mechanics and Geotechnical Engineering Laboratory, a new non-continuous model pile system with adjustable rigidity has been developed and manufactured. Afterward, various non-continuous model pile tests are conducted in the previous studies.

One of the primary objectives of this study is to develop a new continuous pile system. In this way, it is aimed to verify the test results obtained from the non-continuous pile tests. Additionally, the advantage of the continuous pile system is that

the developed beam equations can be applied to the pile model. The other significant objective of the study is to develop a continuous pile system with adjustable rigidity. This study in accordance with this purpose is primarily aimed to reach a similar range of pile-soil modulus ratios with the non-continuous pile system. A confined rubber cylinder is used as the pile material, and the rigidity of the cylinder is adjusted by controlling the water pressure inside them. The other important objective of the study is to perform the pile group tests. Due to the size of the non-continuous pile system, the pile group tests cannot be conducted in the previous studies. On the other hand, the size of the continuous pile group system is adjusted to be able to perform the group tests. The potential use of adjustable rigidity in continuous pile groups is investigated, and the effect of pile-soil modulus ratio at large horizontal displacement is observed. In summary, the segmental pile system is a non-continuous system, and there is a question of whether it can be treated as a beam. The rigidity can be adjusted. The working mechanism is through shear developed at the joints. The primary objective of this study is to compare this behavior with a continuous pile with adjustable rigidity. Due to its continuity, beam behavior will be applicable in this system. To be able to adjust the rigidity of the continuous pile system, water pressure in a confined rubber cylinder is regulated.

2. LITERATURE REVIEW

For the literature review, the general concepts associated with pile properties, group work of pile, laterally loaded piles, modulus of elasticity for soils and piles are concisely reviewed; afterwards, the laboratory experiments for laterally loaded piles are briefly reviewed.

2.1. Piles

Piles are mostly preferred when shallow foundations are incapable of carrying the structural loads. In addition, the piles are used in engineering projects in which the load capacity of the soil is low, and the soil is prone to excessive settlement [10].

The resistance that piles provide comes from end bearing and side friction. First of all, side friction develops through the interface friction between the surface of piles and the soil around the piles; side friction provides a critical amount of resistance for the piles. Secondly, the general concept of end-bearing piles is to convey the structural loads to deeper layers of soil where the load capacity is high. At this point, the soil at depths underlying the piles has a significant role in the resistance that piles provide.

2.1.1. Group of Piles

Piles are placed under large structures such as towers, skyscrapers and bridges to provide allowable lateral capacity. In some cases, piles can be used as single piles to convey the loads to depths. However, piles are used as a group in most of the cases. It is all known that vertical loads are considered as the main concern to design a pile, but horizontal loads are also needed to be taken into consideration. Earthquake (large ground deformation due to Rayleigh waves), wind and wave forces or failure of slopes may be given as the examples of powerful horizontal loads. Figure 2.1 displays the stress conditions under both a single pile and a group of piles [11].

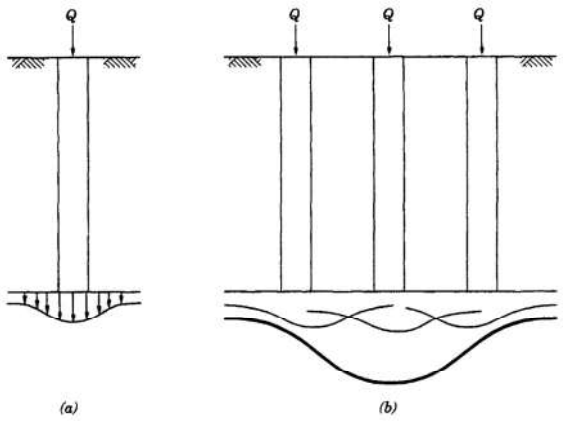


Figure 2.1. Stress Conditions Under Piles (a) Single Pile (b) A Group of Piles [10].

Using piles as a group decreases their individual lateral capacity values; this effect is called "group effect". Therefore, this term indicates that the group of piles has less total lateral capacity compared to the sum of lateral capacities of each pile. This effect happens since each pile in the group has an impact on the soil surrounding the other piles. The decrease in the horizontal resistance – horizontal displacement (p-y) curve is shown in Figure 2.2

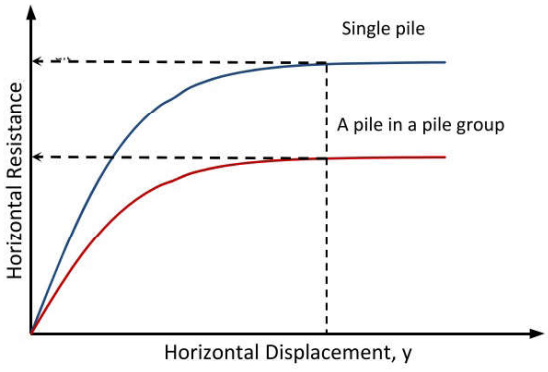


Figure 2.2. Group Effect.

During a lateral movement, every pile pushes the soil in front of it, and the movement develops a shear zone. As the movement continues, the shear zones start expanding and converging. If the piles are placed too close to each other, the possibility of converging the shear zones of each pile increases considerably. Converging may occur

between the piles both in the same row and different rows (Figure 2.3). If it occurs in the same row, it is named as "edge effects". On the other hand, if the converging occurs in the different rows it is called "shadowing effects". As a result of all these effects, the individual lateral load capacity of each pile decreases [12].

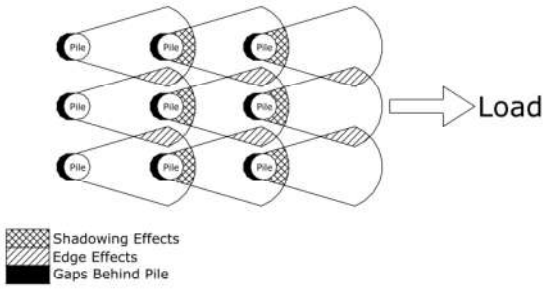


Figure 2.3. Shadowing and Edge Effects in a Laterally Loaded Group of Piles [13].

Brown et al. (1988) proposed one of the most commonly used methods related to the group effect of piles. This method identifies a p-multiplier and by using the parameter, the single pile curve is adjusted as seen in Figure 2.2 above. There are some parameters that affect p-multiplier. These effects are the arrangement of rows in the group of piles, type of soil and the distance between piles. Hence, p-multiplier can only be handled by experimenting since the parameter is correlated with soil variables.

2.1.2. Pile Properties

It is widely known that nearly all of the structures are exposed to lateral forces and moments as a consequence of waves, earthquakes, wind force, and lateral earth pressure. The piles have to be modeled carefully for such lateral forces mentioned above if it is planned that the piles are used as reinforcement for the structures [14].

The piles can be categorized into two groups as active and passive piles.

The piles are named "passive piles" under the circumstance that they are exposed to lateral soil movement. The upcoming conditions are counted as lateral soil movement when piles are used in practice; near to deep excavation, tunneling operation, slope movement, landslide, and embankment loading. Through the forces mentioned above, the soil moves against the piles; and then the presumptions regarding the force resulting from soil movement are performed to design the piles. Figure 2.4 exhibits passive piles placed in a bridge abutment [15].

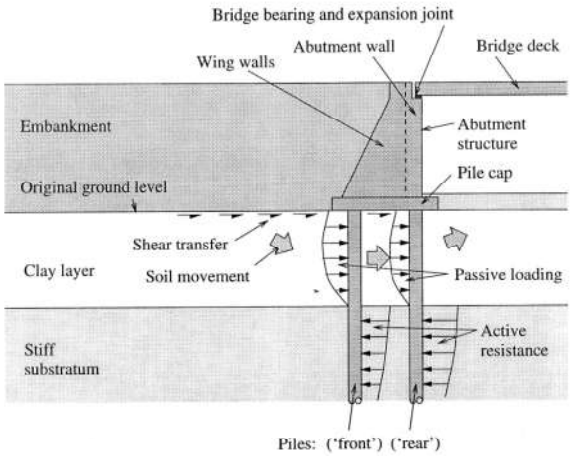


Figure 2.4. Passive Piles [16].

Secondly, the piles loaded at the top are counted as "active piles". The external horizontal force coming from the top of the piles is transferred to the soil and depths. The piles named active may be placed under towers and offshore platforms.

Chen et al. (1997) mentioned that the piles are designed by solely taking into consideration active forces, in most of the cases. However, an existing pile may be subjected to passive forces additionally. For example, lateral loads resulting from an excavation may cause extra settlement, deflections, and moments for piles; and it can be end up with structural failure. It is all a complicated issue that a lateral movement affects an already existing pile and it results in harder to predict the reaction of the

pile. Figure 2.5 shows an active pile in practice [17].

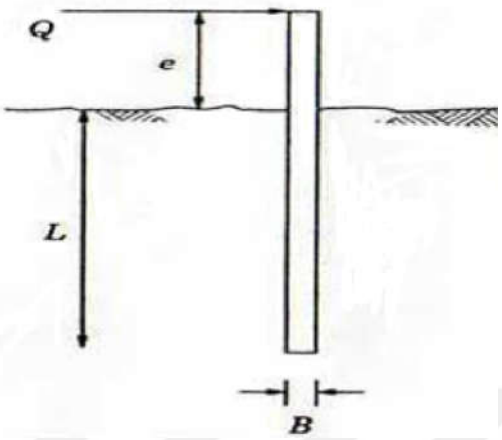


Figure 2.5. An Active Pile [18].

A failure in a group of laterally loaded piles happens inevitably when each pile in the group fails one by one; afterward, the characteristic length T of the pile has a crucial role on the pile behavior and the failure mechanism at the same time. The characteristic length T of a pile is calculated with equation (2.1) given as in [18] as

$$\mathbf{T} = \left(\frac{\mathbf{E}_p \mathbf{I}_p}{\eta_h} \right)^{0.2}. \tag{2.1}$$

It is proposed that the piles can be categorized into two groups as "short" and "long" piles. In addition, short piles are called rigid piles, while long piles are named as flexible piles. When the length of the pile is equal to or more than 5T, the pile can be categorized as a long pile. On the other hand, if the length of the pile is equal to or less than 2T the pile is classified as a short pile [19].

The characteristic length T of the pile is defined as a function of Young's modulus of a pile (E_{pile}), moment of inertia of a pile (I_{pile}), and unit subgrade modulus (η_h).

- L$\geq 5T$, long flexible piles.
- L$\leq 2T$, short rigid piles.

In practice, each kind of pile has its own response against lateral movements. Commonly, four different circumstances are observed. These different cases can be listed as; [20]

- Free-head long piles, the head of the pile is free to rotate and translate, but the base of the pile is completely restrained against rotation and translation.
- Free-head short piles, both the head and base of the pile is free to rotate and translate.
- Fixed-head long piles, the head of the pile is free to translate but completely restrained against rotation, and the base of the pile is completely restrained against rotation and translation.
- Fixed-head short piles, the head of the pile is completely restrained against rotation.

All these circumstances are shown in Figure 2.6., respectively.

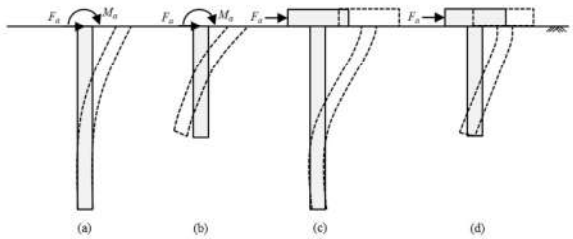


Figure 2.6. (a) Free-Head Long Piles, (b) Free-Head Short Piles, (c) Fixed-Head Long Piles, and (d) Fixed-Head Short Piles [20].

2.1.3. Analytical Models for Laterally Loaded Piles

In literature, there are several analytical models conducted in designing single or group laterally loaded piles. Each case possesses its own conditions, and different models offer the most suitable solution for the cases. The main consideration to design laterally loaded piles is not the ultimate lateral capacity that piles have but the maximum deflection that piles can endure. Designing single or group laterally loaded

piles may be complex in most cases. Several nonlinearities in the soil make the cases harder to solve.

First of all, as the pile moves in the soil, the mobilization of the soil resistance has a nonlinear pattern. The maximum deflection of the pile occurs at the top of it. As the load transferred to the pile increases, the soil layers at depths mobilize more actively. Moreover, the stiffness of soil also shows a nonlinear pattern. The range of the deformation affects the soil stiffness. The soil behaves stiffer in large deformations. Besides, the pile diameter and the soil depth are important factors affecting nonlinearities in soil [21].

In designing piles to resist lateral loads, the structural response and geomaterial deformation of piles must be assessed cautiously, and the structural resistance must be found out. Figure 2.7 shows the soil resistance against laterally loaded piles. Afterward, the deformation of piles regarding the service loads must be determined, and the considered results must be compared to the performance factor of the foundation [22].

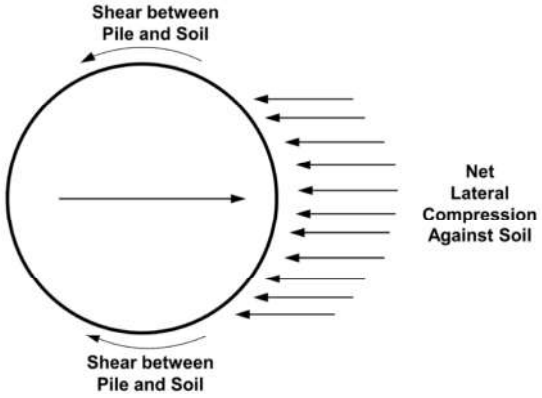


Figure 2.7. Soil Resistance Against Laterally Loaded Piles [22].

A full understanding of the laterally loaded piles demands both geotechnical and structural engineer skills. If the topic is considered on the part of geotechnical engineering, analyzing the structure-pile interaction may be a problem. At the same time, determining the spaces and sizes of the piles is not the main consideration of

structural engineering. Both conditions also affect the response of the soil. Under these conditions, an interdisciplinary approach between structural and geotechnical engineering is required [22].

There are a lot of significant parameters that can influence the resistance of laterally loaded piles. These parameters are related to soil, pile, and load conditions. In this context, the factors that affect the parameters mentioned above must be evaluated as follows [22]:

- Soil parameters,
  - (i) Soil type and its properties such as friction angle, GWL, moisture content, and shear strength.
  - (ii) Coefficient of horizontal subgrade reaction. The coefficient can be identified as the ratio between the pressure and deflection at a point.
- Pile parameters,
  - (i) Pile properties, for instance; its shape, dimensions, and material.
  - (ii) Pile head states such as fixed-head and free-head.
  - (iii) Placement method of the piles.
  - (iv) Group piles effect.
- Load parameters,
  - (i) Load type such as monotonic or cyclic.
  - (ii) Eccentricity.

Analytical models conducted in designing single or group laterally loaded piles are listed as follows.

2.1.3.1. Subgrade-Reaction Analysis. The theory [9] is based on the Winkler soil model. This analysis method firstly aims to find out a subgrade reaction modulus, which is denoted by k_h. Reese and Matlock [23]; Davisson and Gill [24] regularly referenced this modulus in their studies. In cases in which a horizontal loading is a matter, a modulus of subgrade reaction k_h can be found regarding the pressure p and deflection

ρ at a point. k_h has units of $force/length^3$ and is formulated as

$$\mathbf{p} = \mathbf{k}_h \rho. \tag{2.2}$$

Afterward, soil reaction per unit-length of a pile, w can be calculated through the modulus of subgrade reaction. Subgrade-reaction modulus is defined as K, which has units of $force/length^2$ ($K = k_h d$) and d refers to the diameter of a pile. And, equation (2.2) has been formed as equation (2.3) written as

$$\mathbf{w} = \mathbf{K}\rho. \tag{2.3}$$

In the method, the pile is thought of as a thin strip, and the behavior of the pile is governed by the beam equation. The equation can be defined as a function of Young's modulus of a pile (E_p), moment of inertia of a pile (I_p), soil depth (z), deflection(ρ), and diameter of the pile (d). The Equation is given as

$$\mathbf{E}_p\mathbf{I}_p \frac{\mathbf{d}^4\rho}{\mathbf{dz}^4} = -\mathbf{pd}. \tag{2.4}$$

Hereby, the impact of axial load in the pile can be ignored when the theory of bending of beam is taken into account and then the deflection in laterally loaded piles can be calculated as the main purpose of the method. The governing equation for the deflection of a laterally loaded pile is formulated in equation (2.5) as a combination of equation (2.2) and equation (2.4) and written as

$$\mathbf{E}_p\mathbf{I}_p \frac{\mathbf{d}^4\rho}{\mathbf{dz}^4} + \mathbf{k}_h\mathbf{d}\rho = 0. \tag{2.5}$$

2.1.3.2. Broms' Model (1964). Broms [25] developed the model to find out the ultimate lateral capacity for laterally loaded piles. Primarily, the model was developed for free-head and short piles in cohesive soils. In time, the model was also improved to use for fixed-head and long piles in cohesionless soils.

There are some assumptions to calculate the ultimate lateral capacity for short and long piles. If the short piles are considered, it is assumed that the ultimate lateral capacity is governed by the passive earth pressure of the soil around the piles. On the other hand, if the piles with large penetration depths, so long piles are considered, the ultimate lateral capacity is governed by the ultimate resistance of the pile. Figure 2.8 shows the soil reaction for short and long piles.

Besides, the type of soil must be evaluated that such as it is sandy or clayey. This is because the soil has a major effect on the ultimate lateral capacity. For clay soils, laterally loaded piles in a cohesive soil are subjected to the lateral earth pressure at failure and, that pressure is roughly equal to two times the undrained cohesive strength C_u at the ground level. At depths, the earth pressure is greater than the value at the ground level. The pressure can reach a value of eight to twelve times the undrained cohesive strength at three pile diameters below the ground level. Moreover, the reaction of the clay soil varies from depth to depth at failure. Broms' model presents that the soil positioned in front of the pile from the ground level up to three pile diameters below the ground moves through upwards. As a result of the move, the soil swells at that layer. On the other hand, the reaction of the soil is different where the soil moves laterally at depths three diameters below the ground level. For sandy soils, laterally loaded piles in a cohesionless soil are subjected to the lateral earth pressure at failure and, that pressure is safely equal to three times the passive Rankine earth pressure.

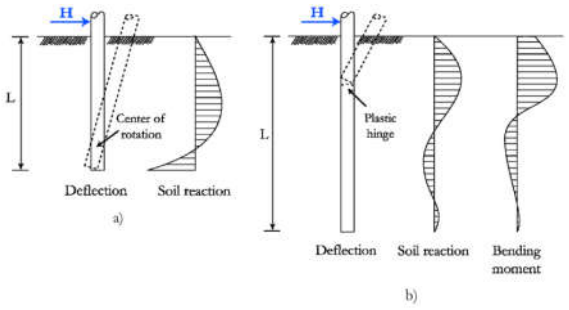


Figure 2.8. Soil Reaction and Failure Mechanisms for Short (a) and Long Piles (b) [25].

As comparing the results between Broms' model and field experiments for laterally loaded piles, the results obtained by the model differ greatly from the measured results. When the strength parameter is considered, Broms' model can be counted as conservative for the sandy soils. Additionally, the results for the strength are accurate for the clayey soils [21].

Broms' model is quite usable and offers a quick method to design a pile. On the contrary, the model is undependable because the results are not satisfying, as mentioned above. There are lots of limitations in the model that the most accurate results are obtained for the cases that the piles are placed into only homogeneous soils. Furthermore, cyclic and axial loads are not taken into account in the calculations. When all the factors are observed, the accuracy and the reliability of the model are reduced because there is a great difference between the calculation and the measurement [21].

2.1.3.3. Elastic Analysis. In this model, it is assumed that the soil is like an elastic continuum. Many significant names like Douglas and Davis (1964) [26], Spillers and Stoll (1964) [27], and more described and detailed this method in their studies. All the analyses conducted are basically the same, but the differences originate from the details. Each study has a different aspect regarding the action of the piles. In this thesis, the analyses of Poulos [4], [5] are briefly summarized below.

As a beginning, Poulos [4] focuses on floating piles in which the geometry of a floating pile is rectangular with width d, length L, and a constant elasticity. The analyses can be applied to a circular pile also while the width d can be counted as the diameter of the pile. The analysis does not consider the potential horizontal shear stresses between the pile and the soil surrounding the pile. Afterward, the pile is separated into $n + 1$ pieces as shown in Figure 2.9, and it is assumed that each piece is subjected to a uniform horizontal stress ρ along the width of the pile. The soil is also assumed as homogeneous, and the soil surrounding the pile, positioned at the back of it, adheres to the pile. If elastic conditions dominate the soil perfectly, the lateral displacements of the pile and the soil are equal to each other. In this model, the lateral

displacements are equated at the center of each piece. Lateral soil displacements for all center of pieces along with the pile, where $\{_{\mathbf{s}}P\}$ indicates the lateral soil displacement of $n+1$ column vectors and $\{\mathbf{p}\}$ does horizontal stress between the pile and the soil. $[\mathbf{I_s}]$ is the matrix of soil-displacement-influence factor, and displacements are given as

$$\{_{\mathbf{s}}P\} = \frac{\mathbf{d}}{\mathbf{E_s}}[\mathbf{I_s}]\{\mathbf{p}\}. \tag{2.6}$$

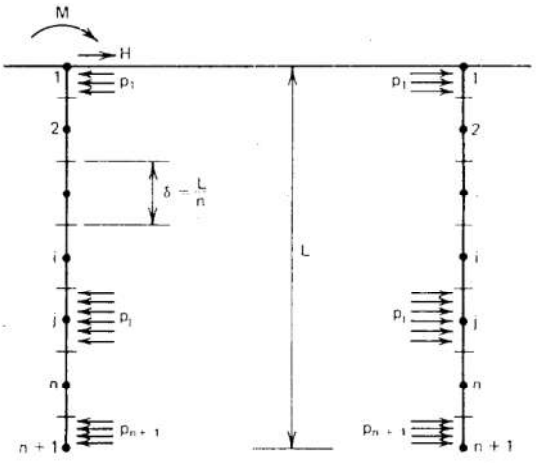


Figure 2.9. A Floating Pile [4].

The differential equation for bending of a thin beam (equation (2.4)) is used to determine the pile displacements. Different formulations are needed to calculate the lateral displacements for free-head and fixed-head piles. The formulations can be arranged in a finite-difference model by determining the boundary conditions from the top of the pile to the tip.

In addition to floating piles, Poulos [5] also focuses on socketed piles in which similar conditions related to floating piles regarding the behavior of the soil and the pile are assumed. However, the soil is described as a rigid and rough bearing stratum in this model, and so the tip of the pile is limited by the soil from moving laterally. Lateral

pile displacements for socketed piles where p is $n-1$ column vectors for load, $\{_{\mathbf{p}}\rho\}$ is lateral pile displacement, and $[D_2]$ and $\{\mathbf{C}\}$ are the matrices of finite-difference coefficients limited by the top and the tip boundary conditions. The working mechanism of socketed piles is shown in Figure 2.10, and displacements are given as

$$-\{\mathbf{p}\} = \{\mathbf{C}\} + \frac{\mathbf{E_p I_p n^4}}{\mathbf{dL}^4}[\mathbf{D_2}]\{_{\mathbf{p}}\rho\}. \tag{2.7}$$

Poulos [4] indicates that in-situ soils are expected to yield at relatively low loadings. Therefore, a large amount of displacement occurs since the elastic analysis exhibits that high pressures are observed around the top of the pile. As a result, local yields of soil are observed. Moreover, the elastic analysis supposes that the soil positioned at the back of the pile always adheres to the pile. It is expected to develop separation around the top of the pile where large stresses are taken into account. This is because tension develops behind the pile while compression does in front of the pile. The local yield and the separation near the top of the pile are the major effects regarding the expected nonlinearity in load and deflection behavior mostly encountered in lateral loading tests.

2.1.3.4. Blum's Model (1932). Blum's model [28] is one of the oldest models that it is widely used in the world even today. Some of the features of the model, such as being simple and giving fast results, make it valuable in contrast with brand new models, which are pretty complicated and relatively expensive.

The model includes some essential assumptions just because the period when the model is developed is the lack of computers executing the complex calculations easily. It is assumed that the pile is fixed at a theoretical depth t_0 where the moment is zero. A lateral force is assumed at the depth t_0. There are two lateral loads on the pile above the critical depth t_0. The first one is loaded at the top of the pile and the other one is induced by the resistance in the soil. The soil is considered to induce all passive resistance, which is pushed upwards by a lateral deflection along with the pile. The passive resistance can be calculated by imagining a soil wedge. Figure 2.11 shows the

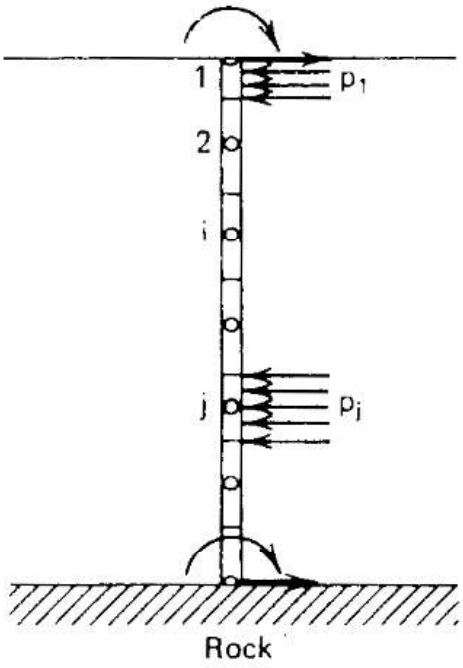


Figure 2.10. A Socketed Pile [5].

soil wedge causing the resistance and the lateral loads on the pile regarding Blum's assumptions.

The model primarily aims to calculate displacements, and Blum does it in the ultimate state by conducting the basic rules of the mechanics. In the model, it is assumed that the moment and all rotations are restricted and must be zero at the critical depth t_0.

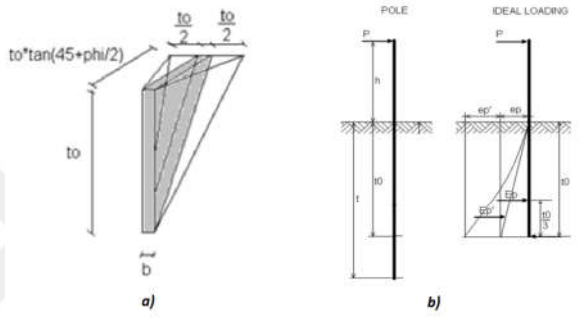


Figure 2.11. The Soil Wedge (a) and The Pile Scheme (b) [28].

The limitations of Blum's model are briefly listed below;

- The study of Blum is not available for long piles. The model is only reliable for the short piles in sandy soils. The cohesion effect is not included in the study.
- The model is counted as an ultimate strength model. Therefore, the main aim of the model is not to design serviceable piles.
- The behavior of the pile-soil interaction is not considered in the model at all. Hence, the model is preferred only to have an idea of the final pile design.
- Cyclic and axial loads are not taken into account in the calculations in the model.

2.1.3.5. P-y Curves. The p-y method is the most extensively used nonlinear analysis model for laterally loaded piles. Attention to the model first appeared in the '50s when off-shore structures were built by energy firms that preserve them from lateral loads caused by waves. Firstly, p-y curves were referred to by the studies of Terzaghi and

Skempton in the ‘50s. The p-y method is enhanced in time and is now capable of analyzing all kinds of cases. Moreover, the model is still developed even today [21].

In the p-y model, p indicates the soil resistance per unit pile length and y does the lateral pile or soil displacement. Basically, the resistance of the soil is modeled as a series of nonlinear springs along the pile length regarding the lateral loads. The series of springs are illustrated in Figure 2.12 [21].

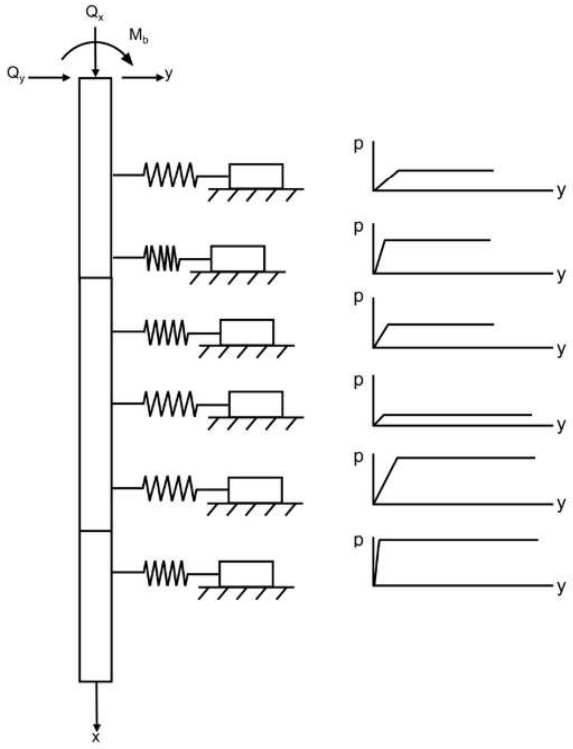


Figure 2.12. An Analysis of P-y Soil-Pile Model [22].

Reese [6,7] introduced some procedures, which help to understand, the soil behavior around the laterally loaded piles in different cases by conducting the p-y method. The main objective of the procedures is to form the most accurate curves. Tests using full size instrumented piles and technics regarding the soil response under load are the major considerations that Reese took into account to create the procedures.

There are two types of p-y curves, typically. The first one is ductile p-y curves mostly encountered in soft clays during static loading. The other type is brittle p-y curves that express the response of stiff clays during dynamic loading. Typical ductile and brittle p-y curves are shown in Figure 2.13 as an example.

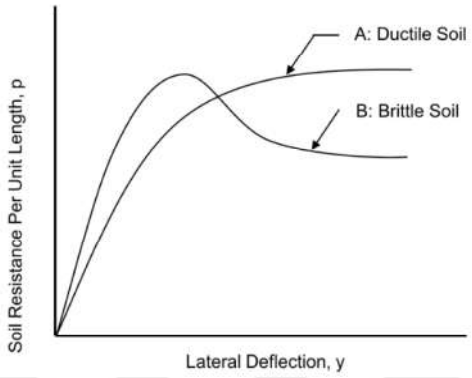


Figure 2.13. Examples of P-y Curves in Ductile (A) and Brittle (B) Soils [29].

It is important to emphasize that several factors can affect the fluctuation on p-y curves. The main factor is the soil properties, for sure. On the other hand, there are also minor factors that can influence the curves as listed below;

- The soil relationship in between stress and strain,
- GWL,
- Pile diameter,
- The type of loading,
- Depth.

The initial goal of the model is to solve the nonlinear differential equation. The solution is provided by using the finite-difference formulation introduced by Reese [6] as detailed in his analyses. Also, the solution regards the condition of lateral loads and the behavior of the soil-pile interaction. The model offers an iterative solution. In the end, a reliable result is achieved in the p and y values in every element of the case.

An ordinary p-y analysis performed presents the input data and the results of the analysis. Firstly, the input information consists of soil and pile properties. Afterward, the output information gives the force and deflection values at various depths presented as p-y curves. Moreover, bending moments, stresses, and modulus of soil can be found in the output data. In the light of all information given by the model, an analysis regarding the structural resistance of a pile can be performed. The model also includes graphical output exhibiting the computed moment, force, and slope diagrams at various depths. Consequently, it can be said that the p-y model has no limitations, and every condition can be modeled by using the method [22].

2.1.3.6. Strain Wedge Model. FHWA [22] presents that the strain wedge model offers a more reliable solution for short, rigid piles, unlike the p-y model is usually preferred for the long piles that can deflect and bend. On the other hand, short piles tend to rotate instead of deflecting or bending.

Norris (1986) [30] and Ashour et al. (1998a) [31] brought into the open the basic details of the model. Fundamentally, a passive wedge is designed against the laterally loaded piles in the strain wedge model. The wedge is modeled as three dimensional and integrated into the beam on an elastic foundation. The model offers various conditions regarding depth, loading and shape because of changes in strain. The mobilized strains in the wedge constitute the connection between horizontal displacement and passive resistance. The development of a wedge in the soil is exhibited in Figure 2.14. The point is to get the stress-strain behavior of the soil. The behavior can be straightly taken from experiments or estimated. Afterward, the information is added to the wedge design.

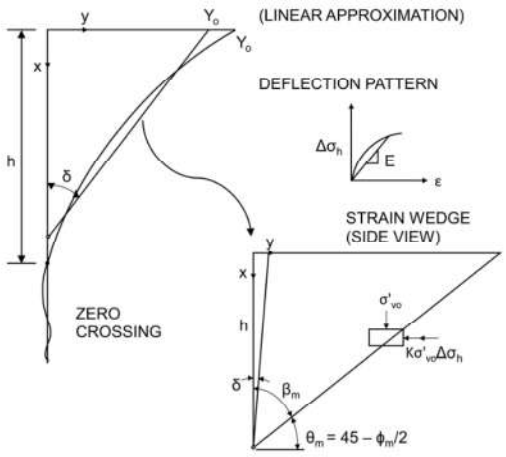


Figure 2.14. Strain Wedge Developed in Soil [31].

Additionally, Ashour et al. 2002 [32] improved the model in further studies, which have added the capability of calculating the impact of pile head conditions and multiple soil layers. For implementing the multiple soil layers, the soil properties of each layer must be assigned one by one in the wedge model. The various wedge shapes are observed depending on soil properties as exhibited in Figure 2.15.

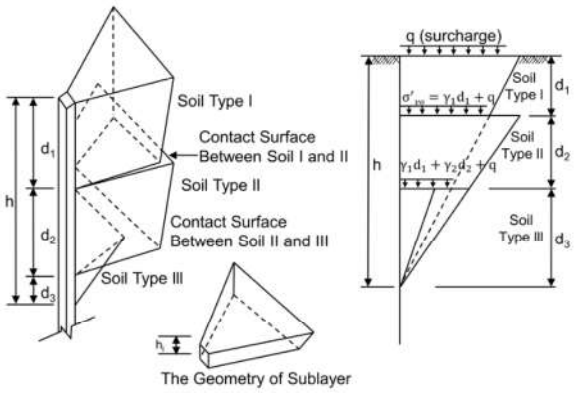


Figure 2.15. Geometry of Wedges in Soil [31].

As a result, the strain wedge method takes modeling laterally loaded piles one step further from the traditional p-y method. In the wedge design, the series of elastic springs are dependently modeled through all the pile length as depicted in Figure 2.16. Additionally, the group effect of piles can also be modeled by overlapping the wedges

of every single pile.

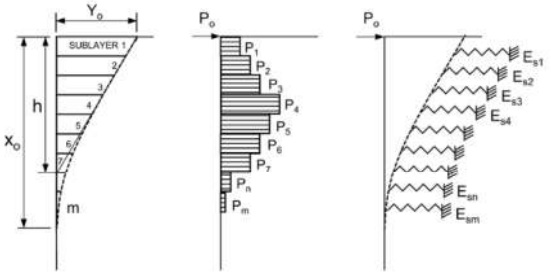


Figure 2.16. Interaction Between Soil and Pile within Multiple Soil Layers [31].

2.1.3.7. Analysis of Pile Groups. One of the important design criteria of a pile group is to resist lateral loads. It is assumed that the lateral displacement of a pile group is approximately 3 times larger than the lateral displacement of an individual pile under lateral loads. An illustration of pile groups is shown in Figure 2.17. Brown et al. 1988 [33] emphasized that a leading row in a pile group has more resistance to lateral loads than trailing rows of a pile group. Hence, greater lateral displacement is observed for trailing rows. The reason behind the case is the pile-soil-pile interaction that ends up with less resistance in a pile group against lateral loads. Consequently, the sum of the lateral resistance that single piles have is greater than the lateral resistance of a group pile.

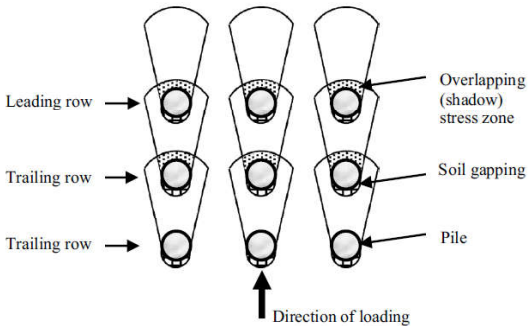


Figure 2.17. Illustration of a Pile Group [33].

The study of Brown et al. 1988 [33] indicates that the lateral resistance of every single pile in a group of piles varies depending on the position in the group. A p-multiplier, P_m is defined to adjust the change in the lateral resistance of a single pile by taking into consideration the row position of piles. P-y curves are adapted by the p-multiplier as exhibited in Figure 2.18. The P_m values for piles in the same row are equal, and the P_m value for a single pile is valid along all the pile length. According to an experiment, 3 x 3 pile group in dense sand, performed by Brown, the P_m values for piles positioned in the leading, middle and back rows found 0.8, 0.4, and 0.3, respectively.

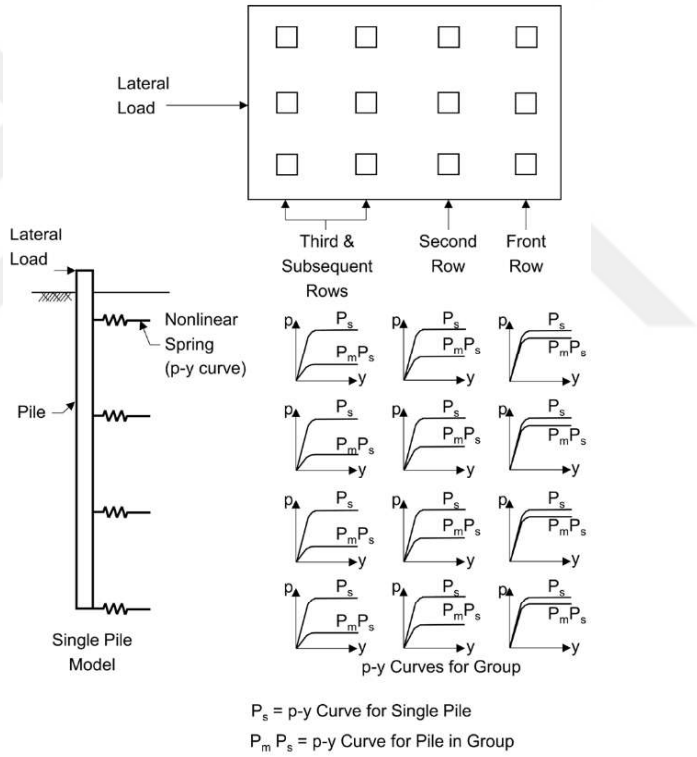


Figure 2.18. Concept of P-multiplier for Pile Groups [22].

A study of FHWA [22] presents a stepwise design methodology for laterally loaded pile groups regarding the analysis used for laterally loaded single piles.

(i) Find out factored lateral loads.

(ii) Draw p-y curves for single piles.

- Find out p-y curves for single piles according to instrumented in-situ lateral pile load tests.
- Draw p-y curves regarding the published correlations with soil properties.
- Draw p-y curves regarding the in-situ test data.

(iii) Run the software-based analysis.

- Find out Pm values for every row of pile group and run the p-y analysis. (P-multipliers are exhibited in Table 2.1 suggested in AASHTO, 2012.)
- Get load-deflection and moment-deflection data from the analysis.
- Determine and plot load-deflection graphics for every row in the pile group.

Table 2.1. Pile P-Multipliers, P_m, for Multiple Row Shading.

Pile Center to Center Spacing	**Row 1**	**Row 2**	**Row 3 and Higher**
3B	0.8	0.4	0.3
5B	1.0	0.85	0.75

(iv) Presume group deflection during lateral loading.

- Find out an average load for given deflections from every pile in the group and determine the average group response.
- Divide the total lateral load by the number of piles and determine the average lateral load.
- Plot the load-deflection curves for all the piles in the group and draw the average curve representing the pile group behavior.
- Presume group deflection from the group average curve.

(v) Assess the structural acceptability of the pile.

- Draw maximum bending moment-deflection curves for each row in the group regarding the data from software-based analysis.
- Check the structural competence for each pile and determine maximum bending moments for every single pile; by using presumed deflection values during the lateral loading.
- Find out the maximum pile stress from the data from software-based analysis associated with the maximum bending moment.
- Observe the comparison between pile yield and maximum pile stresses.

(vi) Compute refined pile group assessment regarding the interaction between structure and substructure.

2.2. Elastic Modulus of Soil and Pile Rigidity

It is important to emphasize that deformation is the response of the soil against an applied load. When piles are considered, limit states of structures are determined by allowable deformations. Modulus parameters are provided from strain values through laboratory and in-situ tests. Elastic modulus, E can be found out with the help of Hooke's Law. The measurement of a strain against to load applied to soil gives the modulus parameter given as in [22] as

$$\sigma = \mathbf{E}\epsilon. \tag{2.8}$$

Here, σ is the parameter which is referring to the stress and ϵ is the strain parameter.

The shear modulus, G is also related to the stress-strain parameters. Equation (2.9) is formulated to find out the elastic modulus by considering Poisson's ratio, ν and the shear modulus written as

$$\mathbf{G} = \frac{\mathbf{E}}{\mathbf{2(1+\nu)}}. \tag{2.9}$$

The publication of AASHTO 2012 [34] compiled the values of Young's modulus of soil, E_s and Poisson's ratio, and tabulated the values as shown in Table 2.2 below. Table 2.3 and Table 2.4 also cover the estimating soil Young's modulus values with the correlation of the SPT N and CPT static cone resistance values, respectively. It is also suggested that additional laboratory or in-situ tests must be performed to double-check the given values.

Table 2.2. Range of Soil Modulus Values, E_s Based on Soil Type (AASHTO 2012).

Soil Type	**Young's Modulus (MPa)**	**Poisson's Ratio, ν**
Clay: Soft Sensitive	2.4-14.4	0.40-0.50 (undrained)
Clay: Medium Stiff	14.4-48	0.40-0.50 (undrained)
Clay: Very Stiff	48-96	0.40-0.50 (undrained)
Sand: Loose	9.6-28.8	0.20-0.36
Sand: Medium Dense	28.8-48	
Sand: Dense	48-76.8	0.30-0.40
Gravel: Loose	28.8-76.8	0.20-0.35
Gravel: Medium Dense	76.8-96	
Gravel: Dense	96-192	0.30-0.40
Loess	14.4-57.6	0.10-0.30
Silt	1.9-19	0.30-0.35

Table 2.3. Soil Modulus Values, E_s From SPT N value (AASHTO 2012).

Soil Type	**E_s (MPa)**
Silts, Sandy Silts, Slightly Cohesive Mixtures	$0.38(N_1)_{60}$
Clean Fine to Medium Sands, Slightly Silty Sands	$0.67(N_1)_{60}$
Coarse Sands and Sands with Little Gravel	$0.96(N_1)_{60}$
Sandy Gravels and Gravels	$1.15(N_1)_{60}$

On the other hand, pile properties have a significant effect on the structural resistance. Pile rigidity is one of the critical parameters for when the capacity of driven piles is considered. Piles are mostly made of concrete, steel, or wood, and each material has its unique properties. The most widely preferred material is steel that is used for meeting the minimum design yield stress values. According to ASTM A572 [35] requirements, the minimum yield stress of 345 MPa is asked for the steel pile sections to be fabricated. Furthermore, AASHTO (2012) [34] specifications require that the

Table 2.4. Soil Modulus Values, E_s From Cone Resistance, q_c (AASHTO 2012).

Soil Type	E_s **(MPa)**
Sandy Soils	$0.1q_c$

elastic modulus for steel piles, E_{st} is supposed to be 200 GPa. In addition to steel piles, AASHTO (2012) specifications have similar recommendations for concrete piles. The elastic modulus of the concrete pile is directly related to the concrete strength, which can be improved by adding reinforcing steel. Finding out the elastic modulus of the concrete pile as mentioned in the specification is proposed in equation (2.10) given as

$$\mathbf{E_c} = 1820\sqrt{\mathbf{f'_c}}. \tag{2.10}$$

Here, elastic modulus of the concrete pile is defined as the function of the compression strength of concrete at 28 days, f'_c in ksi.

For wooden piles, tree species is the dominant factor for the property of piles. Relevant compression stress values and reference design values in terms of the type of lumber are presented in AASHTO [35] specifications. The values can be adjusted through the size and shape parameters of the pile.

As a side note, the pile shape also contributes to the structural resistance at transferring loads to the pile. The relative thickness of the material has a direct effect on this. Flexural rigidity depends on the shape of the pile too. Figure 2.19 exhibits a common pipe pile dimension.

In a pile section, the observed stress increases from the center of the pile through the edges during a loading. For a single pile, the largest stresses are observed in the outer parts of the section. When it is aimed to find out the maximum stress on a pile during loading, the parameters: area of the pile, the rigidity and distance from the pile

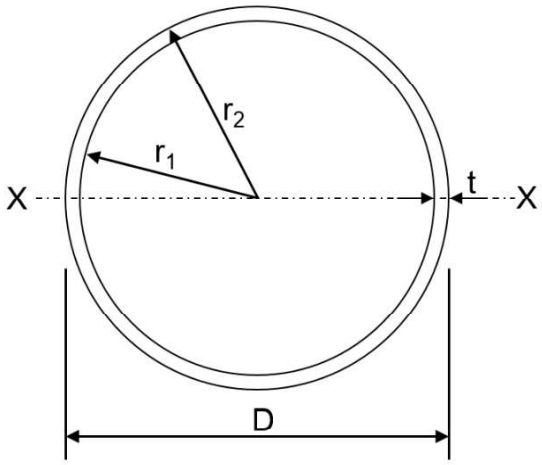


Figure 2.19. Shape Dimensions for Pipe Pile [34].

center to the edges in the section must be known. Equations (2.11)-(2.13) present how to compute the moment of inertia, I for different pile shapes [22].

For circular sections,

$$\mathbf{I} = \frac{\pi(\mathbf{D})^{\mathbf{4}}}{\mathbf{64}}. \tag{2.11}$$

For voided circular sections,

$$\mathbf{I} = \frac{\pi[(\mathbf{D})^{\mathbf{4}} - (\mathbf{D_1})^{\mathbf{4}}]}{\mathbf{64}}. \tag{2.12}$$

For square sections,

$$\mathbf{I} = \frac{\mathbf{b}^{\mathbf{4}}}{\mathbf{12}}. \tag{2.13}$$

Here, D indicates the outer diameter, D_1 does the inner diameter; and lastly, b does the width of the square.

2.3. Review of Laterally Loaded Pile Group Studies in Literature

Several studies regarding the laterally loaded piles at different pile spacings and group configurations in various types of soils and pile-soil modulus ratio behaviors are presented. Table 2.5 and Table 2.6 exhibit a summary of the reviewed studies. Pile types, pile group patterns, pile spacings, pile and soil properties, test types and additional conditions can be found in tables. The further knowledge related to the studies is presented below the tables.

The study of Rao et al. [1] highlights that marine structures, supported by piles, are designed against lateral loads, and afterward; the interested parameters behind the idea have been detailed in the study. These parameters are listed as flexural rigidity of piles, different models of pile group layouts considering the direction of the lateral load, and embedment length of piles. The clay soil used in the experiments is from a deposit off the coast. The Atterberg limits of the soil are 52% of LL, and 22% of PL. The range of the water content of the soil varies between 33-42%. The experiments are performed in a rectangular strongbox apparatus with internal dimensions of 1.2 m x 0.8 m x 1.1 m. The experiment mechanism is considered as a free-head pile test. The dimensions of the test apparatus are large enough to neglect wall effects as mentioned in Prakash, 1962 [43]; 8-12D in the way of lateral loading and 3-4D in the way of perpendicular to the lateral loading. The piles used in the tests are made of aluminum and mild steel pipes covering different diameters, and an extensive range of L/D ratios varied from 20 to 40. The details of pile materials and soil properties are listed in Table 2.7.

In the study, the experiments have been conducted with various combinations of pile configuration to analyze and observe the stress zones along the pile and load-deflection curves of the pile groups. Figure 2.20, Figure 2.21, and more are depicted by the authors considering the test results.

The authors [1] concluded that the critical spacing of the piles is one of the decisive factors for the behavior of structures supported by piles exposed to lateral loading. The

Table 2.5. Test Types and Notes for the Reviewed Studies in Literature.

Reference	**Test Type**	**Notes**	**Keywords**
[1]	Large Scale Laboratory	Free-Head, Static Lateral Loading	Flexural Rigidity, Embedment Length, Pile Arrangement
[36]	Large Scale Laboratory, Numerical Analysis	Free-Head, Static Lateral Loading	Soil and Pile Rigidity, Subgrade Reaction
[37]	Large Scale Laboratory	Static Lateral Loading	Flexible Piles, Large Deflection
[38]	Large Scale Laboratory	Fixed-Head, Static Lateral Loading	Flexural Rigidity, Pile Spacing, Pile Arrangement
[39]	Large Scale Laboratory	Static Lateral Loading	Pile Arrangement, Installation Method
[33]	Large Scale In-Situ	Free-Head, Cyclic Lateral Loading	Shadowing Effect, Group Effect
[40]	Parametric	Static Axial Loading	Soil and Pile Stifness, Skin Resistance
[11]	Parametric (Full-Scale)	Free-Head, Lateral Loading	Group Factor, Pile Spacing, Continuum Model
[41]	Parametric	Lateral Loading	Group Behavior, FEM
[42]	Centrifuge	Free-Head, Lateral Response	Pile Spacing Lateral Resistance

Table 2.6. Test Conditions for the Reviewed Studies in Literature.

Reference	**Pile Type**	**Pile Configuration**	**Pile Spacing**	**Embedment Depth Ratio (L/D)**	**Soil**
[1]	Aluminum and Mild Steel Pipe Piles	1 x 2, 2 x 1, 3 x 2, 2 x 3	-	20, 30, 40	Marine Clay
[36]	Steel Piles	-	-	12.5, 20.3	Clay, Silt, Rock
[37]	Steel Pipe Piles	-	-	28	Low Plasticity Silt
[38]	Steel Pipe Piles	2 x 3, 3 x 2, 3 x 3	1D, >D	21	Sand
[39]	Steel and Concrete Piles	-	-	from 10 to 35	Medium to Highly Plastic Clay
[33]	Steel Pipe Piles	3 x 3	3D	11	Poorly Graded Sand
[40]	-	3 x 5	2 m	16.67, 50	-
[11]	Steel Piles	3 x 3	5.65D, 3.29D	-	Sand
[41]	-	2 x 1, 2 x 2, 3 x 2	2D, 4D, 6D, 8D	15	Cohesive, Cohesionless Soils
[42]	Prototype Pipe Piles	3 x 3	3D, 5D	5	Poorly Graded Sand

Table 2.7. Relative Stiffness Factors, K_{rc} of Piles Tested.

Pile Material	**Pile Modulus E_p (kPa)**	**L/D**	**Soil Modulus E_s (kPa)**	E_p/E_s	K_{rc}
Mild Steel	$2.1x10^6$	40	$0.292x10^3$	7191	$0.92x10^-2$
Aluminum	$0.754x10^8$	20	$0.292x10^3$	258219	$3.78x10^-2$
Aluminum	$0.754x10^8$	40	$0.292x10^3$	258219	$0.24x10^-2$
Aluminum	$0.754x10^8$	20	$0.292x10^3$	258219	$3.21x10^-2$
Aluminum	$0.754x10^8$	20	$0.292x10^3$	258219	$0.21x10^-2$

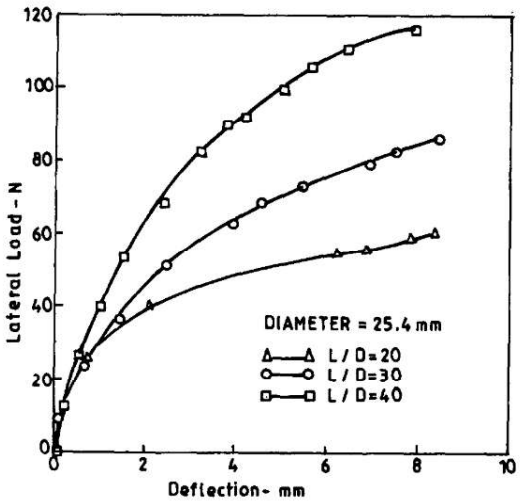


Figure 2.20. Lateral Load - Deflection Curves (Single Pile) [1].

critical spacing of piles is dependent to the pile group layout corresponding the load direction and the embedment depth of the piles. The critical spacing of the piles is figured out in below: (L denotes the length of the piles, S does the spacing between piles, and D does the outer diameter of the piles.)

(i) For a series combination of two piles:
- L/D = 20; S/D = 5,
- L/D = 30; S/D = 6,
- L/D = 40; S/D = 8.

(ii) For a parallel combination of two piles:
- L/D = 20; S/D = 4,
- L/D = 30; S/D = 5,
- L/D = 40; S/D = 7.

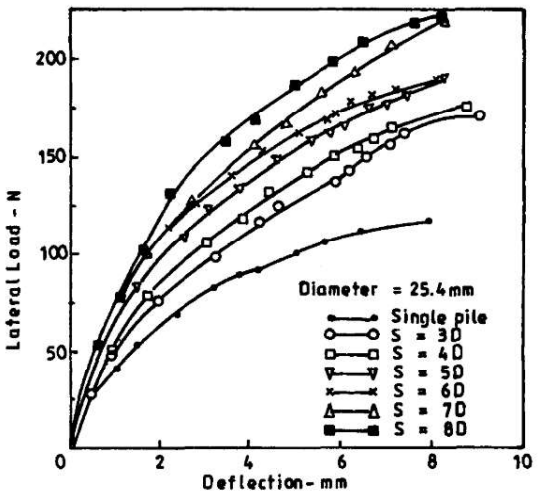


Figure 2.21. Lateral Load - Deflection Curves for Two-Pile Group [1].

At last, it is concluded in the study [1] that long and flexible piles show greater resistance to lateral loading in the form of a parallel combination compared to that for short and rigid piles. The opposite case is valid for the rigid piles under lateral loading in the form of a series combination.

The study of Youngho Kim et al. [36] concerns deformations and the load pattern in offshore piles. Afterward, the relation between soil and pile rigidity of laterally loaded piles is also specifically detailed in this study by conducting flexible and rigid pile analyses. Both in-situ and laboratory model tests, and also numerical analysis methods are performed to have a comprehensive comparison. The soil properties used in the in-situ and laboratory tests are listed in Table 2.8. The experiments are performed in a transparent cylinder strongbox apparatus with internal dimensions of 800 mm diameter and deep enough to prevent any influence coming from the walls of the box. The properties of the pile models used in the laboratory tests are listed in Table 2.9. Various types of instruments such as LVDT's, strain gauges, and load cells are used to measure deflections, bending moments, and forces during the experiments.

Table 2.8. Soil Properties (Field Load Test).

Soil	**Upper Clay**	**Lower Clay**	**Silt**	**Residual Soil**	**Weathered Rock**	**Soft Rock**
Total Unit Weight, (kN/m^3)	17.5	17.5	17.8	17.8	20.2	20.5
N Value	1-3	4-7	12-19	44	50-10	100
Average Undrained Strength, c_u**(kPa)**	18	42	-	-	-	-
ϕ**(Deg)**	-	-	24	34	32	33
Plasticity Index PI(%)	25-30	30-35	35-40	-	-	-
Poisson's Ratio	0.3	0.3	0.3	0.3	0.25	0.25
OCR	0-2	1-2	<2	-	-	-

The authors [36] obtained the p-y curves by conducting lateral load tests through double differentiating the pile bending moment. When the parametric study of the relation of pile and soil rigidity is examined in the study, the authors mentioned that the study of Broms (1964) is related to the pile characteristics, β and pile length, L.

The pile diameter, D, flexural rigidity of the pile E_pI_p, and the modulus of subgrade reaction, K are primary variables interesting the pile characteristics. The equation, p indicates the soil resistance per unit length and z does the depth, is formulated as

$$\mathbf{p} = \frac{\mathbf{d^2M}}{\mathbf{dz^2}}. \tag{2.14}$$

In the study [36], after all the experiments and analyses were done, the forthcoming comments are deduced: $\sqrt{D}$ is much more fitted instead of D (the pile diameter), through calculating the modulus of subgrade reaction. Hence, it is needed to take into additional consideration for widely used methods calculating the subgrade reaction. Furthermore, the presented p-y curves in the study are quietly proper, corresponding to a pile-soil relationship for large diameter piles after the comparative studies. About the parametric study of the pile-soil rigidity, it is observed that the flexible piles are affected much more compared to rigid piles by the p-y curves. It is also recommended that the flexible piles should be designed more carefully because of the sensitivity against the distribution and magnitude of the p-y curves. In conclusion, when the pile and soil rigidity are closer to each other, the soil gets inclined to resist much more against the pile.

Table 2.9. Pile Properties (Laboratory Load Test).

Type	c_u **(kPa)**	**Load Type**	**Diameter (mm)**	**Pile Depth (mm)**	E_pI_p (Nm^2)	**Pile Tip Condition**
Short Pile	18	One-Way	32	400	4360	Free
Short Pile	42	One-Way	32	400	4360	Free
Long Pile	18	One-Way	32	650	4360	Free
Long Pile	42	One-Way	32	650	4360	Free

The study of Zhu et al. [37] recommends finding out new design criteria for flexible piles since the present specifications solely consider the rigid piles. It is mentioned in the study that large displacement is mobilized in piles. The study has been conducted by using large-scale lateral static load tests and three impact tests, where performed in

a soil apparatus with internal dimensions of 15 m x 5 m x 6 m, as shown in Figure 2.22. The soil used for the tests is composed of 80% silt, 12% sand, and clay size material for the rest. The soil is categorized as low plasticity silt, ML (according to ASTM, 2010) with the specific gravity which is 2.69. The soil is laid out in the apparatus layer by layer with 0.2 m thickness each one. The length, outer diameter, and thickness of the steel pipe piles used in the experiments are 4.5 m, 0.159 m, and 0.0045 m, respectively. The flexural rigidity for the piles has been calculated as 1.417 MN/m2.

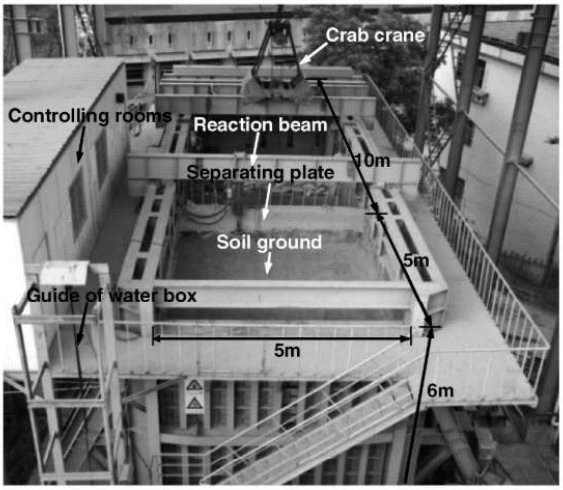


Figure 2.22. Soil Apparatus [37].

In the study [37], static and dynamic load pressures are observed around the pile; afterward, the p-y curves are obtained from the lateral load tests by differentiating the bending moment with the soil reaction along the pile length at different depths. Derived p-y curves beside the values corresponding to Reese et al. (1974) are shown in Figure 2.23. Constant damping coefficients are also suggested for the model. The authors deduce from the experiments that the drainage condition shows different behavior under static and dynamic loadings that results in that static soil stiffness is less than a dynamic one. Moreover, the coefficient of damping can be put to good use in p-y curves, and the damping of the soil and flexural rigidity of the pile has an important effect on the load/displacement relation of the pile. Hereby, the authors presented a dynamic analysis method considering the p-y curve model.

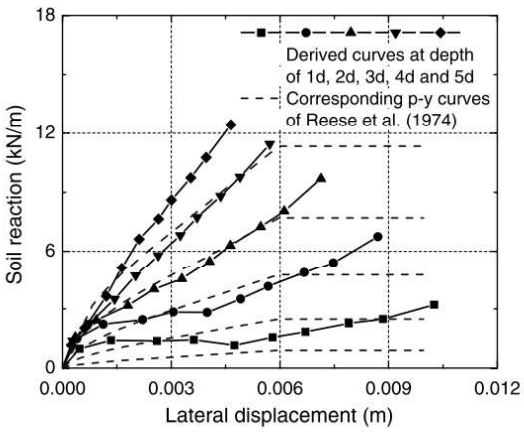


Figure 2.23. Derived p-y Curves at Depths [37].

The study of Kim et al. [38] focuses on detailing pile group interaction factors by preparing six types of pile group layouts (see in Figure 2.24) with various pile spacing values in the soils varied from loose to dense. A static fixed-head test model has been preferred in the study. The experiments are performed in a laboratory strongbox apparatus with internal dimensions of 0.8 m x 0.8 m x 0.6 m. The soil layer below the pile tip is kept six times the diameter of the pile to prevent any influence coming from the walls of the box. In the study, five factors are considered at different values: pile diameter, displacement, area, force, and flexural rigidity of piles. The length, outer diameter, and thickness of the piles used in the experiments are 250 mm, 12 mm, and 0.25 mm, respectively. The flexural rigidity for the piles, EI_p has been calculated as 45 GNm^2. The main characteristics of the soil used in the experiments are presented in Table 2.10. The sandy soil has been prepared at various relative densities of loose (27%), medium (50%), and dense (73%) conditions.

In the study [38], Kim et al. performed 50 pile group tests and gathered an enormous amount of data considering lateral load, lateral displacement, and shear forces on the piles. Figure 2.25 exhibits the correlation between the average load on the piles in each three-row which are lead, middle, and trail. Furthermore, the impact of different soil density values on the load-displacement relationship for the pile group

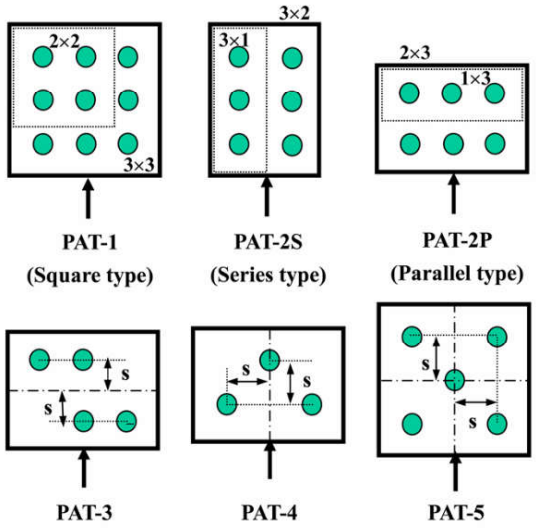


Figure 2.24. Pile Array Types (PAT's) [38].

Table 2.10. The Main Characteristics of The Soil.

Specific Gravity, G_s	2.67
Mean Particle Size, d_{50} **(mm)**	0.26
Uniform Coefficient, C_u	2.0
Curvature Coefficient, C_c	1.2
Maximum Void Ratio, e_{max}	1.19
Minimum Void Ratio, e_{min}	0.81
Peak Friction Angle, ϕ_{peak}	40 ($D_r = 73\%$) 35 ($D_r = 50\%$) 27 ($D_r = 27\%$)

is depicted in Figure 2.26.

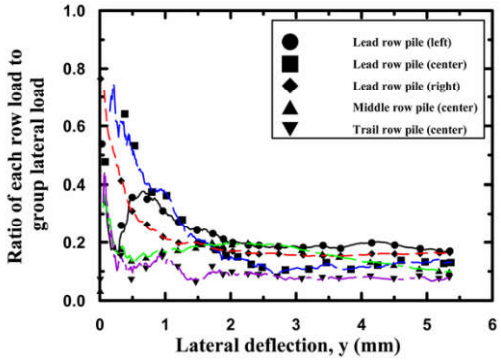


Figure 2.25. The Correlation Between The Average Load on The Piles in Each Three-row [38].

The authors [38] state that the pile group shows displacement two times more than the individual pile under the same conditions. It is deduced that the maximum load-carrying capacity of piles in each row in the pile group has dramatically dropped compared to the individual pile performance because of the group effect factor. It is also stated that the p-multiplier is dependent to pile group arrangement and pile spacing. The multiplier is fluctuating between 0.2 and 0.5 at various pile spacing values with different relative soil densities. The study carries out that the ratio between the pile spacing and pile diameter should be six times larger to eliminate pile group effects for loose/medium soil conditions. On the other hand, the ratio should be over eight times larger to eliminate the effect for medium/dense states. Beyond the ratios, as mentioned here, every single pile in the group behaves the same as an individual pile.

The study of Mohamedzein et al. [39] aims to detail the impact of variables like pile material, pile properties, and installation method by conducting laboratory lateral load tests on piles in plastic clay. The study also covers an extensive range of L/D ratios varied from 10 to 35. The experiments are performed in a laboratory strongbox apparatus made of 3 mm thick steel plates with internal dimensions of 1 m * 1.25 m * 1.4 m. As the soil used in the experiments, medium to highly plastic clay has

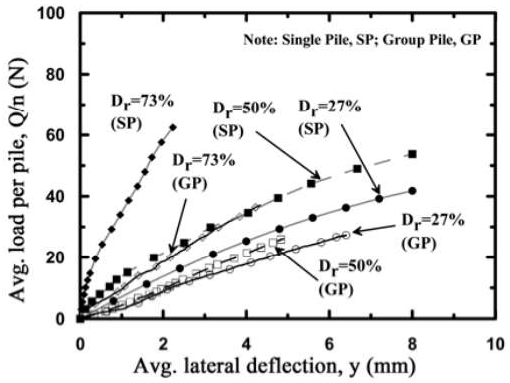


Figure 2.26. The Load-Deflection Response (3x3 Pile Group, 3d Pile Spacing) [38].

been preferred which the properties of the soil are presented in Table 2.11. As the pile materials used in the experiments, steel and concrete piles have been preferred since they are the most common materials used for piles. The concrete piles have length and diameter which are 500-1000 mm and 50-100 mm, respectively. The length, outer diameter, and thickness of the steel pipe piles are 580-1160 mm, 31-58 mm, and 1.1-1.5 mm, respectively. The soil placement has been done layer by layer of a thickness of 200 mm each one and prepared for needed density. Afterward, two installation methods are used in the study, bored and pre-installed methods.

Table 2.11. The Main Characteristics of The Soil.

LL, %	50
PL, %	25
Percentage Passing Sieve #200	97
Specific Gravity	2.6
Optimum Moisture Content, %	24.5
Curvature Coefficient, C_c	0.2704
Initial Young's modulus, kNm^{-2}	4600

The results in the study [39] have been stated in regards to the distribution of bending moments, load and displacement curves, and lastly the p-y curves. The

authors deduced from the experiment results that load-displacement curves show non-linear behavior, especially for large L/D ratios and large pile diameters. Larger L/D ratio and pile diameter mean an increment in the ultimate lateral capacity of piles and the maximum moment. The maximum bending moment is observed at a depth of around 0.13L to 0.32L. The p-y curves also have non-linear behavior, and the resistance of the soil increases as the depth increases. Furthermore, for the small pile diameters, it is found out that there is a considerable difference between the actual and experimental p-y curves. The difference is not observed for the larger pile diameters. At last, it is stated that greater soil resistance is ensured when bored installation method is used instead of the pre-installed method.

The study of Brown et al. [33] consists of a series of two-way cyclic lateral loading experiments conducted to a large-scale steel pipe pile group and an individual pile for a comparison. The experiments are performed on the campus of the University of Houston and the soil is medium-dense sand classified as SP by the USCS. The soil has an internal friction angle, ϕ of 38.5° for a dry density. The pile group used in the experiments comprises nine piles with an outer diameter of 273 mm and a thickness of 9.27 mm. The spacing between the piles is 3 times the diameter of a pile.

The results in the study [33] are presented as plots of pile deflection against the pile head load for each pile and each row in the group. It is concluded that the pile deflection of an individual one is relatively less compared to the pile group during a loading equal to the average per pile. The main factor behind the results is highlighted as the "shadowing" effect. The soil resistance in the trailing rows reduces sharply. When it is compared to the bending moment values, it is observed that the value is quite similar between the leading row and an individual pile. Furthermore, it is recommended that a constant, p_m which is indicating the drop in soil resistance because of group effect should be used to modify p-y curves.

The study of Ahmed Mufty [40] focuses on the effects of various pile stiffness and soil stiffness values how the skin resistance capacity of piles can be increased by using RSPile pile analysis software. The study also aims to find out that shorter piles can ensure an important cost-saving compared to long piles under acceptable conditions. In the test, three groups of a 15-pile group with a modulus of elasticity varying from very stiff to highly flexible were installed in a 3 x 5 configuration. The piles are spaced from outer wall-to-wall at a distance of 2 m. Three different soil conditions with a different range of stiffness having ultimate skin resistances (60 kPa, 90 kPa, and 120 kPa) have been used. Beyond the soil and piles, 18 boreholes are used to characterize the soil zones as exhibited in Figure 2.27.

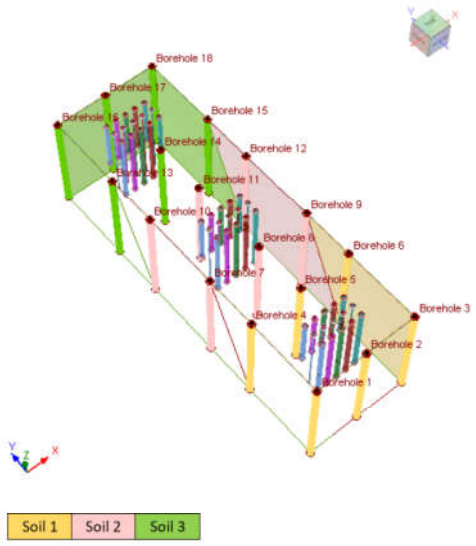


Figure 2.27. Piles and Boreholes [40].

The author [40] discussed the results regarding the behavior of the pile groups of various diameter, length, and rigidity values under three soil conditions. The key point in the study is to find out that how the skin resistance along the pile and settlement is influenced by various rigidities of piles. Afterward, it is deduced that if the pile is flexible, the effective length becomes shorter. Additionally, if the pile is long enough beyond the effective length, how much longer the pile has no impact on the skin resistance. It is also found out from the study that more skin resistance is ob-

served in the stiffer soil under the same conditions, and herewith, the effective length becomes shorter. Besides, the area is the major reason regarding the elastic shortening compared to the pile diameter.

The study of Fayyazi et al. [11] aims to investigate the effects of different pile spacings on the group factor for certain pile groups. In the study, a continuum model is used to simulate the response of pile groups by using Flac3D software. The test results of an existing full-scale, in-situ study of Christensen, 2006 [12] is used as a validation of the continuum model here. Steel piles with a 3 x 3 configuration are used in the experiments and the outer diameter of each pile is 0.324 m. The piles are spaced from center-to-center at a distance of 5.65D in the direction of loading and 3.29D in the perpendicular direction to the loading. The free-head model is used in the study. The properties of the soil, divided into eight layers and used in the model, are exhibited in Table 2.12. The moment of inertia, I for the six side-piles is $1.16x10^8$ mm^4 and $1.43x10^8$ mm^4 for the three middle-piles.

Table 2.12. Soil Properties.

Distance From Ground Surface (m)	**Unit Weight** (kN/m^3)	**Shear Modulus** (kN/m^2)	**Bulk Modulus** (kN/m^2)	**Friction Angle (Degree)**	**Cohesion** (kN/m^2)
0	16.7	29615	64166	40	0
2.1	16.7	15884	34416	40	0
2.4	19.1	7000	15166	0	41
2.7	19.1	7000	15166	0	50
3.7	19.1	8076	17500	0	40
4.6	18.1	17769	38500	38	0
6.3	19.1	6461	14000	0	57
8	16.7	22615	49000	33	0

In the continuum model used in the study [11], every pile in the group is subjected to equal displacement values from the head of piles. Total pile head forces are shown

in Figure 2.28 that is a comparison between in-situ experiments and the continuum model. Besides, p-multipliers are calculated for each row of the group, and the values are averagely found out as 1.01, 0.74, and 0.61, respectively. The study uses an average p-multiplier used for every single pile in the group instead of determining p-multipliers for every row. That average p-multiplier is named as the group factor. As a result, it is deduced that this study can be used as a basis for determining group factors for various cases. In the research, a specific group factor has been determined for a specific case, but in reality, it is predicted significant errors in calculating the maximum bending moments for trailing rows. Furthermore, the study showed that the measured and computed maximum bending moments for the leading row of a pile group are comparatively close to each other. Hence, it is recommended to use the group factor for designing and analyzing the pile groups.

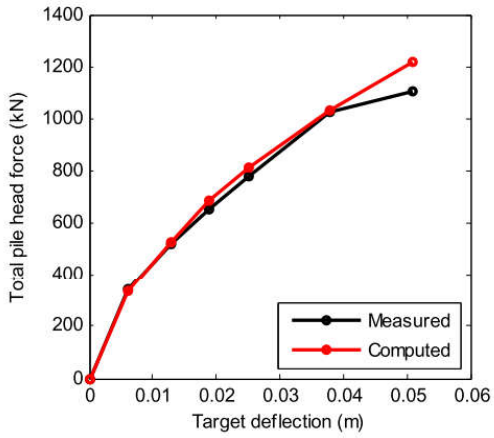


Figure 2.28. Total Pile Head Forces at Target Deflections [11].

The study of Abbas et al. [41] concentrates on detailing laterally loaded piles and their group behavior by using an analytical model which is a three-dimensional FEM. In the study, various pile spacing values are combined with different group configurations, and then the results are presented regarding the lateral displacement, lateral loading, and soil resistance. The diameter of each circular pile is 1.0 m with a length of 15 m. Two soil types are used in the study where both soil properties are listed in Table 2.13. As the pile spacings: 2D, 4D, 6D, and 8D are chosen with three types of configurations

which are 2 x 1 a single row order, 2 x 2 square order, 3 x 2 rectangular order. Each pile group is subjected to an equal lateral load of 450 kN.

Table 2.13. Soil Properties.

Parameter	**Unit**	**Cohesionless Soil**	**Cohesive Soil**
Unit Weight	kN/m^3	20.0	18.0
Young's Modulus	MPa	$1.3x10^4$	$1.0x10^4$
Poisson's Ratio	-	0.3	0.35
Cohesion Intercept	-	0.0	5.0
Angle of Internal Friction	-	30	25

The authors [41] compared the design equation with existing cases in order to validate the model. It is found out that the results are not satisfied for the leading row, but the first and second trailing rows. After evaluating the results, the following arguments are obtained: the lateral displacement for the individual pile is more than the value obtained from all pile groups. Due to the group effect, the lateral soil pressure is redistributed, and the lateral displacement per pile in the group increased. 6D pile spacing is observed as the critical limit; below the limit, large lateral displacements are observed under the loading. When the pile spacing is 6D and more, the individual pile and piles in the group have a reasonably close response in terms of pile deflection and observed soil pressure against the loading. Additionally, a p-multiplier is observed for each row and it is concluded that the p-multiplier of the leading row is always greater compared to the value for trailing rows. Besides, the soil types are analyzed, and the p-multiplier for the pile group in cohesive soil is almost less than the value for piles in cohesionless soil under the same conditions.

The study of McVay et al. [42] aims to observe the lateral response of laterally loaded pile groups at different pile spacing. Centrifuge tests are conducted on an individual pile and pile group which is installed in a 3 x 3 configuration. The piles are spaced from center-to-center at a distance of 3D and 5D during the tests. A load cell is used to measure the lateral load, and also an LVDT is used to measure the

deflections. All experiments are conducted with free-head pile conditions. The soil used in the study is categorized as SP in the USCS. The maximum unit weight of the soil is 16.74 kN/m^3 with an e_{min} of 0.55, and the minimum unit weight is found out as 13.59 kN/m^3 with an e_{max} of 0.91. In the tests, two relative densities of 33% and 55% are used. The centrifuge equipment is modeled at a 1/45 scale. The prototype piles modeled in the study are exhibited in Figure 2.29. It is also mentioned that the piles in a group should not be placed less than at a distance of 2D.

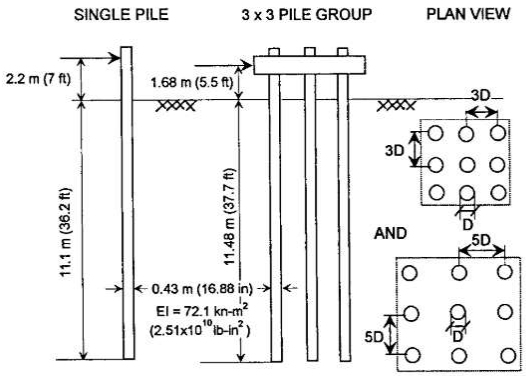


Figure 2.29. Single Pile and Free-Head Pile Group (3 x 3 Configuration) [42].

The authors [42] conducted several centrifuge tests and arrived at the following conclusions: soil density and pile spacing are the major factors regarding the shadowing factor in pile groups. The group efficiencies for 3D and 5D are observed as 0.74 and 0.94, respectively. The group distribution for the group pile at a 3D spacing from the leading row to the second trailing row is found as 45%, 32%, and 23% for very dense soil; 41%, 32%, and 27% for medium dense soil; and 37%, 33%, and 30% for medium loose soil. The same at 5D spacing is found as 36%, 33%, and 31% for medium dense soil; and 35%, 33%, and 31% for medium loose sands. As it is seen, the distribution does not fluctuate at 5D spacing. Triaxial compression tests are also conducted on the soil at different densities to reach p-y curves in the study. According to the test results, the multipliers for p-y curves at a 3D spacing from the leading row to the second trailing row are found as 0.8. 0.4, and 0.3 for very dense and medium dense soils; and 0.65, 0.45, and 0.35 for medium loose soil. The multipliers at 5D spacing are

1.0, 0.85, and 1.70 for the medium dense and loose soils.

The study of Laman et al. [44] concerns the behavior of short rigid piles subjected to lateral load and the behavior of granular soil by conducting experimental and numerical analyses. In the study, different testing methods are used to have a comprehensive comparison of the lateral capacity of model piles placed in granular soil, which is categorized as poorly graded sand. The soil properties used in the tests are listed in Table 2.14. The experiments are performed in a steel strongbox apparatus with internal dimensions of 960 mm x 800 mm x 500 mm. The length and diameter of the circular model piles used in the experiments are 200 mm and 50 mm, respectively. Moreover, Young's modulus and L/D ratio of the model pile are given as 210000 MPa and 4, respectively.

Table 2.14. Soil Properties.

D_{10}	c_u	c_c	$\gamma_{dry,loose}$	$\gamma_{dry,dense}$	ϕ_{loose}	ϕ_{dense}
0.18	2.78	1.0	15.3	17.06	38°	44°

In the study [44], after all the experiments and analyses were done, the following comments are deduced. When the experiments conducted on laterally loaded piles placed in dense and loose soils are compared, the lateral capacity of the model pile is observed five times higher in tests performed in dense soil. It is also observed that the lateral capacity of the pile model is related to the thickness of the upper loose soil layer. As the thickness of the layer increases, a drop in the lateral capacity of the pile is obtained. Furthermore, the sand with the value of higher dilatancy is mobilized much more through the lateral movement in the tests. Hence, increment in the lateral capacity of the model piles is observed with the values of higher dilatancy of the soil.

The study of Laman et al. [45] aims to detail the impact of variables like Young's modulus of granular soil, pile properties, L/D ratio, and eccentricity of loading by conducting numerical analysis on short piles in sandy soil. Loose and dense state sandy soils have been preferred in the analyses, and the properties of the soils are

presented in Table 2.15. Concrete piles have been used in the analyses, and properties of the pile are presented in Table 2.16.

Table 2.15. Soil Properties.

Parameters	**Loose Sand**	**Dense Sand**
ϕ_{peak}	39°	49°
Cohesion (kN/m^2)	0.25	0.25
Unit Weight (kN/m^3)	14.40	16.40
Dilation Angle	9°	19°
Young's Modulus (kN/m^2)	11397	35913
Poisson's Ratio	0.30	0.30

Table 2.16. Pile Properties.

Diameter (m)	**Length (m)**	**Material**	$E_p(kN/m^2)$	γ_{pile} (kN/m^3)
1	3	Concrete	$30x10^6$	24

The results in the study [45] have been stated in regards to the comparison of the lateral capacity of short piles between the present design methods and 3-D non-linear FEM. Figure 2.30 exhibits the correlation between the lateral load and displacement for loose and dense state soils. Furthermore, the impact of different soil density values on the distribution of the lateral effective stresses with depth is depicted in Figure 2.31. The authors deduced from the results that the relative density of the granular soils has a significant effect on the lateral load and moment capacity of the piles, and higher lateral capacity values are obtained when the soil is compacted to a dense state. Cross-section of the pile is also an important parameter that higher lateral load and moment capacity values are obtained with a square cross-section instead of that pile with a circular cross-section. Pile diameter and L/D ratio are also main parameters having an impact on the lateral capacities of the piles. An increment in pile diameter and pile length provides higher lateral capacities. This is because an increment is observed in the passive pressure.

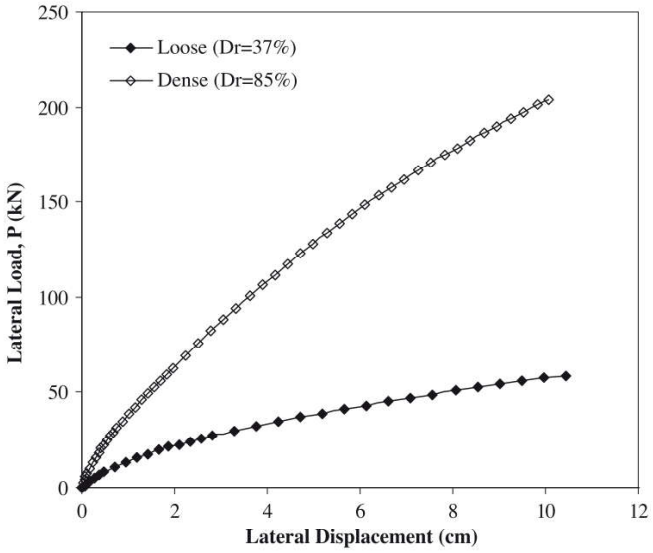


Figure 2.30. Lateral Load and Displacement for Loose and Dense State Soils [45].

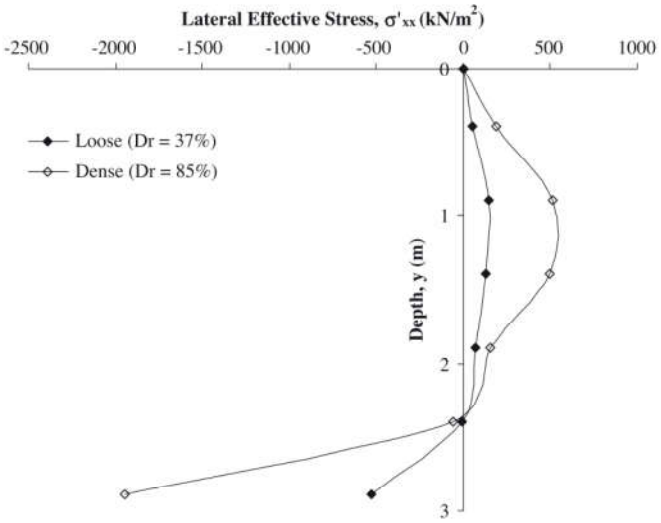


Figure 2.31. Distribution of the Lateral Effective Stresses with Depth [45].

2.4. Review of Related Studies Done at Boğaziçi University Karl Terzaghi Soil Mechanics and Geotechnical Engineering Laboratory

A new pile system called a segmental pile with variable flexural rigidity (SPVFR) is developed at Boğaziçi University Karl Terzaghi Soil Mechanics and Geotechnical Engineering Laboratory. The segmental pile system consists of mortar blocks and rubber material; and afterward, the components are linked together with a steel cable. The flexural rigidity of the segmental pile can be adjusted by increasing or decreasing the post-tension on the steel cable. Through the laboratory experiments, it is observed that the lateral capacity of the segmental piles can be sustained at large displacement. The view of the pile system is given in Figure 2.32. Table 2.17 exhibits a summary of the previous related studies. A brief review of previous related studies is presented below.

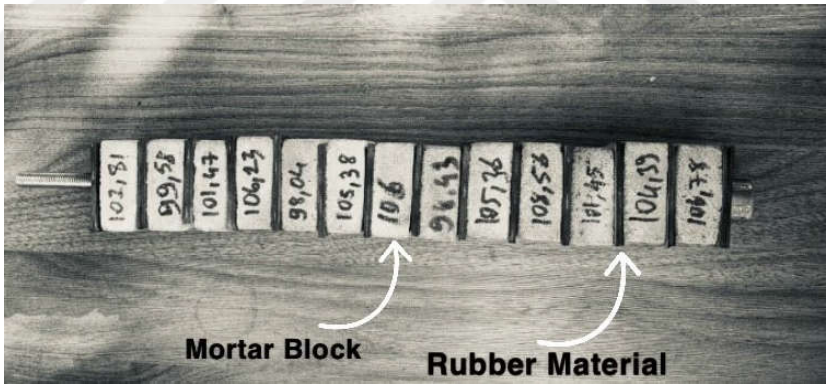


Figure 2.32. Segmental Pile with Variable Flexural Rigidity.

The study of Yahia et al. [46] focuses on the behavior of the pile model subjected to horizontal loading. For that purpose, the pile model is placed on manufactured elastic springs. Then, the behavior of the pile model is partially modeled and observed in sandy soil with various relative densities. Different flexural rigidity values are obtained for the pile model by applying post-tension forces (750 N, 1500 N, and 2250 N) on the steel cable; afterward, the load-displacement curves for the pile model are determined by conducting three-point bending tests. All other experiments for the pile model are conducted by placing it on the elastic springs (Figure 2.33). Static and cyclic loads are

Table 2.17. Test Conditions and Notes for the Previous Studies.

Reference	**Number of Mortar Block**	**Length (m)**	**L/D**	**Piles Post-Tensioned with (N)**	**Keywords**
Yahia [46]	15	0.35	7	750 1500 2250	Behavior of Segmental Pile with Adjustable Rigidity and Prescale Films
Sengez [47]	13	0.34	6.8	750 1500 2250	Lateral Capacity of Segmental Piles under Cyclic Loading
Keklik [48]	12	0.32	6.4	750 2250	Lateral Capacity of Segmental Piles under Static Loading and Inclinations of Piles
Ozturk [49]	14	0.325	6.5	750	Stress and Displacement Measurement for Geotechnical Modelling Using Open Platform

applied to the pile model at both the top and middle points with a maximum displacement of 4 mm (equals to 8% of the pile model diameter); afterward, the lateral load and displacement values are recorded. The p-y curves are obtained through the records. The behavior of the pile model, which has a post-tension of 2250 N, is observed during the loading process. Moreover, the pre-scale films are placed between mortar blocks and rubber material to obtain the contact stress maps during the loading.



Figure 2.33. Segmental Pile System Prepared for Winkler Tests [46].

At last, it is concluded in the study [46] that the segmental pile model can be manufactured in the laboratory; and then the flexural rigidity of the pile model can be adjusted by changing the post-tension on the steel wire. Figure 2.34 exhibits the p-y curves of the segmental pile system placed on elastic springs 1K-2K-3K/static load, respectively. In the comparison of cyclic and static loadings, it is observed that the lateral capacity of the pile model slightly decreases under cyclic loading. In any case, the elastic springs used in the experiments limit the comprehension of the study, and the results may not represent the expected behavior of the actual soil under cyclic loading. The pile model has the capability to sustain its lateral capacity at the maximum displacement (with 600 cycles applied for cyclic loading) without failure. Furthermore, the results of the moment distribution obtained from the load-displacement values and pre-scale films have a similar trend. However, it is observed that the magnitude of the moment values obtained from the pre-scale films are two times higher compared to the other calculation. The study proves that the use of pre-scale films is a repeatable and reliable method that is to obtain the contact stress maps and measure the stress distri-

bution between mortar block and rubber material. The pre-scale technique contributes to the laboratory study with back calculating the bending moments.

The study of Sengez et al. [47] aims to investigate the behavior of the segmental pile model under cyclic loading, which is applied by using stress-controlled pneumatic muscles. In the study, three-point bending, oedometer, and large-scale model pile tests are conducted. Pre-scale films are used in this study too. The manufactured segmental piles consist of 13 mortar blocks and 12 rubber materials placed between mortar blocks. The pile length is 34 cm, and the length / pile diameter ratio is less than 10. The steel cable is post-tensioned with the forces of 750 N, 1500 N, and 2250 N to adjust the flexural rigidity of the segmental pile. Subsequently, the model pile is embedded into the coarse sand with various relative density values (loose, medium dense, and dense states). In this way, an opportunity reveals to investigate various pile-soil modulus ratios; afterward, the impact of the elasticity modulus ratio (E_{pile} / E_{soil}) on the segmental pile model is observed. During the experiments, the lateral displacements on the pile in depth are measured with LVDT's placed at five different points.

In the study [47], after all the experiments are done, the following comments are deduced: due to the increase in the relative density of the soil, a decrease in the corresponding displacement values of the non-continuous pile system is observed. In addition, a similarity in the corresponding displacement values of the non-continuous pile system post-tensioned with 750 N and 1500 N is observed. Another similarity is also observed for the mortal beam and piles post-tensioned with 2250 N. Although the difference in displacement values between the pile models post-tensioned with forces of 750 N and 1500 N is considerably small, the displacement value of the pile model post-tensioned with forces of 2250 N can be easily distinguished from the other two piles. An increment in the number of cycles on loading also increases the corresponding displacement values measured of the segmental piles. Through the experiments conducted within the scope of the study, the pile-soil modulus ratio, E_{pile} / E_{soil} varies in the range of 6 and 36. The displacement values, along the segmental piles placed in

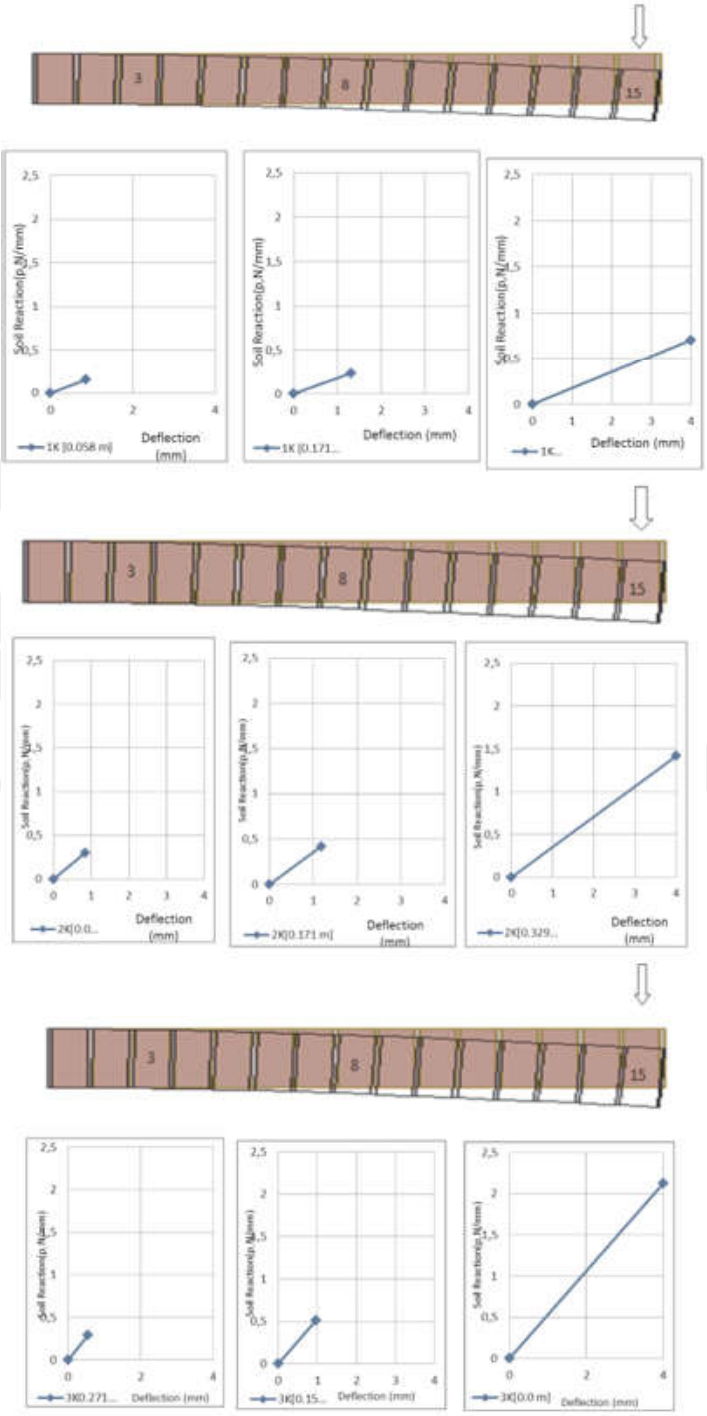


Figure 2.34. P-y Curves of the Segmental Pile System Placed on Elastic Springs 1K-2K-3K-Static Load [46].

loose, medium dense, and dense state soils, are shown in Figure 2.35, Figure 2.36, and figure 2.37, respectively.

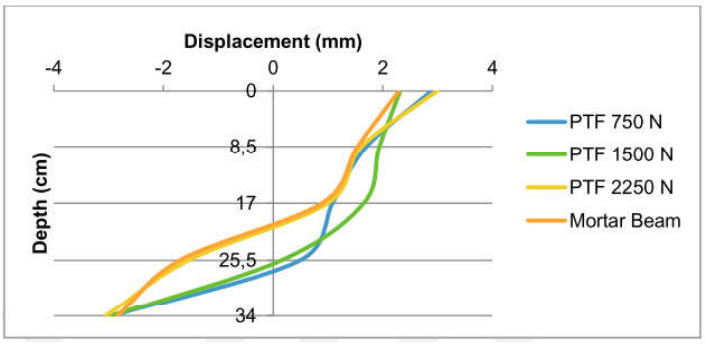


Figure 2.35. Displacement Values for the Piles Placed in Loose Soil [47].

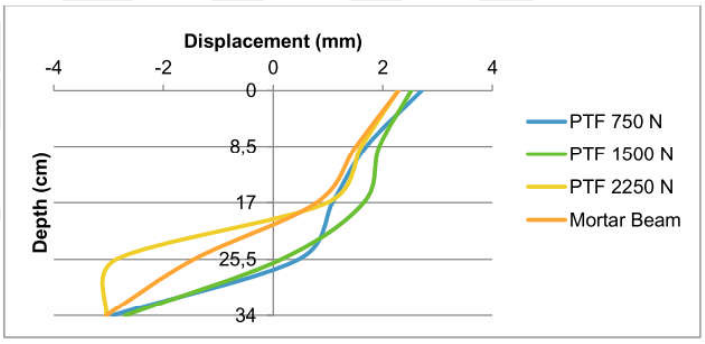


Figure 2.36. Displacement Values for the Pile Placed in Medium Dense Soil [47].

The study of Keklik et al. [48] consists of a series of large-scale, constant-contact area direct shear experiments conducted to the segmental pile model. The study aims to observe the impact of the change in the flexural rigidity of piles when they are laterally loaded. The manufactured segmental piles consist of 12 mortar blocks and 11 rubber materials placed between mortar blocks. The pile length is 32 cm, and the length / pile diameter ratio is less than 10. The soil used for the tests is unsaturated-coarse sand prepared at loose and medium dense conditions. A constant rate of displacement is applied to the pile cap, and the corresponding lateral force is measured with a load cell. In the large-displacement direct shear experiments, Arduino boards and magnetometers are preferred to obtain lateral displacements along with the segmental pile.

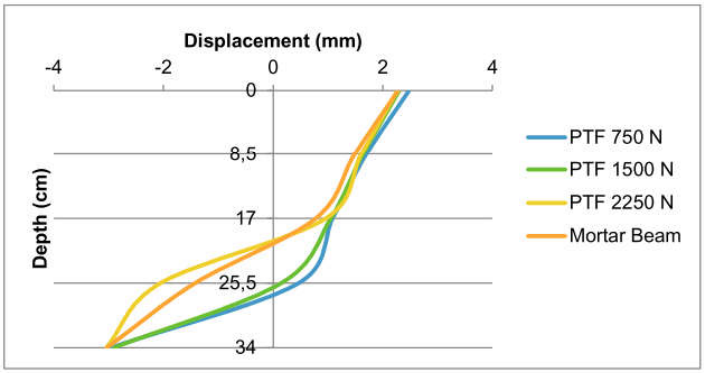


Figure 2.37. Displacement Values for the Pile Placed in Dense Soil [47].

It is concluded in the study [48] that the segmental pile model has the capability to reach larger displacement values without failure compared to conventional pile systems. It is also observed that the flexural rigidity of the pile has a straight impact on the bending behavior and the lateral capacity of the laterally loaded segmental pile. The lateral displacement of up to 50 mm is conducted with strain control, and the loading rate is 1 mm per minute in the lateral direction from the pile cap level. The load-displacement curves obtained for the segmental piles, post-tensioned with forces of 750 N and 2250 N, placed in loose and medium dense soils are shown in Figure 2.38. Moreover, the positions of the segmental piles, post-tensioned with forces of 750 N and 2250 N, after the tests are shown in Figure 2.39 and Figure 2.40, respectively..

The study of Ozturk et al. [49] aims to observe various stress and deflection measurement methods and devices in laboratory experiments. In the study, magnetometers, pre-scaled films, gyroscopes, and accelerometers are used to measure the deflection and stress values during the tests. Pre-scale films and required sensors are placed on the segmental pile system, which is embedded in the test apparatus. The manufactured segmental piles consist of 14 mortar blocks and 13 rubber materials placed between mortar blocks. The pile length is 32.5 cm, and the length/pile diameter ratio is 6.5. The soil used for the tests is poorly graded sand prepared at a loose state.

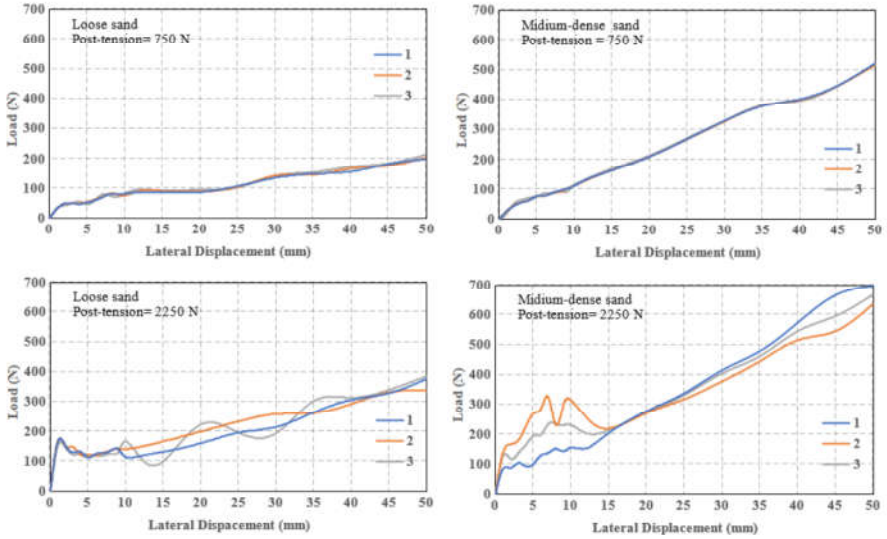


Figure 2.38. Load-Displacement Curves for Segmental Pile Model [48].

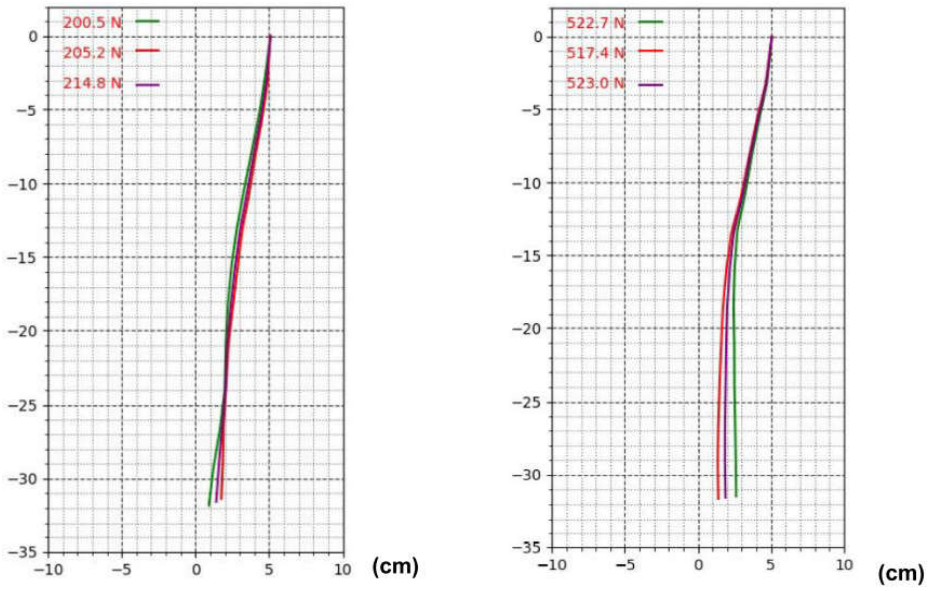


Figure 2.39. 750N Pile in a) Loose Sand b) Medium Dense Sand (x-axis displacement, y-axis depth) [48].

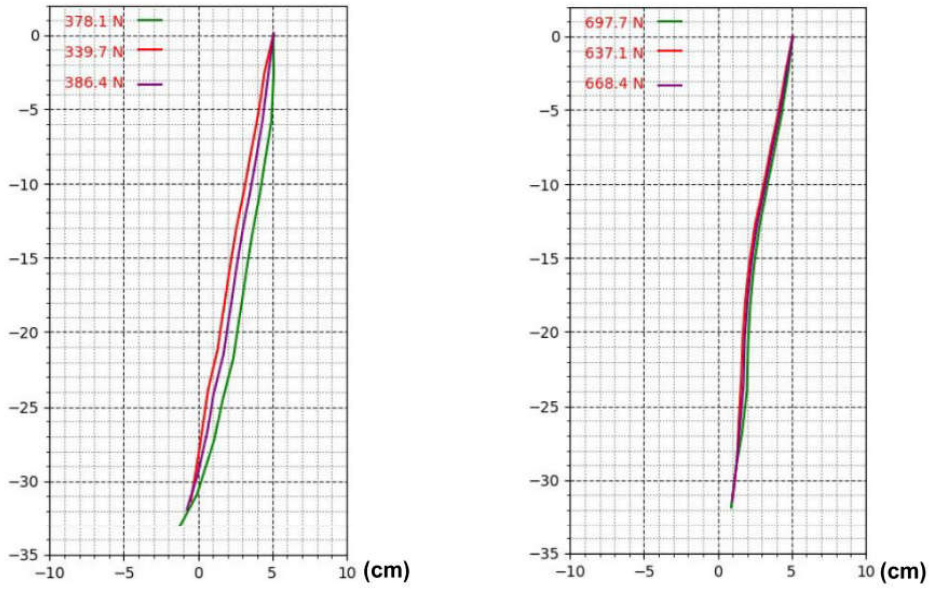


Figure 2.40. 2250N Pile in a) Loose Sand b) Medium Dense Sand (x-axis displacement, y-axis depth) [48].

The author [49] conducted several tests and arrived at the following conclusions: magnetometers, accelerometers, and gyroscopes are available to determine the deflection of piles (Figure 2.41). This technique can be used if the error range is limited to a tolerable level. In addition, a pressure transducer is adjusted to be used as embedded in the soil during the experiments. It is also seen that this technique is available to measure the stress values in the soil, but multiple repetitions of experiments are required. Moreover, pre-scaled films can be used to measure the stress in the soil, and the stress distribution is successfully obtained by using this method. However, they are produced to be used in between smooth surfaces. Therefore, the stress value measured is higher than it is expected.

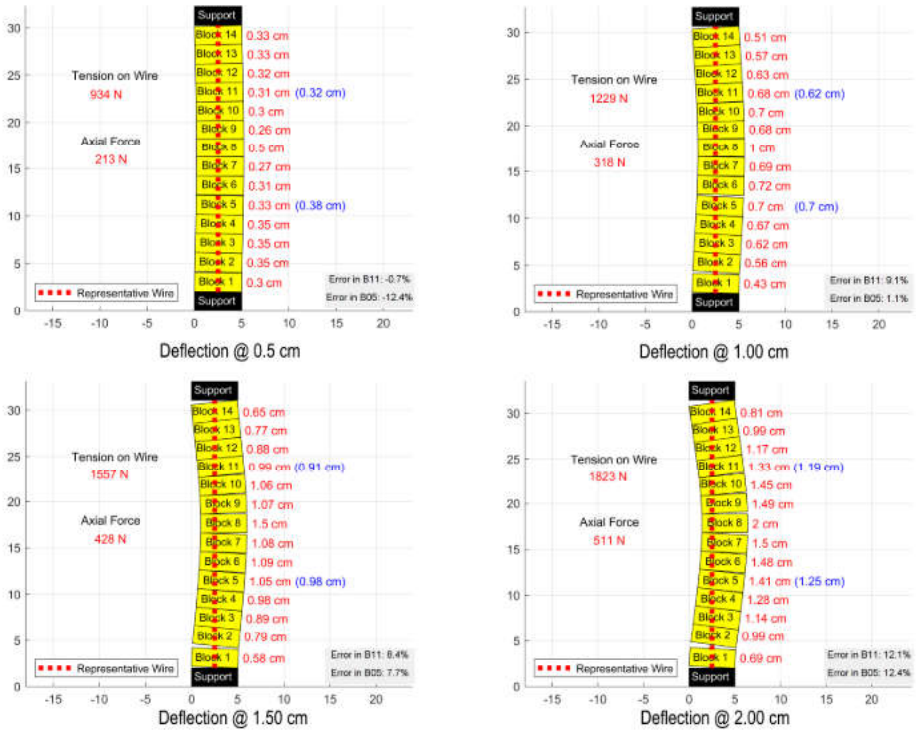


Figure 2.41. Estimation of Deflection in Blocks [49].

3. METHODOLOGY

3.1. Soil Material and Soil Placement

The soil material used in the study is classified as poorly graded sand, SP according to ASTM D2487 [50]. The sand is obtained from Akpinar, Istanbul. The grain size distribution of the sand is exhibited in Figure 3.1. The sieve analysis method is conducted through ASTM D6913 [51]. The properties of the sand and related standards are presented in Table 3.1.

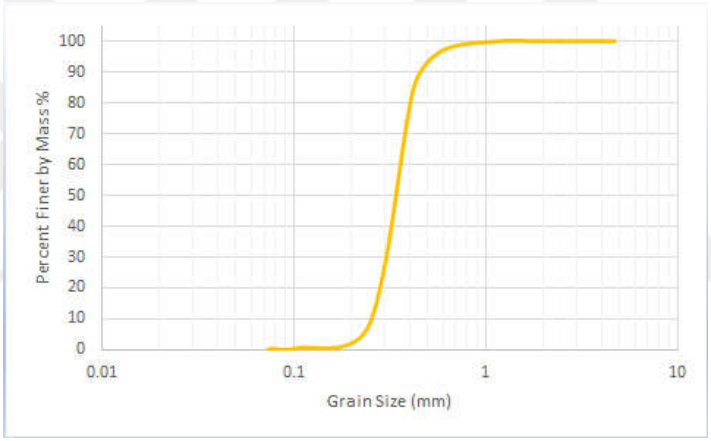


Figure 3.1. Grain Size Distribution.

The soil is placed in layers into the test apparatus. The thickness of each layer is 50 mm, and the soil is compacted through the required density. The soil is manually compacted layer by layer by using a burden. In the study, the goal is to compact the soil at different relative densities, which are loose (30%), medium dense (50%), and dense (65%) states. Relative density is calculated in equation (3.1) given as

$$\mathbf{D_r} = \frac{\mathbf{e_{max}} - \mathbf{e}}{\mathbf{e_{max}} - \mathbf{e_{min}}}.\mathbf{100}(\%). \tag{3.1}$$

Table 3.1. Soil Properties.

Property	**Value**	**Standards**
Specific Gravity	2.63	ASTM D854 [52]
Maximum Void Ratio, e_{max}	0.80	ASTM D4253 [53]
Minimum Void Ratio, e_{min}	0.47	ASTM D4253 [53]
D_{10}	0.27	ASTM D6913 [51]
D_{50}	0.32	ASTM D6913 [51]
Coefficient of Curvature, c_c	0.96	ASTM D6913 [51]
Uniformity Coefficient, c_u	1.24	ASTM D6913 [51]
Maximum Unit Weight, γ_{max} (kN/m^3)	17.9	ASTM D4253 [53]
Minimum Unit Weight, γ_{min} (kN/m^3)	15.1	ASTM D4253 [53]
Internal Friction Angle, $\phi_{avg.}$ $(^\circ)$	38.3	ASTM D3080 [54]

Figure 3.2, Figure 3.3, and Figure 3.4 exhibit shear stress - horizontal displacement and vertical displacement - horizontal displacement curves for loose state, medium dense state, and dense state soils, respectively.

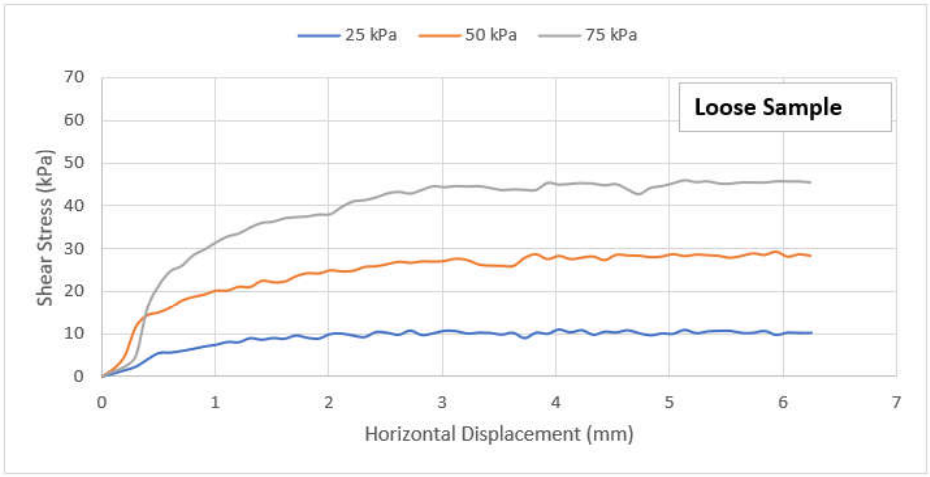
Through the tests performed, the peak and residual internal friction angles are given in Table 3.2.

Table 3.2. Peak and Residual Internal Friction Angles for Sand.

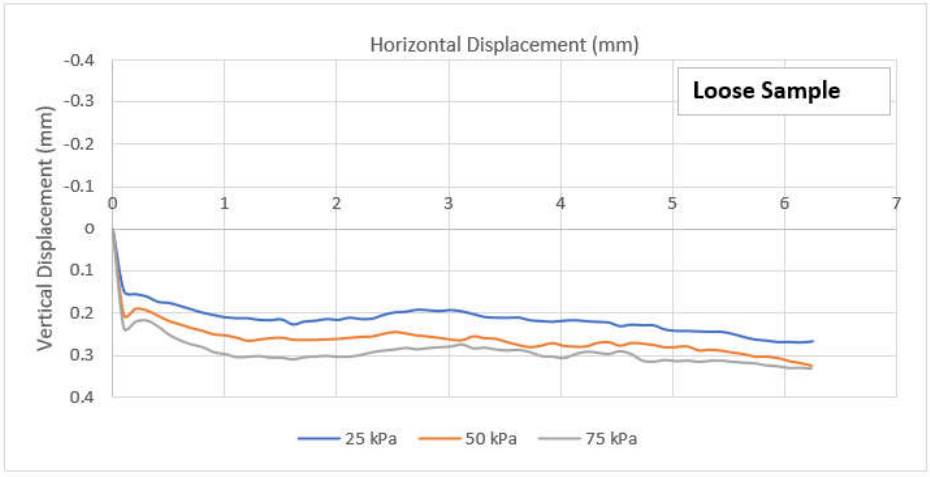
Internal Friction Angle	**Loose**	**Medium Dense**	**Dense**
ϕ_{peak}	30.02	34.45	36.89
$\phi_{residual}$	29.18	31.20	31.45

3.2. Pile Material

A pile group with continuous piles, which are widely used in literature, is preferred in the study. The piles are designed to have adjustable rigidities. The piles used in the study are made of fire hoses which can be pressurized to different rigidities

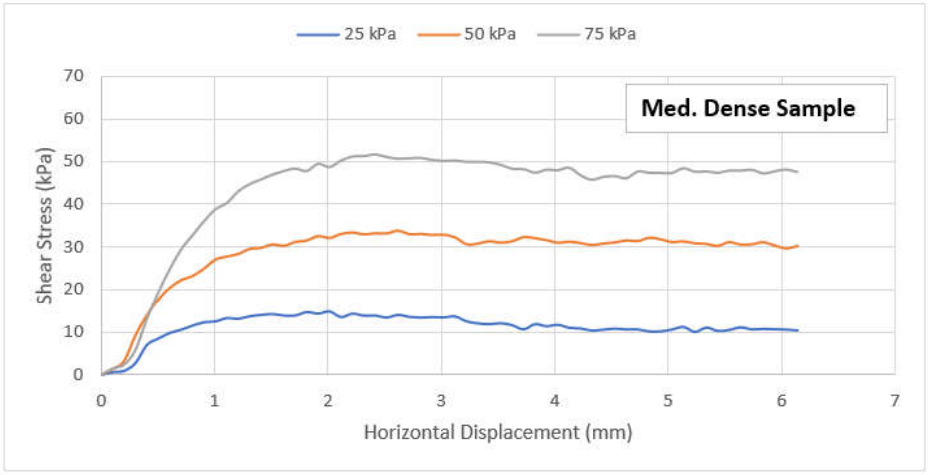


(a)

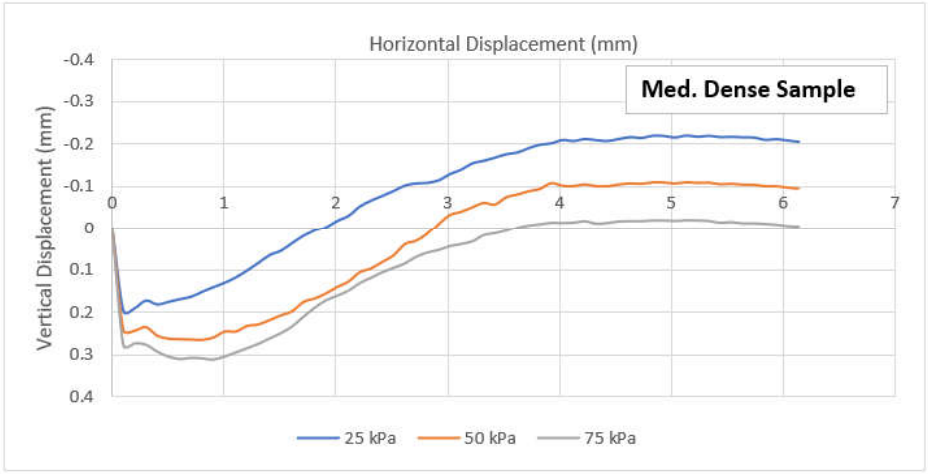


(b)

Figure 3.2. a) Shear Stress - Horizontal Displacement b) Vertical Displacement - Horizontal Displacement Curves For Loose Soil.

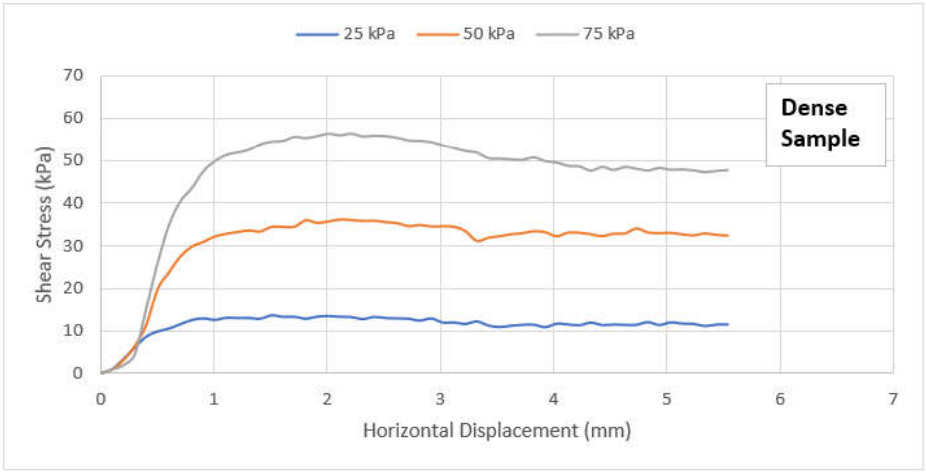


(a)

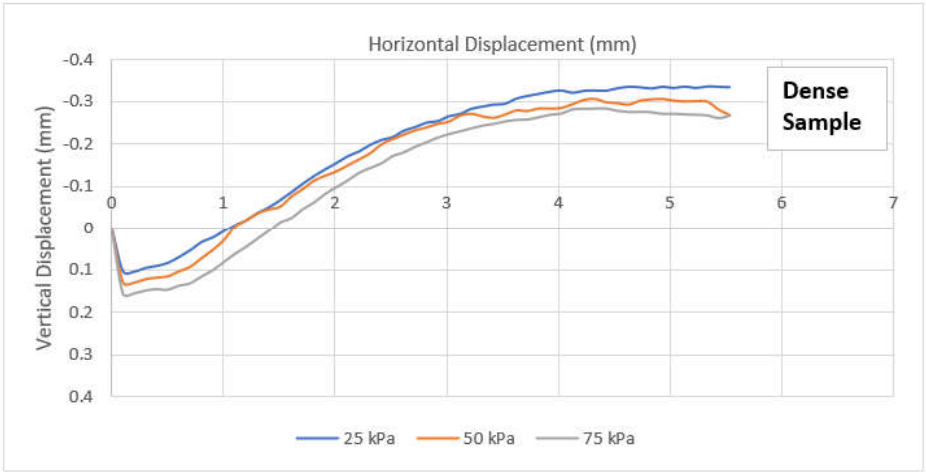


(b)

Figure 3.3. a) Shear Stress - Horizontal Displacement b) Vertical Displacement - Horizontal Displacement Curves For Medium Dense Soil.



(a)



(b)

Figure 3.4. a) Shear Stress - Horizontal Displacement b) Vertical Displacement - Horizontal Displacement Curves For Dense Soil.

by controlling the water pressure inside the piles. A single continuous pile and nine continuous piles with a 3 x 3 configuration are used in the experiments. The outer diameter and length of each pile are 35 mm and 340 mm, respectively. The piles are spaced from center-to-center at a distance of 2.4D in both straight and perpendicular directions to the loading. The equipment of the pile group system is detailed below.

- Fire hoses as piles: Fire hoses are used for designing piles because the flexural rigidity of the material can be easily adjusted with the water pressure inside. Fire hoses are used as confined rubber cylinders in the study. The idea behind using a fire hose as a continuous pile is that the material is resisted up to 50 bar pressure and connection fittings are quite accessible and economical. The piles are pressurized to 500, 1000, and 1500 kPa during the tests in the study. The thickness of the material is 2 mm. The tip of each pile is closed with pipe couplings. The view of the piles made of fire hoses is given in Figure 3.5.



Figure 3.5. Fire Hoses as Piles.

- Water pump: The pressure pump system is shown in Figure 3.6. The required pressure is transferred to the pile group with the pumping lever (1) and pump. When the specified test pressure is reached, the valve (4) is closed. The pressure is monitored by the gauge (6) having a precision scale with three measuring units, which are bar, psi, and MPa. The maximum pressure range of the pump is 0-50 bar.

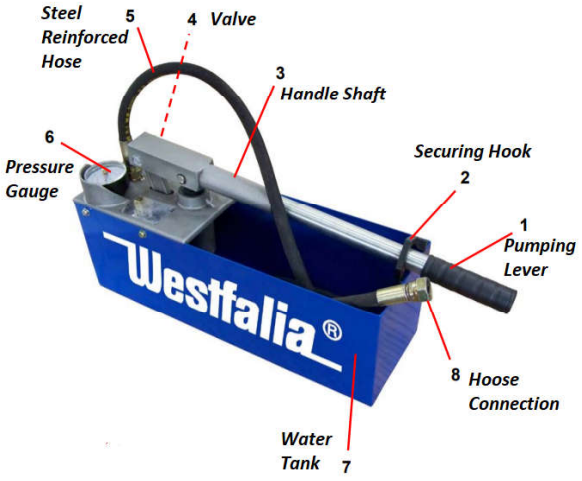


Figure 3.6. Water Pump.

- Water distribution hoses: The hoses are designed for transferring the water from the water tank to the piles. Hoses equally distribute the water to the piles, so each pile is pressurized to the same rigidity. The steel-reinforced hoses are strong enough to withstand high amounts of pressure. The hoses are shown in Figure 3.7.



Figure 3.7. Water Distribution Hoses.

- Pile cap plate: The pile cap plate is made of steel and designed to keep the pile group in order. The pile cap plate restrains all the deflection and rotation at the head of piles. Therefore, the pile group head used in the study is called a fixed-

head. The laterally loaded pile group experiments are performed with fixed-head pile head conditions. Figure 3.8 shows the pile cap plate used in the study.



Figure 3.8. Pile Cap Plate.

- Additional wearing layer: The same material with the fire hose is used as a wearing layer. The thickness of the wearing layer is 2 mm. In the study, both single and double wearing layers are tested. The point of using an additional layer is to increase the thickness of each pile. With increasing the thickness, it is aimed to reach a higher amount of moment of inertia values for pipe piles. Hence, the bending stiffness of the pile with the additional wearing layer is increased, and more rigid piles are obtained. The wearing layer is fixed to the piles with clamps. Figure 3.9 exhibits the piles after the wearing process.

- Clamps: Worm drive clamps, shown in Figure 3.10, are used for fixing the additional wearing layer onto the piles. The clamps ensure a high clamping force with low tightening torque. The product is light and compact enough to minimize the potential effects caused by the clamp during the tests. The clamps are only used for fixing the wearing layer, not for adjusting the pile rigidity. The width and thickness of a clamp is 13.5 mm and 0.6 mm, respectively. Twelve clamps are spaced with an equal interval of 15 mm along with the pile. Figure 3.11 shows the pile group system with all equipment during a test.



Figure 3.9. Additional Wearing Layer.



Figure 3.10. Clamps.

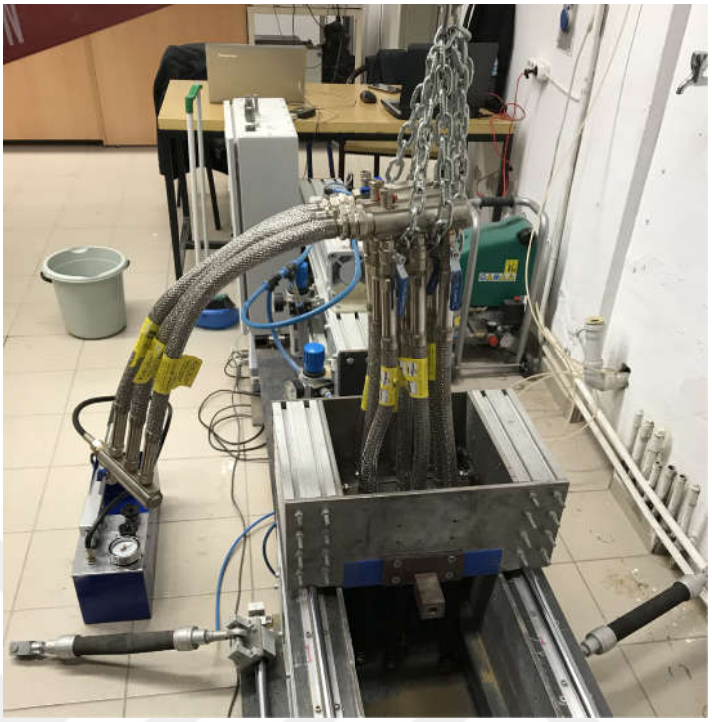


Figure 3.11. Pile Group System.

3.3. Test Setup and Instrumentations

The developed large-size model pile test device, designed and manufactured by Baykal, G. 2015 [55] and Baykal G. 2016 [56], [57], has been used during the laterally loaded pile group tests at large displacement. The view of the test apparatus used in the study and related sections of the apparatus is given in Figure 3.12. The sections are enumerated in the figure; afterward briefly detailed below [58].

- The first section comprises an antagonistic loading system than can run independently. The system applies cyclic loads by using stress-controlled pneumatic muscles. In the study, this part of the test device is not used.
- The second section consists of the upper box with internal dimensions of 300 mm length, 200 mm height, and 300 mm width. The upper box moves forward and backward over the lower box. Aluminum beams are fastened to both sides of the upper box to convey the static and cyclic lateral loads generated by the first and



Figure 3.12. Large-Size Model Pile Test Device.

fourth sections. The pile cap plate is placed into the upper box during lateral loading tests.

- The third section consists of the lower box with internal dimensions of 900 mm length, 400 mm height, and 300 mm width. The height of the box is adjustable between 200 mm and 400 mm. The length of the lower box creates the opportunity for model pile tests at large displacement. The piles (Figure 3.13) are embedded into the lower box where is filled with the soil afterward. Then, the soil is compacted to the required density in the box.
- The fourth section comprises a linear actuator with a stepper motor used for generating both static and cyclic lateral loads. The actuator can apply 167 kPa shear force to the upper part of the apparatus. This section is controlled by software providing controls over the frequency of the static and cyclic loads, displacement rate, and the direction of the horizontal loads. In the study, this section of the device is used. Static lateral load, 1 mm per minute, is applied to the pile head plate. Lateral displacement of up to 50 mm (143% of pile diameter) is conducted to pile heads through tests.

The other use of the test apparatus is also possible, such as the application of normal loads provided with pneumatic muscles. The muscles are tied with the beams on both sides of the upper box moving along the lateral loads. The normal load is applied through the upper box. In the case of a single 40 mm diameter muscle, 6.5 kN force can be developed. Besides, S-type load cells are placed at the specified locations in order to measure the applied loads. Each load cell has a capacity of 20 kN. A laboratory portable jib crane is used to hang the entire pile group system, as exhibited in Figure 3.14. The advantage of the crane is to keep the pile system stable during the experiments. The crane is quite useful in the tests because of its being-portable, and it synchronously moves together with the lateral loads.

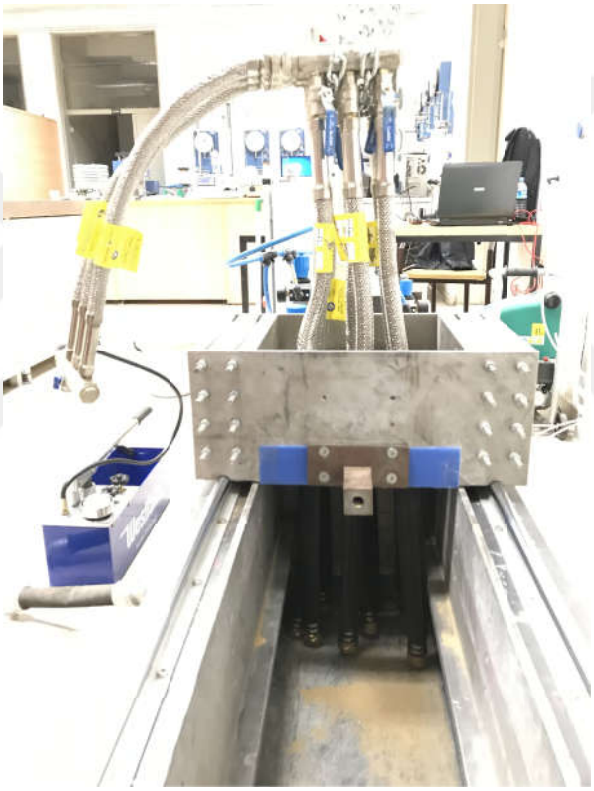


Figure 3.13. Embedded Piles into the Lower Box.



Figure 3.14. Portable Jib Crane and Pile Group System.

3.4. Testing Program and Conditions

3.4.1. Three-Point Bending Test

The flexural properties of the piles pressurized to different rigidities are determined through the specifications in ASTM D790 - 17 [59]. The testing program covering the determination of flexural property of the material is presented below:

- A bar of circular cross-section is placed on two supports. Afterward, a loading rod midway between the support applies a force through the material. The view of the testing program is given in Figure 3.15.
- A single fire-hose pile is pressurized to 500, 1000, and 1500 kPa, respectively. The test is conducted for each pile at different rigidity.
- The tests also cover the cases below:
  (i) The pile without a wearing layer: The material with 500-kPa, 1000-kPa, and 1500-kPa pressure is deflected until the strain of 90%, 62%, and 42% is reached, respectively.
  (ii) The pile with a single wearing layer: The material with 500-kPa, 1000-kPa, and 1500-kPa pressure is deflected until the strain of 86%, 74%, and 59% is reached, respectively.
  (iii) The pile with double wearing layers: The material with 500-kPa, 1000-kPa, and 1500-kPa pressure is deflected until the strain of 85%, 69%, and 58% is reached, respectively.
- The point of conducting the test for each case is to figure out the effectiveness of the wearing layer on the flexural rigidity of piles. The testing program is listed in Table 3.3.

- An appropriately calibrated testing device conducts a constant rate of crosshead loading through the distance decided.
- A strain rate of 1 mm/min is preferred in the study.
- Required security measures are taken into account during the deflection process

Table 3.3. Three-Point Bending Test Program.

Test Number	**Number of the Wearing Layer**	**Piles Pressurized to (kPa)**
#1 - #2 - #3	-	500 - 1000 - 1500
#4 - #5 - #6	1	500 - 1000 - 1500
#7 - #8 - #9	2	500 - 1000 - 1500

in the tests.

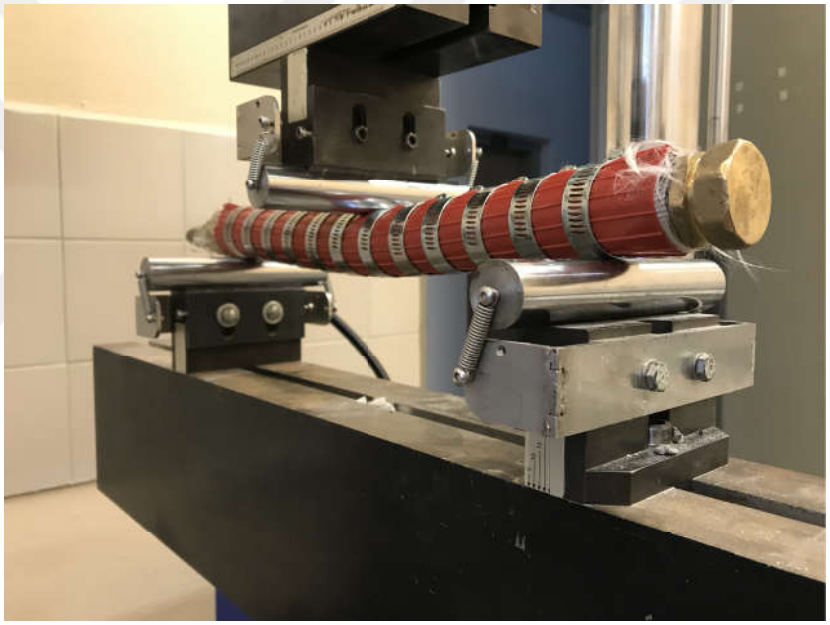


Figure 3.15. Three-Point Bending Test Device.

3.4.2. Oedometer Test

The elastic modulus of the soil used in the study is determined through the specifications in ASTM D2435 - D2435M - 11 (2020) [60]. The testing program covering the determination of one-dimensional consolidation properties of the soil is presented below:

- The specimen is prepared at different relative densities such as loose, medium

dense, and dense states.

- During the testing program, the soil is restrained laterally. The soil is placed in a ring that is fixed to the base. Also, porous discs are placed on each side of the specimen.
- The minimum specimen diameter is required as 50 mm. Therefore, a cap with a diameter of 74.5 mm is used in the study.
- The minimum initial specimen height is required as 12 mm, but cannot be less than $10*D_{max}$. Hence, the specimen height is taken as 25.4 mm.
- The ratio of specimen diameter/height is required minimum of 2.5. In our case, the rate is 2.93.
- The rate and magnitude of consolidation of the soil at different densities are determined.
- An incrementally applied stress loading controlled by an applicator is conducted for each test. The stress applied is performed with multiples ranging through 25-50-100-200-400-800 kPa.
- Each successive load increment is carried out after primary consolidation is done.
- Deformation-time readings are recorded with all load increments.

3.4.3. Laterally Loaded Pile Group Test at Large Displacement

The lateral deflections of a vertical pile and pile group subjected to lateral loading are determined through the specifications in ASTM D3966 - D3966M - 07 (2013) [61]. The testing program covering both single pile and pile group behavior in order to analyze the pile-soil modulus ratio of laterally loaded piles at large displacement is presented below:

- The tests are conducted to both a single continuous pile and a continuous pile group with a 3 x 3 configuration.
- Before the tests, fire hose piles are pressurized to 500, 1000, and 1500 kPa for each test.
- The piles used in the tests are placed into the test apparatus after it is filled with

the soil. The soil is placed with various relative densities like 30%, 50%, and 65%. It is aimed to observe the modulus ratio relation between the pile and the soil.

- ASTM D3966 requires that the pile group cap should be designed as made of steel-reinforced concrete or a steel frame to sustain the system and distribute the loads equally. In our case, the cap is made of a steel frame. Therefore, the requirement is met.
- ASTM D3966 also requires sufficient space under the pile cap to eliminate any pile cap friction. Clear space between the pile cap and the ground surface is ensured during the tests.
- For applying loads, the standards demand that the loads should be applied laterally at pile cut-off elevation. The load should also be applied through the central axis of the pile group. It is aimed to minimize or eliminate undesired eccentric and vertical loads. Therefore, the load in the study is applied by considering this requirement. The load is applied as exhibited in Figure 3.16.

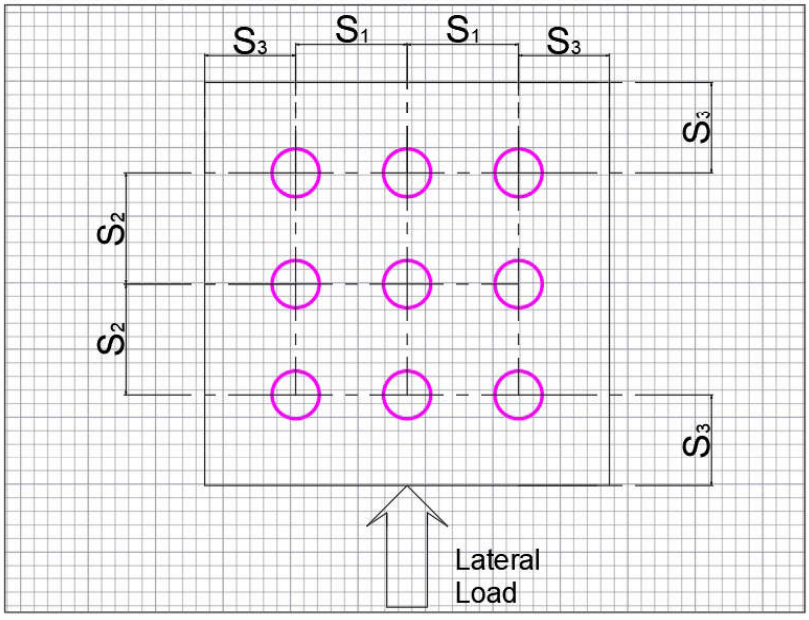


Figure 3.16. Pile Group and Loading Direction ($S_1 = S_2 = 2.4$D, $S_3 = 1.9$D).

- It is also stated in the standards for the lateral loads applied by pulling that the device applying load should be able to create a constant and steady load. In

the study, a linear actuator with a stepper motor can apply up to 167 kPa shear force. Additionally, lateral load, 1 mm per minute, is applied to the pile head plate. Lateral displacement of up to 50 mm is conducted.

- A steel rod is used in the study to connect the device applying force to the pile cap. Hence, the load applied by the device passes through the pile group. A loading gauge is fastened to the steel rod to measure the load applied. The view of the test system is exhibited in Figure 3.17.

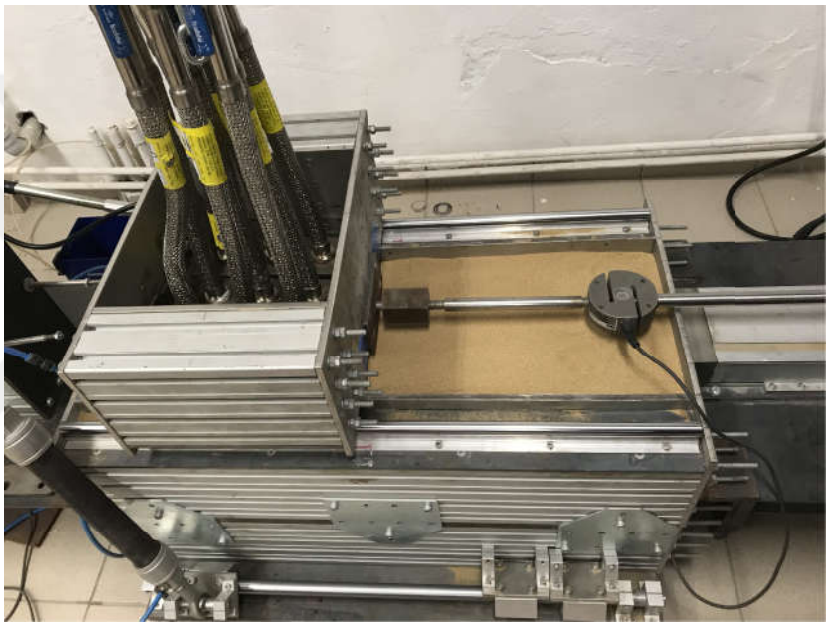


Figure 3.17. Laterally Loaded Pile Group Test System.

- Lateral deflection and corresponding load data of all the experiments are recorded. Each laterally loaded pile test condition is listed in Table 3.4 below.

Table 3.4. Laterally Loaded Pile Test Program.

Test Number	**Number of Piles**	**Number of Wearing Layer**	**Piles Pressurized to (kPa)**	**D_R of Soil (%)**	**Embedment Depth Ratio (L/D)**
#1	9 (3x3)	-	500	30 (Loose)	9.71
#2	9 (3x3)	-	1000	30 (Loose)	9.71
#3	9 (3x3)	-	1500	30 (Loose)	9.71
#4	9 (3x3)	-	500	50 (Medium)	9.71
#5	9 (3x3)	-	1000	50 (Medium)	9.71
#6	9 (3x3)	-	1500	50 (Medium)	9.71
#7	9 (3x3)	-	500	65 (Dense)	9.71
#8	9 (3x3)	-	1000	65 (Dense)	9.71
#9	9 (3x3)	-	1500	65 (Dense)	9.71
#10	1	-	1000	30 (Loose)	9.71
#11	1	-	1500	30 (Loose)	9.71
#12	1	1	1000	30 (Loose)	9.71
#13	1	1	1500	30 (L.)	9.71

4. TEST RESULTS AND DISCUSSION

The behavior of the laterally loaded continuous pile group installed in the sand is presented regarding the load and lateral deflection curves in this chapter. Both the obtained test results and the interpretations of the test results are given in the following sections. The influence of various factors such as flexural rigidity of the pile and relative density of the soil is discussed through the experiments (three-point bending, oedometer, and laterally loaded pile group) conducted in the study. Then, the group efficiency is also studied, and the pile-soil rigidity of the laterally loaded pile group is specially interpreted at the end.

4.1. Test Results

The results of the conducted tests are given in this section.

4.1.1. Three-Point Bending Tests

Three-point bending tests are conducted on the single fire-hose pile pressurized to 500, 1000, and 1500 kPa. During the tests, the piles without a wearing layer, with a single wearing layer, and with a double wearing layer have experimented as listed in Table 3.3 in the previous chapter. The flexural rigidity of the pile, EI_{pile} is determined through the following equation (4.1), where E is Young's modulus of the pile, I is the moment of inertia of the pile section, L is the length of the pile, P is the load applied, and δ is the displacement measured. And, the equation is formulated as

$$\delta = \frac{\mathbf{PL^3}}{\mathbf{48EI}}. \tag{4.1}$$

The following figures show the plots of flexural rigidity of the piles versus displacement for the related piles. The test results are plotted together in order to observe the pile behavior and compare them in detail. During the tests, the displacement is

kept limited for security measures. The displacement values for the piles pressurized to 500, 1000, and 1500 kPa are limited with 30 mm, 25 mm, and 20 mm, respectively. Figure 4.1, Figure 4.2, Figure 4.3 cover tests #1, #2, and #3 (the pile without a wearing layer pressurized to 500, 1000, and 1500 kPa), #4, #5, and #6 (the pile with a single wearing layer pressurized to 500, 1000, and 1500 kPa), and #7, #8, and #9 (the pile with a double wearing layer pressurized to 500, 1000, and 1500 kPa), respectively.

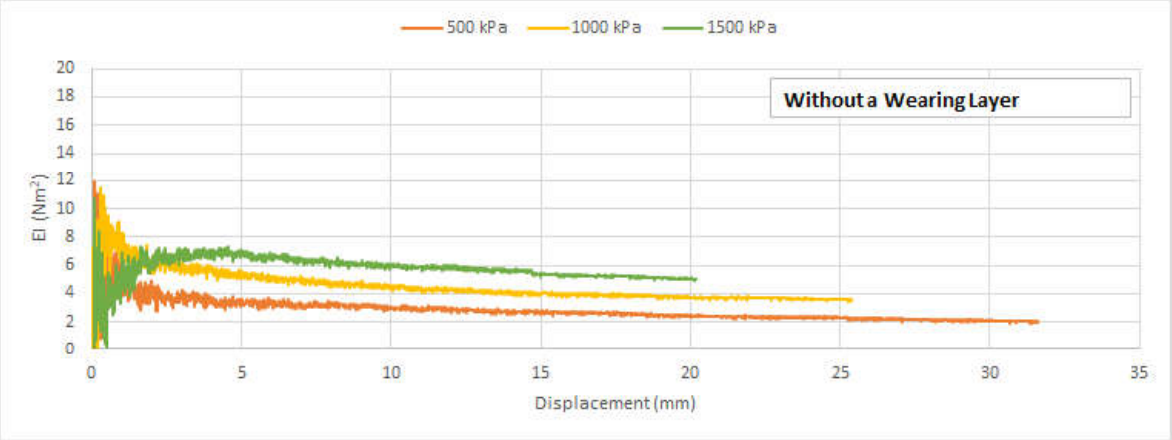


Figure 4.1. Flexural Rigidity-Displacement Curves for Piles Without a Wearing Layer.

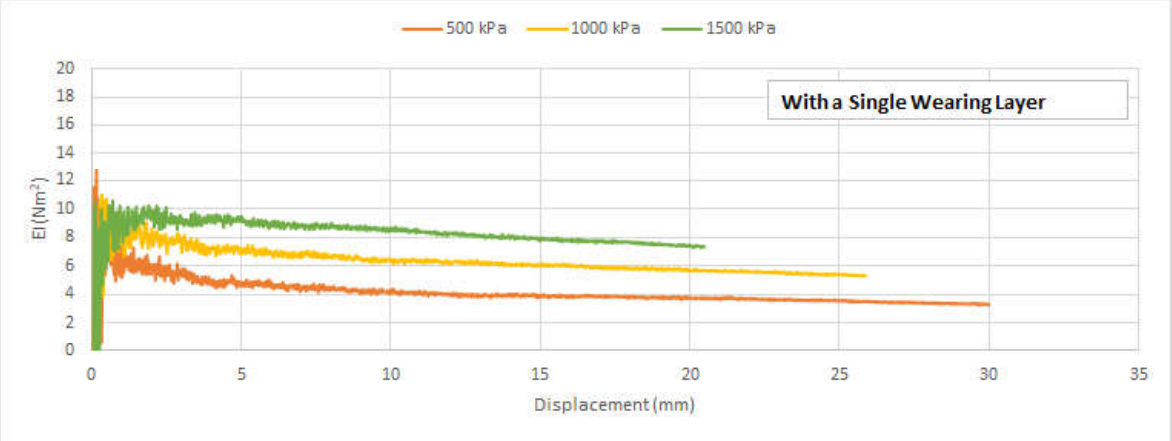


Figure 4.2. Flexural Rigidity-Displacement Curves for Piles With a Single Wearing Layer.

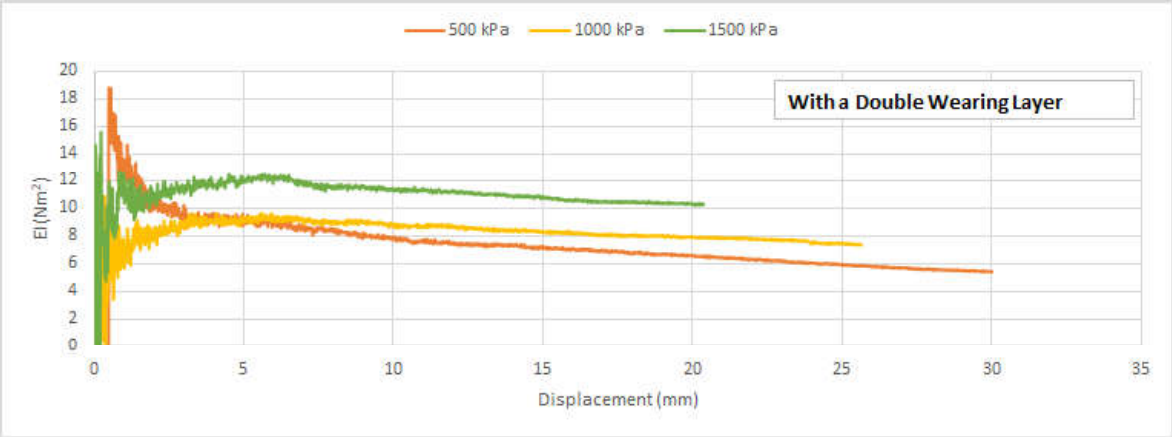


Figure 4.3. Flexural Rigidity-Displacement Curves for Piles With a Double Wearing Layer.

Figure 4.4, Figure 4.5, and Figure 4.6 cover tests #1, #4, and #7 (the pile pressurized to 500 kPa: without a wearing layer, with a single wearing layer, and with a double wearing layer), #2, #5, and #8 (the pile pressurized to 1000 kPa: without a wearing layer, with a single wearing layer, and with a double wearing layer), and #3, #6, and #9 (the pile pressurized to 1500 kPa: without a wearing layer, with a single wearing layer, and with a double wearing layer), respectively.

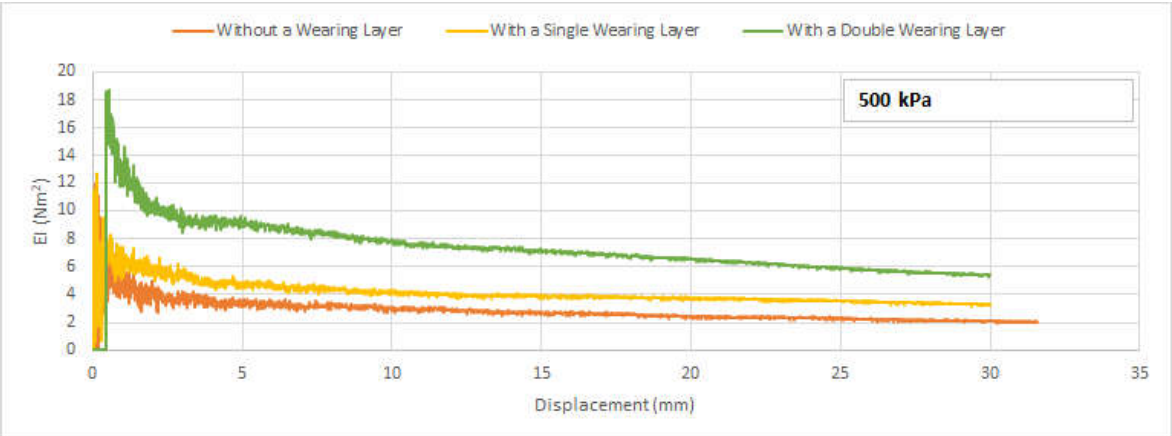


Figure 4.4. Flexural Rigidity-Displacement Curves for Piles Pressurized to 500 kPa.

During the three-point bending tests, the wearing layer is used to increase the moment of inertia of the pile section, I_{pile}. Following this, it is aimed to have the piles

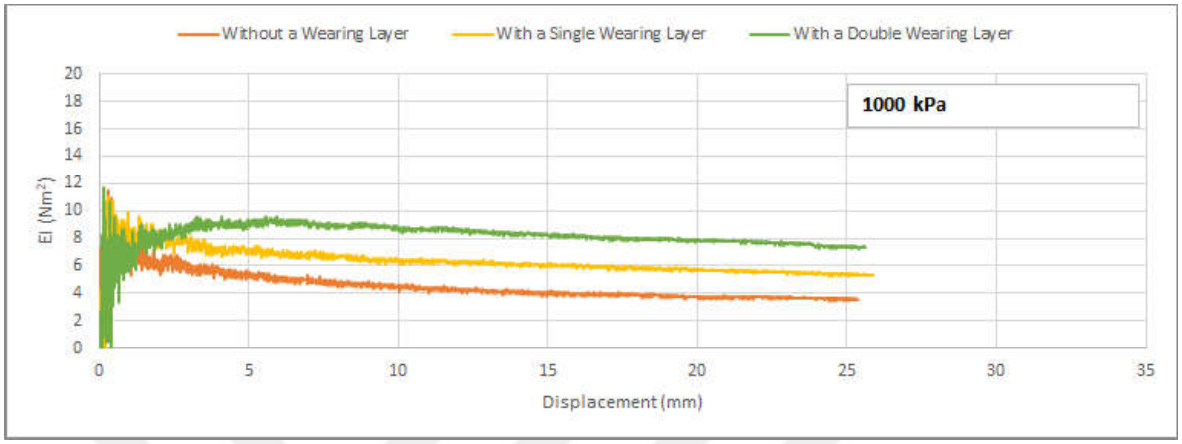


Figure 4.5. Flexural Rigidity-Displacement Curves for Piles Pressurized to 1000 kPa.

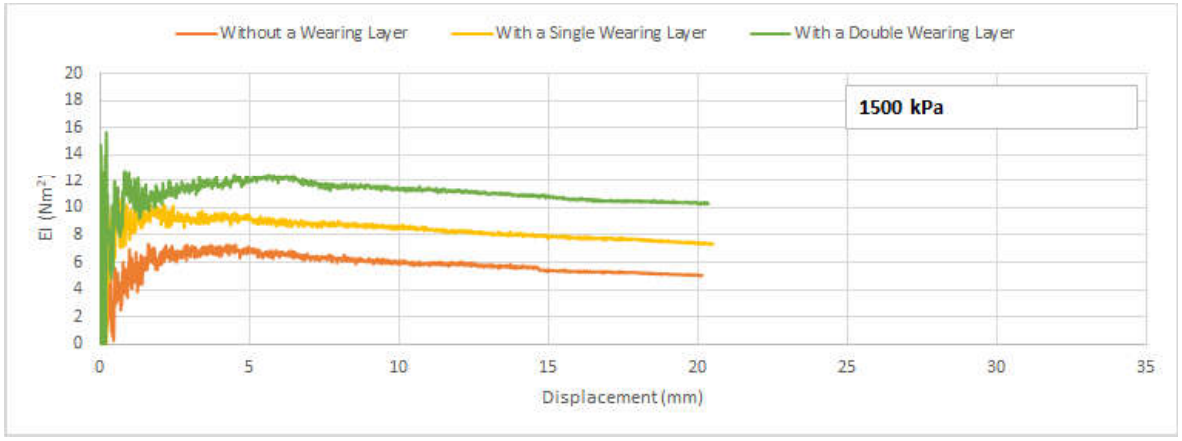


Figure 4.6. Flexural Rigidity-Displacement Curves for Piles Pressurized to 1500 kPa.

with higher flexural rigidities, so a higher E_{pile}/E_{soil} ratio is ensured. Figure 4.7 and Figure 4.8 show tests #1, the pile without a wearing layer and #4, the pile with a single wearing layer.

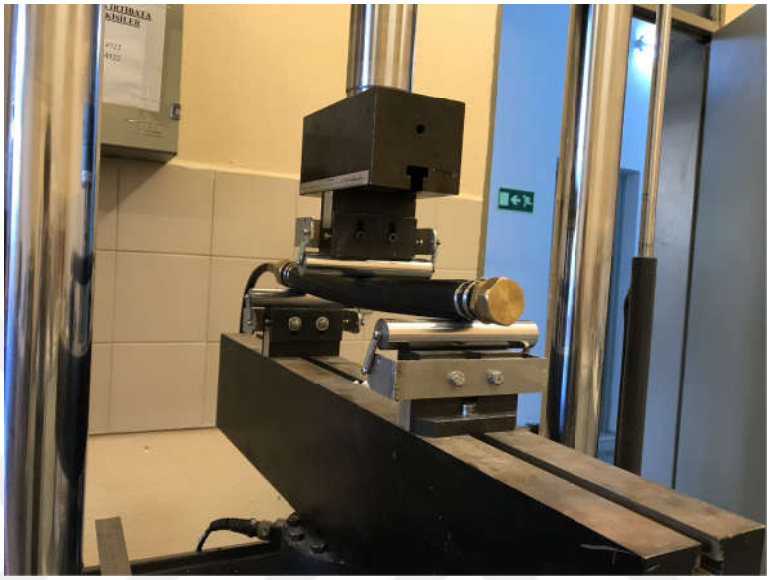


Figure 4.7. The Pile Without a Wearing Layer (Test #1).

After all three-point bending tests are conducted, the flexural rigidity values for the related piles are listed in Table 4.1.

Table 4.1. Flexural Rigidity Values for Piles.

Number of the Wearing Layer	EI_{pile} **for Piles Pressurized to 500 kPa** (Nm^2)	EI_{pile} **for Piles Pressurized to 1000 kPa** (Nm^2)	EI_{pile} **for Piles Pressurized to 1500 kPa** (Nm^2)
-	3.45	5.13	6.82
1	4.81	6.96	9.33
2	8.87	9.90	11.89



Figure 4.8. The Pile With a Wearing Layer (Test #4).

4.1.2. Oedometer Tests

Oedometer tests are conducted on the soil classified as poorly graded sand. The soil specimen is compacted at various relative densities, which are loose (30%), medium dense (50%), and dense (65%) states. Figure 4.9 shows a view of the test equipment.



Figure 4.9. Oedometer Test Equipment.

The elastic modulus of the soil at three different densities is determined through oedometer tests. Vertical stress is applied in a gradual manner from 25 kPa to 800 kPa, and afterward, the vertical strain values for the soil are recorded. Each stress

increment is applied after the primary consolidation of the specimen is completed. Figure 4.10 shows a plot of the vertical stresses against elastic modulus values for each test condition.

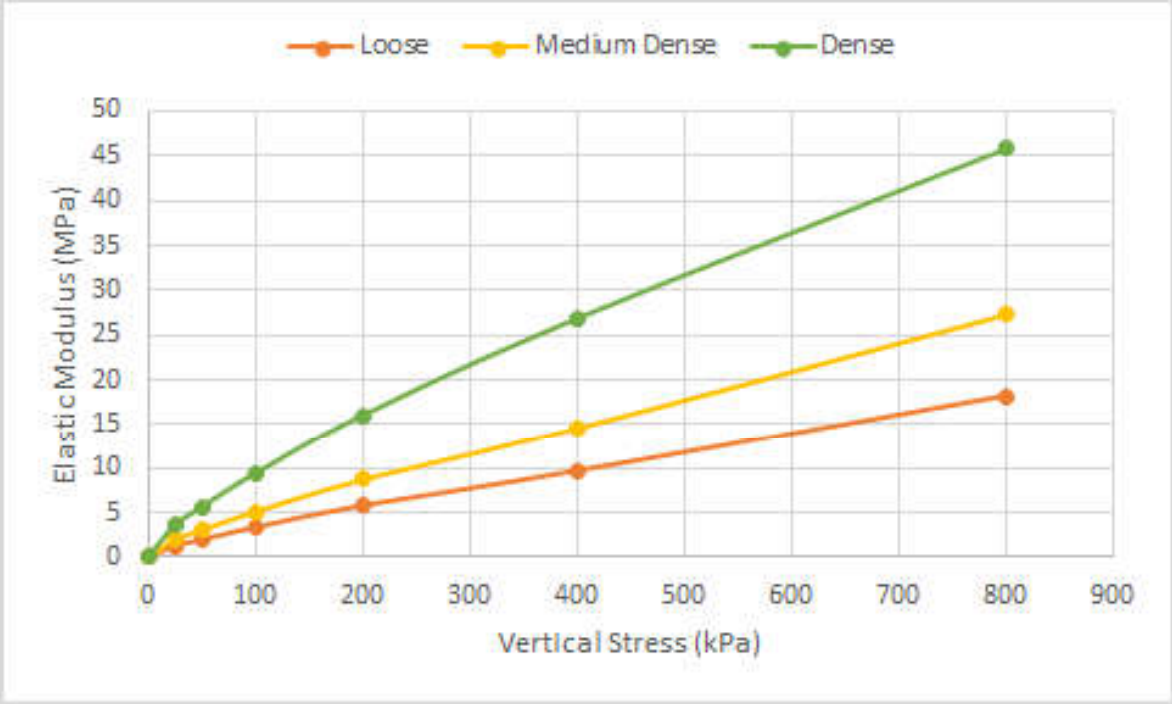


Figure 4.10. Elastic Modulus-Vertical Stress Curves for Soil.

The elastic modulus values for loose-medium dense-dense states of soil are listed in Table 4.2 with intervals of the vertical stresses.

Moreover, vertical stress - vertical strain and void ratio - vertical stress curves for loose-medium dense-dense states of soils are shown in Figure 4.11 and Figure 4.12, respectively.

4.1.3. Laterally Loaded Pile Group Tests at Large Displacement

The response of the pile group is presented with respect to the load and lateral deflection curves. The piles are pressurized to 500, 1000, and 1500 kPa, and then the soil is placed at different relative densities as detailed in the previous subsection. During

Table 4.2. Elastic Modulus Values for Soil.

Stress Range (kPa)	E_{soil} **for Loose State Soil (MPa)**	E_{soil} **for Medium Dense State Soil (MPa)**	E_{soil} **for Dense State Soil (MPa)**
0-25	1.31	1.97	3.60
25-50	2.01	3.07	5.64
50-100	3.40	5.11	9.42
100-200	5.81	8.72	16.02
200-400	9.73	14.60	26.86
400-800	18.23	27.34	45.79

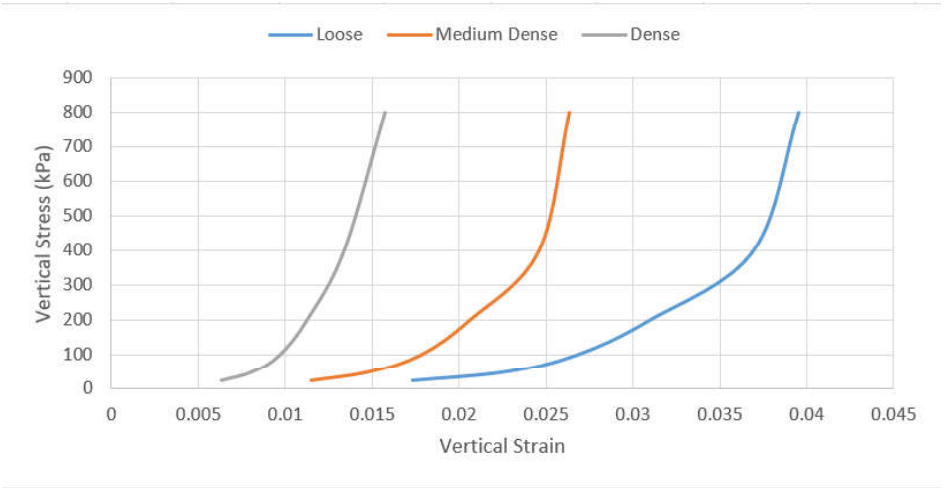


Figure 4.11. Vertical Stress - Vertical Strain Curves.

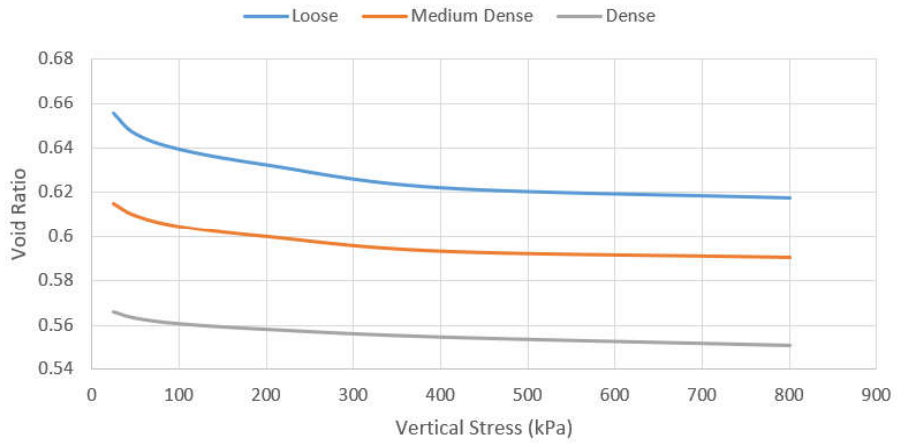


Figure 4.12. Void Ratio - Vertical Stress Curves.

the tests, the pressure inside the piles is kept constant. Both pile group and single pile tests at large displacement are performed to analyze the group efficiency. As mentioned previously, a single pile pressurized to 1000 and 1500 kPa with a wearing layer is also tested at large displacement. All the tests are listed in Table 3.4 as mentioned before.

The following figures show the plots of the load versus the lateral deflection for the pile group and the single piles. The figures show the lateral deflection up to 50 mm, the target deflection in the study. During the tests, the load is measured with time intervals of 1 second and recorded through software. The test results are plotted together to make an appropriate comparison in the following sections.

In the following three figures, the relative density of the soil is kept constant to be able to observe the effect of the change in the pile rigidity of the pile. Figure 4.13 shows a plot of the load versus the lateral deflection for tests #1, #2, and #3. It can be seen in the figure that a continuous increment in the load develops as the lateral deflection increases. Also, the pile group pressurized to 1500 kPa is subjected to the highest load compared to the two other pile groups.

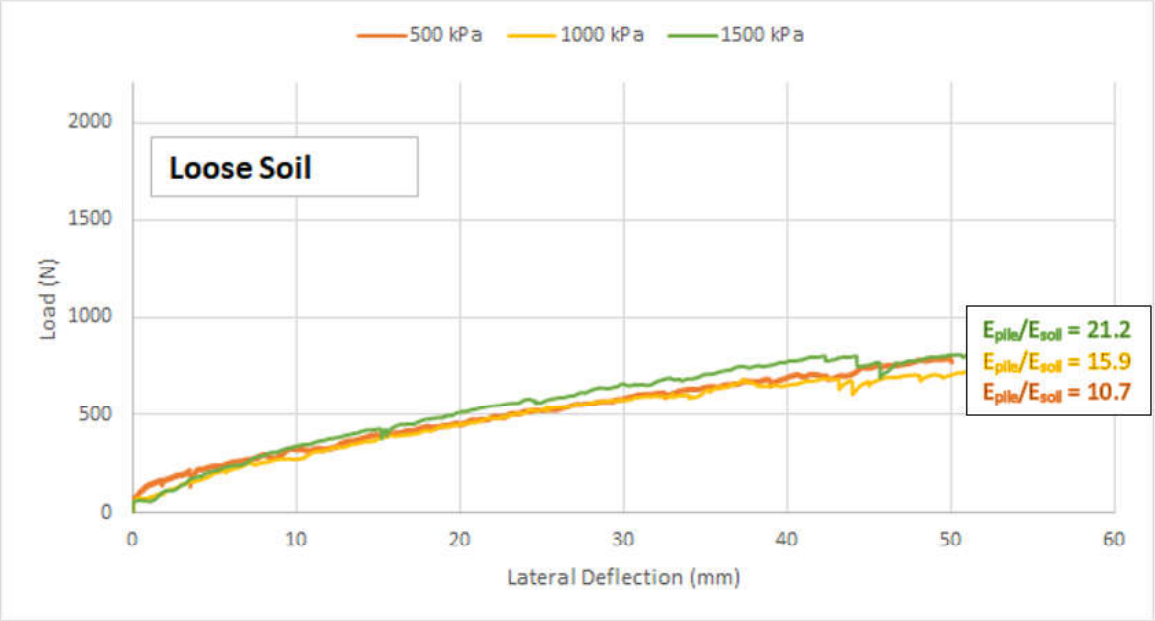


Figure 4.13. Load-Lateral Deflection Curves for Pile Group in Loose Soil.

Figure 4.14 shows a plot of the load versus the lateral deflection for tests #4, #5, and #6. The same behavior observed in Figure 4.13 can also be seen in this figure.

Figure 4.15 shows a plot of the load versus the lateral deflection for tests #7, #8, and #9. The same pattern with Figure 4.13 and Figure 4.14 is observed here.

In the following three figures, the pile rigidity of the pile group is kept constant to be able to observe the influence of the change in the relative density of the soil. Figure 4.16, Figure 4.17, and Figure 4.18 exhibit plots of the load versus the lateral deflection for tests #1, #4, and #7, tests #2, #5, and #8, and tests #3, #6, and #9, respectively. According to the following three figures, higher load values are measured as the relative density of the soil increases.

Figure 4.19 presents a plot of the load versus the lateral deflection for tests #2, #10. It can be seen in the figure that a drop in soil resistance for the pile group is observed because of the group effect. The sum of the lateral resistance that single piles have is greater than the lateral resistance of a group pile. In the study, the group

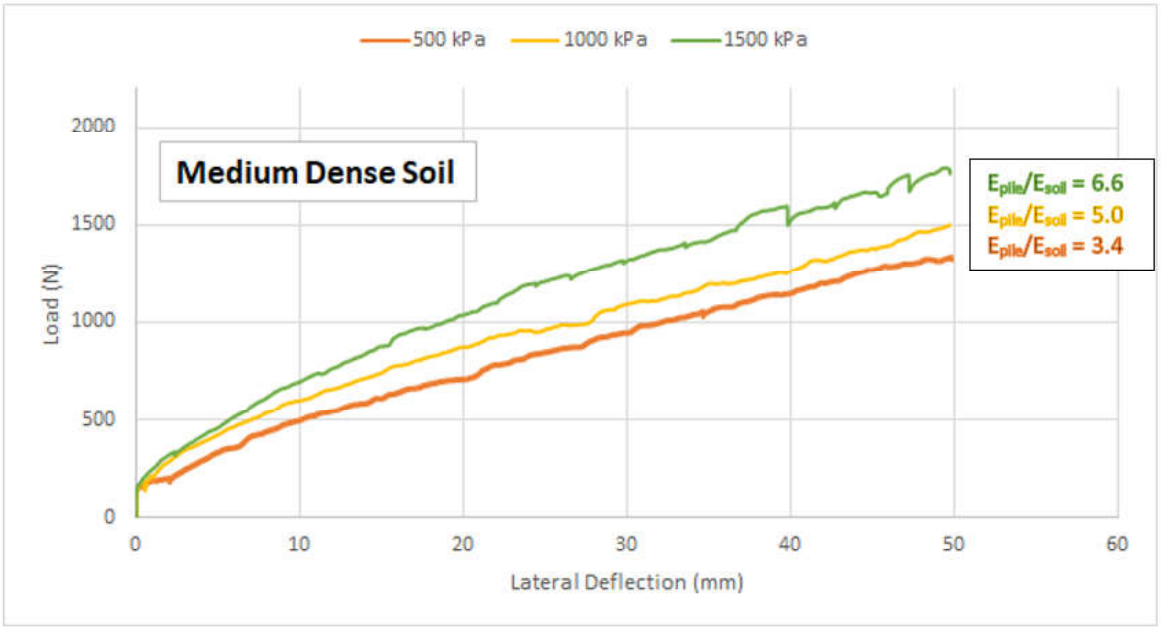


Figure 4.14. Load-Lateral Deflection Curves for Pile Group in Medium Dense Soil.

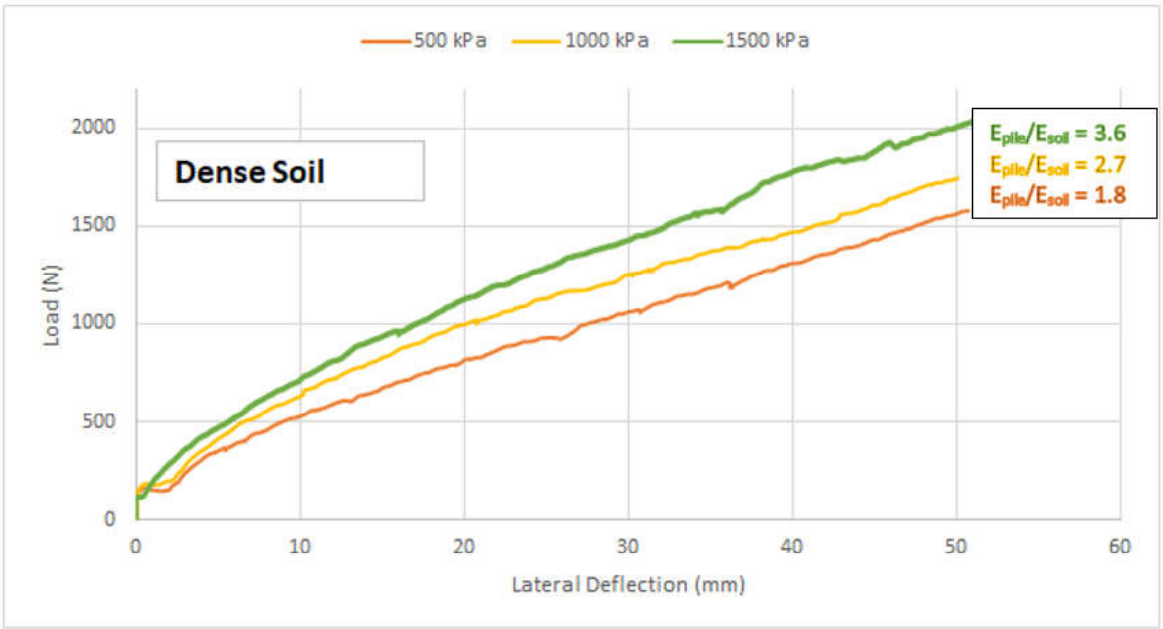


Figure 4.15. Load-Lateral Deflection Curves for Pile Group in Dense Soil.

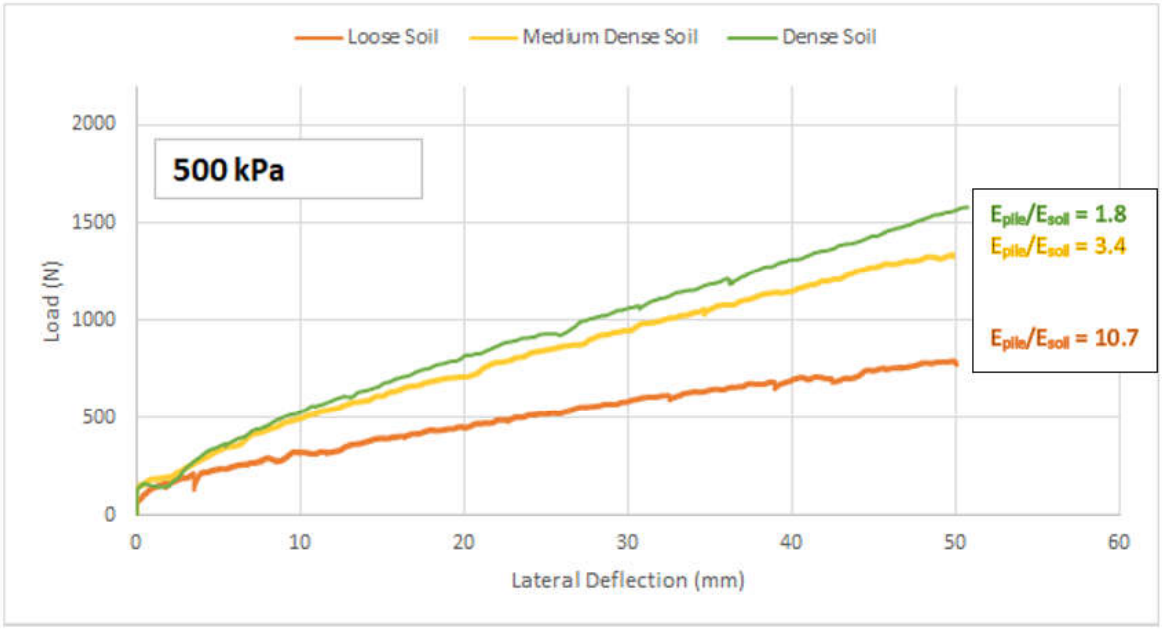


Figure 4.16. Load-Lateral Deflection Curves for Pile Group Pressurized to 500 kPa.

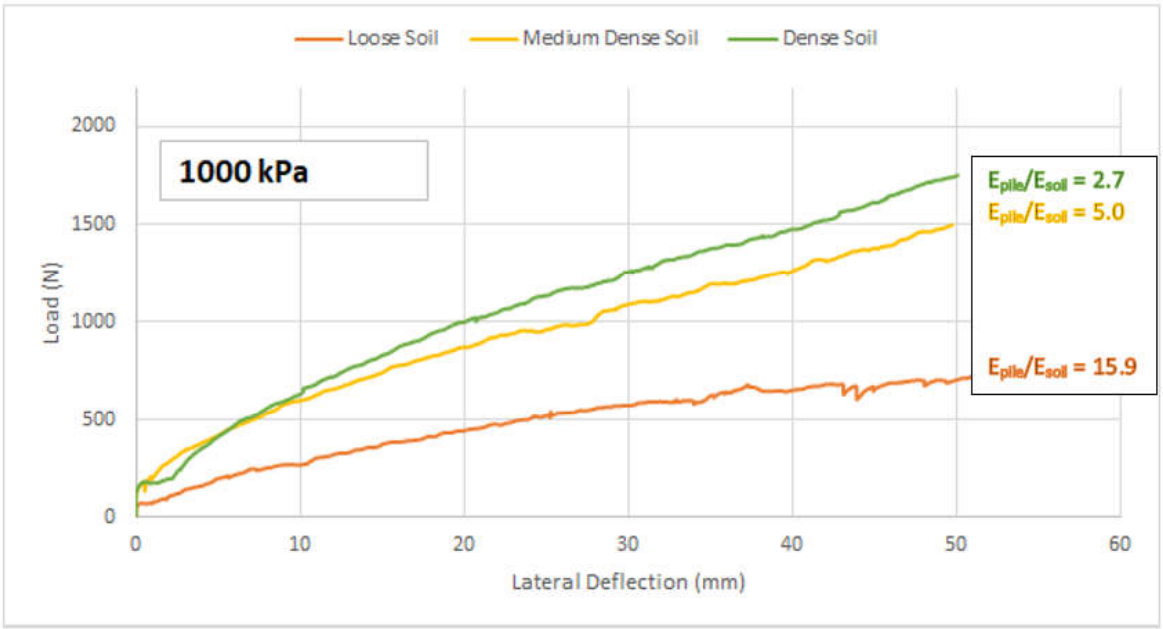


Figure 4.17. Load-Lateral Deflection Curves for Pile Group Pressurized to 1000 kPa.

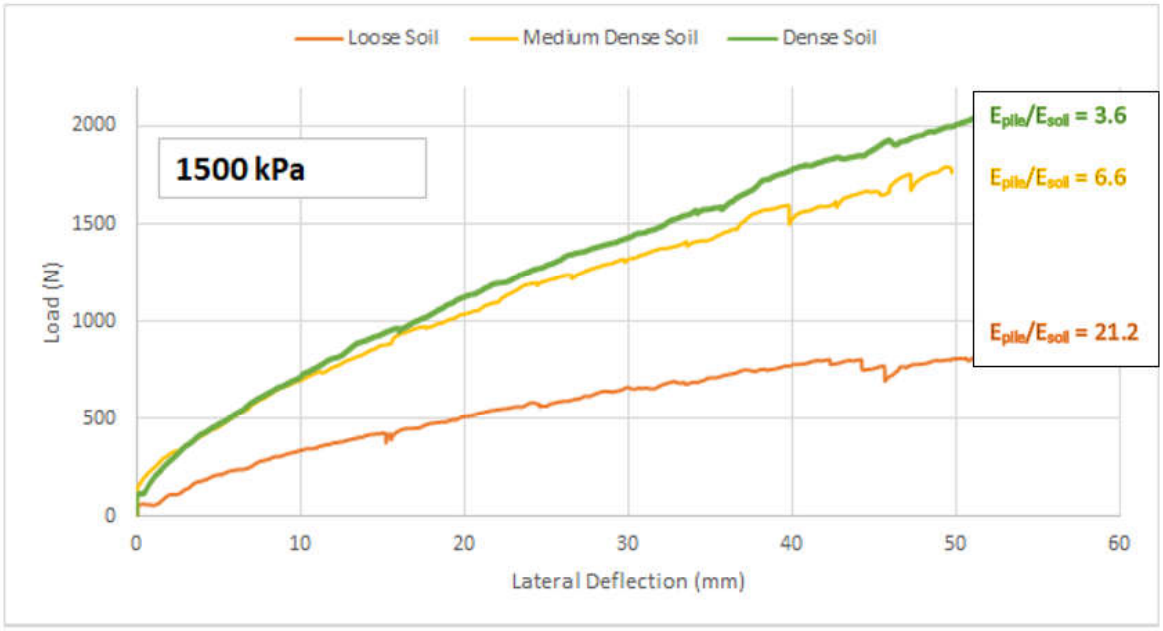


Figure 4.18. Load-Lateral Deflection Curves for Pile Group Pressurized to 1500 kPa.

efficiency fluctuates between 0.50 and 0.60. A p-multiplier, p_m indicating the group efficiency can be determined by using equation (4.2) written as

$$\mathbf{p_m} = \frac{\textbf{Pile Group Capacity / Number of Piles in the Group}}{\textbf{A Single Pile Capacity}}. \qquad (4.2)$$

Figure 4.20 shows a plot of the load versus the lateral deflection for tests #10 and #12. In this figure, it is aimed to compare the single piles with/out a wearing layer. As it is determined in the previous sections, a single wearing layer increases the pile rigidity (pressurized to 1000 kPa) from 5.13 N/m^2 to 6.96 N/m^2 which means an increment of 35.67% in the rigidity. On the other hand, the results show that an increment of 72.45% in soil resistance is observed.

Figure 4.21 shows a plot of the load versus the lateral deflection for tests #11 and #13. In this figure, the same behavior with Figure 4.20 is observed. According to previous test results, a single wearing layer increases the pile rigidity (pressurized to 1500 kPa) from 6.82 N/m^2 to 9.33 N/m^2 which means an increment of 36.80% in the

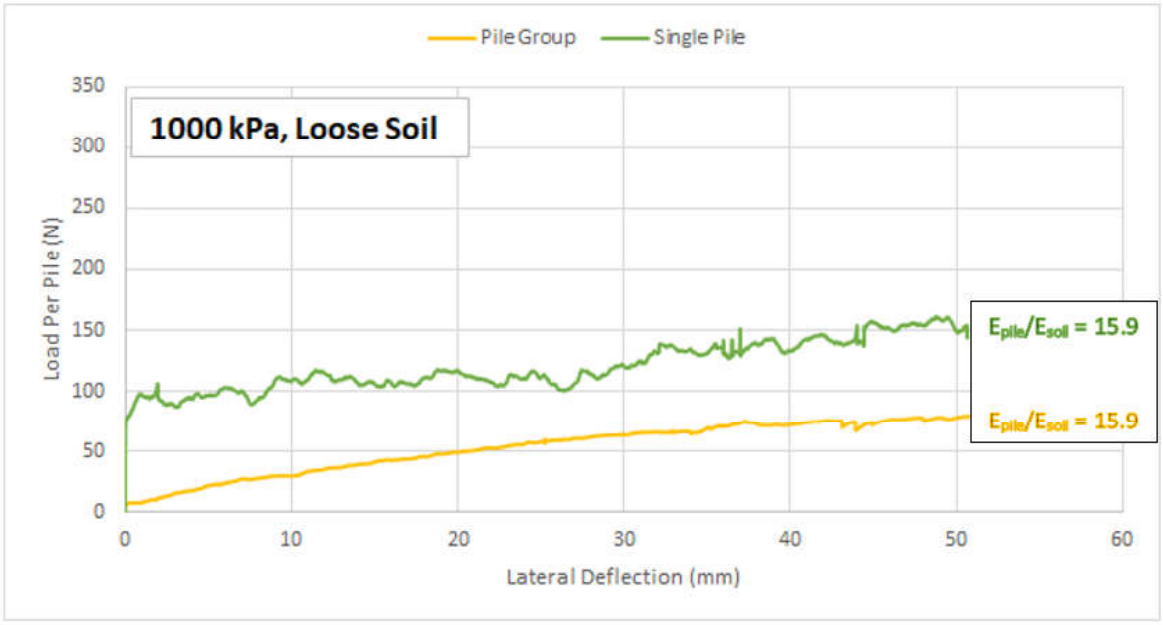


Figure 4.19. Load-Lateral Deflection Curves for both Pile Group and Single Pile.

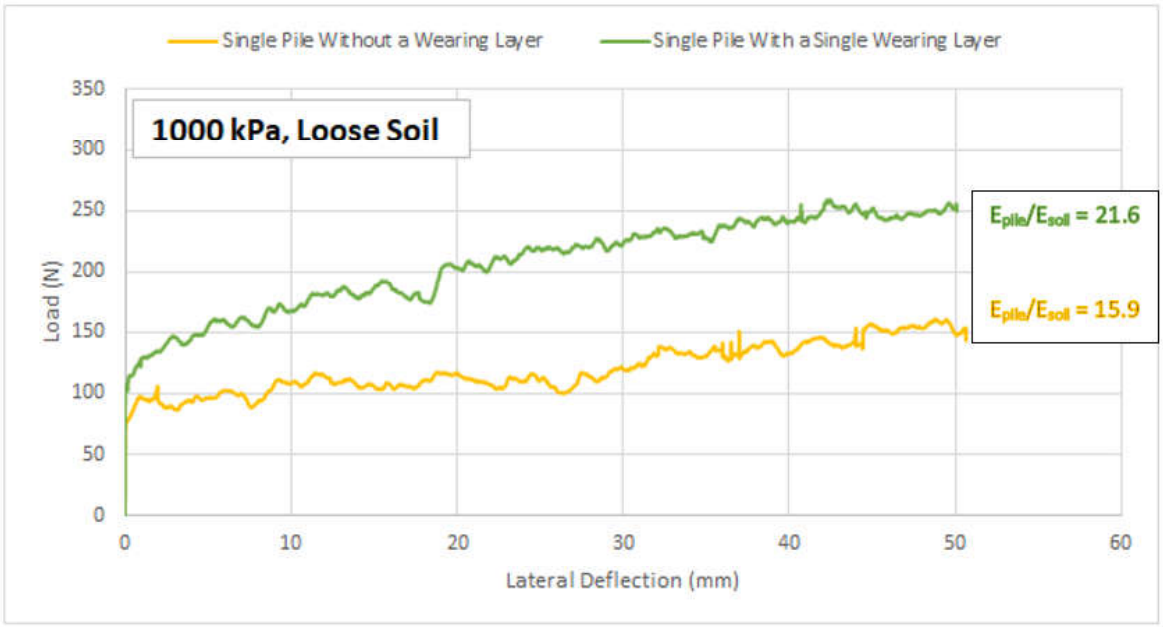


Figure 4.20. Load-Lateral Deflection Curves for Single Piles (1000 kPa).

rigidity. However, it is observed an increment of 58.23% in soil resistance.

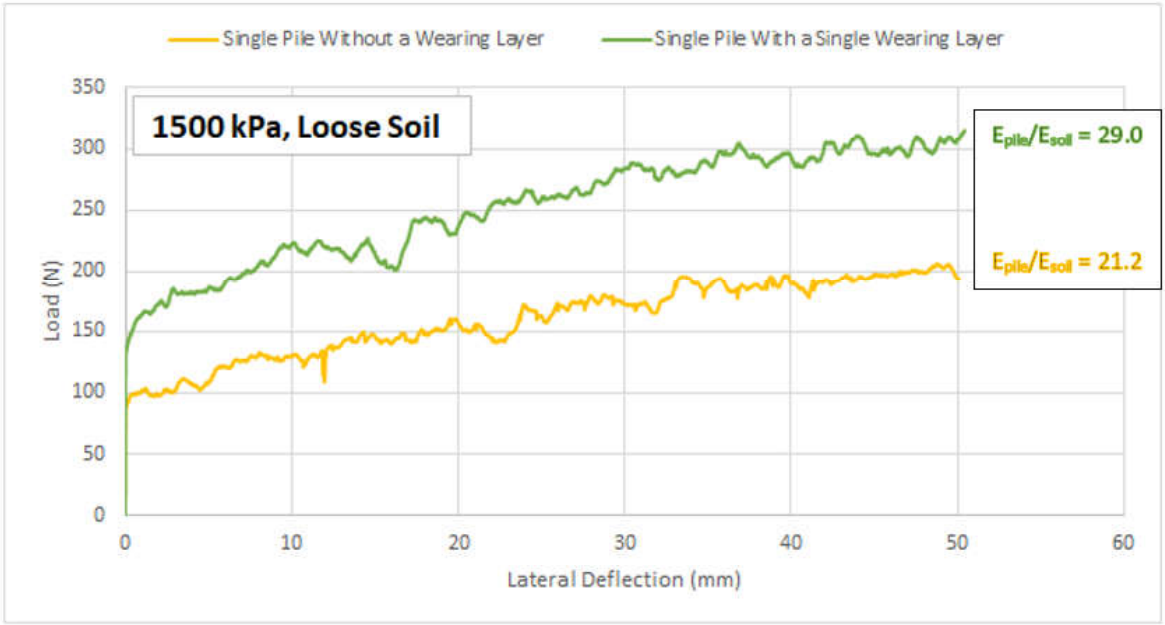


Figure 4.21. Load-Lateral Deflection Curves for Single Piles (1500 kPa).

4.2. Discussion

The interpretations of the test results are given in this section.

4.2.1. Three-Point Bending Tests

The interpretations of the obtained three-point test results exhibited through the figures in the previous chapter are made below.

Flexural rigidity values for the piles without a wearing layer are obtained in the range of 2-7 Nm^2. A parallel response is observed between the flexural rigidity values and the pressure of the piles. An increment of flexural rigidity is noticed in the figure as the pile pressure increases. Increments of 49% and 98% in EI_{pile} are seen by increasing the pile pressure from 500 kPa to 1000 kPa and from 500 kPa to 1500 kPa, respectively.

Flexural rigidity values for the piles with a single wearing layer are obtained in the range of 3.50-9.35 Nm^2. The same behavior with the piles without a wearing layer is also seen here. Increments of 45% and 94% in EI_{pile} are observed by increasing the pile pressure from 500 kPa to 1000 kPa and from 500 kPa to 1500 kPa, respectively.

Flexural rigidity values for the piles with a double wearing layer are obtained in the range of 5.70-12 Nm^2. The same pattern between the flexural rigidity values and the pressure of the piles is also seen here. Increments of 12% and 34% in EI_{pile} are observed by increasing the pile pressure from 500 kPa to 1000 kPa and from 500 kPa to 1500 kPa, respectively.

When the obtained results above are compared, it becomes apparent that the impact of increasing the pile pressure on flexural rigidity for the piles both without a wearing layer and with a single wearing layer is much higher compared to the piles with a double wearing layer. It can be said that as the thickness of the pile increases, the effectiveness of increasing the pile pressure becomes less significant. Moreover, the highest flexural rigidity values are achieved when the piles are pressurized to 1500 kPa for every three cases above.

Flexural rigidity values for the piles pressurized to 500 kPa are obtained in the range of 2-9 Nm^2. A parallel response is observed between the thickness of the piles and the flexural rigidity values. An increment of flexural rigidity is found out in the figure as the thickness of the pile increases. Increments of 39% and 157% in EI_{pile} are seen by increasing the pile thickness from 2 mm to 4 mm and 2 mm to 6 mm, respectively.

Flexural rigidity values for the piles pressurized to 1000 kPa are obtained in the range of 3.80-9.90 Nm^2. The same behavior with Figure 4.4 is also seen here. Increments of 36% and 93% in EI_{pile} are observed by increasing the pile thickness from 2 mm to 4 mm and 2 mm to 6 mm, respectively.

Flexural rigidity values for the piles pressurized to 1500 kPa are obtained in the range of 5.50-12 Nm^2. The same pattern between the flexural rigidity values and the thickness of the piles is also seen here. Increments of 37% and 74% in EI_{pile} are observed by increasing the pile thickness from 2 mm to 4 mm and 2 mm to 6 mm, respectively.

The obtained results above are compared. Afterward, it is clearly seen that the effect of increasing the thickness of the pile on the flexural rigidity values decreases as the pile pressure increases through 500 kPa to 1500 kPa. An increment in pile thickness has the lowest impact on the flexural rigidity when the pile is pressurized to 1500 kPa. On the other hand, the maximum impact is observed for the piles pressurized to 500 kPa. Furthermore, the highest flexural rigidity values are achieved when the piles are dressed with a double layer for every three cases above. Through the three-point bending tests conducted both in this study and the study of Ozturk, B. [49], the load values for continuous and non-continuous piles are listed in Table 4.3.

As mentioned in the previous chapters, the flexural rigidity of a pile and the moment of inertia for a voided circular pile are determined through equation (4.1) and equation (2.12), respectively. Therefore, the pile thickness has a critical and direct impact on the EI_{pile}. In the study, it is planned to achieve increments of 258% and 610% in flexural rigidity by using single and double wearing layers on the piles. However, the targeted increments are not achieved, but only 37% and 108% increments in flexural rigidity are obtained. The main reason is that the wearing layers are fixed to the piles with clamps. Because the pipe wall thickness is not one piece, the expected performance is not ensured in the study.

4.2.2. Oedometer Tests

The interpretations of the obtained oedometer test results presented through Figure 4.10 and Table 4.2 in the previous chapter are made below.

Table 4.3. Load Values (N) for Continuous and Non-Continupus Piles Obtained from Three-Point Bending Tests.

Piles	**Disp. at 5 mm**	**Disp. at 10 mm**	**Disp. at 15 mm**
Cont. Pile Pres. to 500 kPa (No Wearing Layer)	21.07	34.43	51.11
Cont. Pile Pres. to 1000 kPa (No Wearing Layer)	31.58	55.48	72.36
Cont. Pile Pres. to 1500 kPa (No Wearing Layer)	40.91	72.18	100.15
Cont. Pile Pres. to 500 kPa (Single Wearing Layer)	29.56	51.47	72.56
Cont. Pile Pres. to 1000 kPa (Single Wearing Layer)	41.97	77.28	109.85
Cont. Pile Pres. to 1500 kPa (Single Wearing Layer)	55.73	105.76	144.01
Cont. Pile Pres. to 500 kPa (Double Wearing Layer)	55.10	95.80	130.34
Cont. Pile Pres. to 1000 kPa (Double Wearing Layer)	55.75	107.48	151.32
Cont. Pile Pres. to 1500 kPa (Double Wearing Layer)	73.99	134.73	192.47
Non-Cont. Pile Post-Tensioned with 750N	201.55	308.94	417.82

According to the test results, it is observed that the elastic modulus of the soil for each case (loose, medium dense, and dense soil conditions) increases as the magnitude of the vertical stress applied to the soil increases. The expected results are satisfied with the test results obtained. As it is expected, the maximum E_{soil} values are noticed when the soil is prepared in a dense state. On the other hand, the minimum values are observed in the loose state soil. The range of the results for each case is presented below.

- For the loose state soil, E_{soil} values are obtained in the range of 1.31-18.23 MPa.
- For the medium dense state soil, E_{soil} values are obtained in the range of 1.97-27.34 MPa.
- For the dense state soil, E_{soil} values are obtained in the range of 3.60-45.79 MPa.

The elastic modulus for granular soil found in the study and given in the literature are exhibited in Table 4.4. It is seen in the table below that the value of the elastic modulus values for the soils are relatively low compared to the literature.

Table 4.4. Elastic Modulus Values for Sand.

Soil Type	**In This Study**	**AASHTO 2012 [34]**	**Braja M. Das, 2004 [19]**
Sand: Loose	1.31-18.23	9.6-28.8	10.35-24.15
Sand: Medium Dense	1.97-27.34	28.8-48	17.25-27.60
Sand: Dense	3.60-45.79	48-76.8	34.5-55.2

One of the primary goals of the study is to investigate the effect of pile-soil rigidity. With the help of the three-point bending and oedometer tests, various ratios of the pile-soil rigidity, E_{pile} / E_{soil} are obtained. The results are divided into three parts; E_{pile} / E_{soil} ratios for the piles without a wearing layer, with a single wearing layer, and a double layer are presented in Table 4.5, Table 4.6, and Table 4.7, respectively.

Table 4.5. Pile-Soil Modulus Ratios, E_{pile}/E_{soil} (Piles without a Wearing Layer).

Soil Condition	**Soil Stress (kPa)**	**500 kPa (Pile Pressure)**	**1000 kPa (Pile Pressure)**	**1500 kPa (Pile Pressure)**
Loose	**0-25**	10.7	15.9	21.2
Loose	**25-50**	7.0	10.5	13.9
Loose	**50-100**	4.1	6.2	8.2
Med. Dense	**0-25**	3.4	5.0	6.6
Med. Dense	**25-50**	2.2	3.2	4.3
Med. Dense	**50-100**	1.3	1.9	2.6
Dense	**0-25**	1.8	2.7	3.6
Dense	**25-50**	1.2	1.7	2.3
Dense	**50-100**	0.7	1.0	1.4

Table 4.6. Pile-Soil Modulus Ratios, E_{pile}/E_{soil} (Piles with a Single Wearing Layer).

Soil Condition	**Soil Stress (kPa)**	**500 kPa (Pile Pressure)**	**1000 kPa (Pile Pressure)**	**1500 kPa (Pile Pressure)**
Loose	**0-25**	14.9	21.6	29.0
Loose	**25-50**	9.8	14.2	19.0
Loose	**50-100**	5.8	8.4	11.2
Med. Dense	**0-25**	4.7	6.8	9.1
Med. Dense	**25-50**	3.0	4.4	5.8
Med. Dense	**50-100**	1.8	2.6	3.5
Dense	**0-25**	2.6	3.7	5.0
Dense	**25-50**	1.6	2.4	3.2
Dense	**50-100**	1.0	1.4	1.9

Table 4.7. Pile-Soil Modulus Ratios, E_{pile}/E_{soil} (Piles with a Double Wearing Layer).

Soil Condition	**Soil Stress (kPa)**	**500 kPa (Pile Pressure)**	**1000 kPa (Pile Pressure)**	**1500 kPa (Pile Pressure)**
Loose	**0-25**	27.6	30.8	37.0
Loose	**25-50**	18.1	20.2	24.2
Loose	**50-100**	10.6	11.9	14.3
Med. Dense	**0-25**	8.6	9.6	11.6
Med. Dense	**25-50**	5.5	6.2	7.4
Med. Dense	**50-100**	3.3	3.7	4.5
Dense	**0-25**	4.7	5.3	6.3
Dense	**25-50**	3.0	3.4	4.0
Dense	**50-100**	1.8	2.0	2.4

4.2.3. Laterally Loaded Pile Group Tests at Large Displacement

The interpretations of the obtained laterally loaded pile group test results presented through the figures and tables in the previous chapter are made below. A wearing layer is not used during the laterally loaded pile group tests.

The lateral capacity for the laterally loaded pile group in loose soil is obtained in the range of 700-800 N. A continuous increment in pile group capacity is observed for each condition as the lateral displacement increases. In the loose state soil, an increment in the flexural rigidity of the piles does not result in a considerable amount of increment in the pile group capacity. The maximum capacity is observed when the piles are pressurized to 1500 kPa.

The lateral capacity for the laterally loaded pile group in medium dense soil is obtained in the range of 1300-1750 N. A continuous increment in pile group capacity is also seen here. Contrary to the tests carried out in loose soil, a significant increment in

pile group capacity is observed in medium dense soil as the flexural rigidity of the piles increases. Once again, the highest pile group capacity is seen for the piles pressurized to 1500 kPa.

The lateral capacity for the laterally loaded pile group in dense soil is obtained in the range of 1550-2000 N. The same behavior in pile group capacity is seen here as well. The most visible increment in pile group capacity is observed for the tests carried out in dense state soil compared to the others. Once again, the highest pile group capacity is seen for the piles pressurized to 1500 kPa.

When the first three figures are evaluated, it is clearly seen that the maximum increment in pile group capacity by increasing the flexural rigidity of the piles is obtained in dense state soil while the minimum increment is obtained in loose state soil. As it is considered within the scope of Table 4.5, the highest E_{pile} / E_{soil} ratio is seen when the tests are conducted in loose state soil. It can be said that, as the ratio increases, the impact of increasing the flexural rigidity of the piles on the lateral capacity decreases. Additionally, the study of Youngho Kim [36] claims that the soil gets inclined to resist much more against the pile when the pile and soil rigidity are closer to each other. Through Table 4.5, the lowest E_{pile} / E_{soil} ratios are seen when the soil is in a dense state. The maximum lateral capacity is observed where the E_{pile} / E_{soil} ratio is minimum. Therefore, the laterally loaded pile group test results are in accordance with the study of Kim.

The lateral capacities for the laterally loaded pile groups pressurized to 500, 1000, and 1500 kPa are obtained in the range of 700-1550, 700-1750, and 800-2000 N, respectively. A continuous increment in lateral capacity is observed in all three conditions as the lateral displacement increases. When all three figures are evaluated, as the relative density of the soil increases (means that a lower E_{pile} / E_{soil} ratio is ensured), an increment in the lateral capacity is observed. Therefore, the maximum lateral capacities are seen for all three cases when the pile-soil modulus ratio is at the lowest value in the case of dense state soil is prepared.

Additionally, there is a considerable amount of increment in lateral capacity when two experiments, which are conducted in loose and medium dense state soils, are compared. On the other hand, the same amount of increase is expected when the test is conducted in dense state soil. However, the increment in lateral capacity remains limited in comparison with the first increment. The reason behind this might be a critical threshold in E_{pile} / E_{soil} ratio. Within the scope of Table 4.5, E_{pile} / E_{soil} ratio for loose state soil with 0-25 kPa soil stress is in the range of 10.7-21.2. The ratios for medium dense and dense state soils are between 3.4-6.6 and 1.8-3.6, respectively. Further studies are needed to determine a critical limit to understand fully the behavior of laterally loaded piles.

Figure 4.19 is presented to visualize the p-multiplier, p_m that is indicating the drop in soil resistance because of the group effect. A p-multiplier is defined to adjust the change in the lateral resistance of a single pile by taking into consideration the row position of piles. In this study, the group efficiency fluctuates between 0.50 and 0.60. The group efficiency is obtained slightly lower than the data observed in the literature. There are various factors that can influence group efficiency, but pile spacing is one of the most important. In the study of Abbas et al. [41], different pile spacings, which are 2D, 4D, 6D, and 8D, are tested. In this sense, 6D pile spacing is observed as the critical limit. Furthermore, the study of Kim et al. [38] focuses on detailing pile group interaction factors and finds out that the ratio between the spacing and pile diameter should be six times larger to eliminate pile group effects for loose and medium dense soil. In this thesis, the piles are spaced from center to center at a distance of 2.4D. The spacing can be the main reason why the group efficiency is slightly lower compared to the literature.

Single piles are tested to understand whether the system is fully working or not. The single piles are tested in loose state soil (the highest E_{pile} / E_{soil} ratios), which is the most challenging situation for the piles. Moreover, the piles with a single wearing layer are tested for the first time in laterally loaded experiments. It is aimed to observe the efficiency of the wearing layer on the lateral lateral capacity. For the piles pressurized

to 1000 kPa, an increment of 35.67% in pile rigidity, which a single wearing layer brings, causes an increment of 72.45% in lateral capacity (from 150 N to 258 N). Therefore, wearing layers is another way to increase the lateral capacity that piles have. However, it is utile to remember that the increment in pile capacity cannot be explained only with the pile rigidity. Thus, further studies considering E_{pile} / E_{soil} ratio must be done in order to understand fully the behavior of the laterally loaded piles.

Additionally, through large displacement model pile tests, lateral displacement of up to 50 mm is conducted, which means that the piles are displaced 143% of their diameter. Mostly in literature, the piles made of steel and concrete cannot be displaced at these rates. In the study of Rao et al. [1], steel and aluminum piles with an E_{pile} / E_{soil} ratio of 719178 are used. The results would be improved if the ratio was smaller. Also, the piles are displaced 71% and 35% of their diameter. There are other studies [38,39] that the value of lateral displacement is remained at between 35-70%. A comparison of load-displacement curves between this study and the study of Youngho Kim et al. [36] is exhibited in Figure 4.22. In the study of Laman et al. [44], the lateral capacity of the model piles is observed five times higher in the test performed in dense soil. On the other hand, in this study, the lateral capacity of the model piles is observed two times (piles pressurized to 500 kPa), two and four tenths times (piles pressurized to 1000 kPa), and two and five tenths times (piles pressurized to 1500 kPa) higher in tests conducted in dense soil. A comparison of load and lateral displacement curves between this study and the study of Keklik [48] is shown in Figure 4.23. The pile-soil modulus ratios for the non-continuous and continuous pile systems (for the tests conducted in loose state soil) are in the same range (7-29). Also, it has been seen that the non-continuous and continuous pile systems showed similar behavior at the same pile-soil modulus ratios.

A laboratory study is performed to examine the effect of pile-soil rigidities for different soil and pile conditions. Through comparison with case studies and findings, the following comments are made:

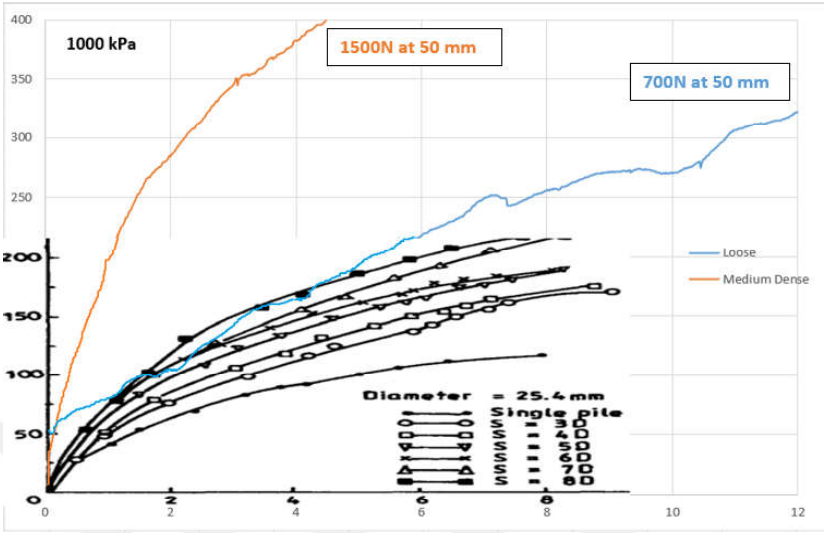


Figure 4.22. Comparison of Load-Displacement Curves (x-axis: displacement (mm), y-axis: load (N)).

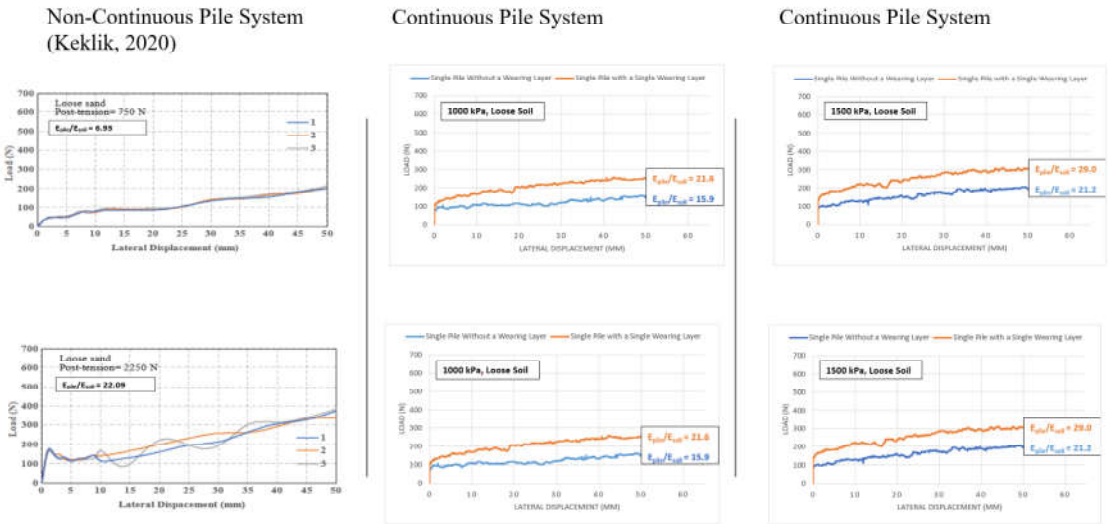


Figure 4.23. Comparison of Load and Lateral Displacement Curves [48].

- In the laterally loaded single pile tests, by taking into account the increment in the pile rigidity with a wearing layer or increasing water pressure inside, an increment in lateral capacity is observed.
- In comparison with the previous studies done in the Boğaziçi University Geotechnical Laboratory, while the flexural rigidity values for the segmental pile system are in the range of 5 and 15 Nm^2, the flexural rigidity values for the piles used in this study are in the range of 3.5 and 12 Nm^2. On the other hand, while the E_{pile} / E_{soil} ratios for the segmental pile system are in the range of 6 and 36, the E_{pile} / E_{soil} ratios for 0-25 kPa soil stress for the piles used in this study are in the range of 5 and 37. As it is clearly seen, both the flexural rigidity of the piles and E_{pile} / E_{soil} ratio values are in the same order, and the primary objective of this study is accomplished.
- For the laterally loaded pile group tests (see in Figure 4.13) conducted in loose state soil (E_{pile} / E_{soil} ratio for 0-25 kPa soil stress is in between 10.7-21.2), it is observed that the increase in the flexural rigidity of the piles does not affect the lateral capacity of the pile group.
- For the laterally loaded pile group tests (see in Figure 4.14) conducted in medium dense state soil (E_{pile} / E_{soil} ratio for 0-25 kPa soil stress is in between 3.4-6.6), the effect of the increase in the flexural rigidity of the piles on the lateral capacity is more remarkable in medium dense soil compared to loose soil.
- For the laterally loaded pile group tests (see in Figure 4.15) conducted in dense state soil (E_{pile} / E_{soil} ratio for 0-25 kPa soil stress is in between 1.8-3.6), the influence of the increase in the flexural rigidity of the piles comes into prominence most in the experiments conducted in dense soil with the lowest pile-soil modulus ratio.
- For all the laterally loaded pile group tests, as the flexural rigidity of the piles increases, the lateral capacity of the pile group is also increased.
- By taking into account the pile-soil rigidity difference effect, it would be appropriate to provide a critical limit for the E_{pile} / E_{soil} ratio.
- The lateral capacity of the piles increases steadily with the increase in lateral displacement.

- It has been obtained through the laterally loaded pile group tests that the lateral capacity of the pile group increases steadily with the increase in lateral displacement.
- The group efficiency, p_m fluctuates between 0.50 and 0.60, which is relatively low. When the result is compared with the existing studies in literature, it is observed that the pile spacing is the main reason for this situation.
- The relation between pile-soil modulus ratios calculated and lateral capacity values obtained in this study is exhibited in Figure 4.24 in order to visualize the correlation between them.

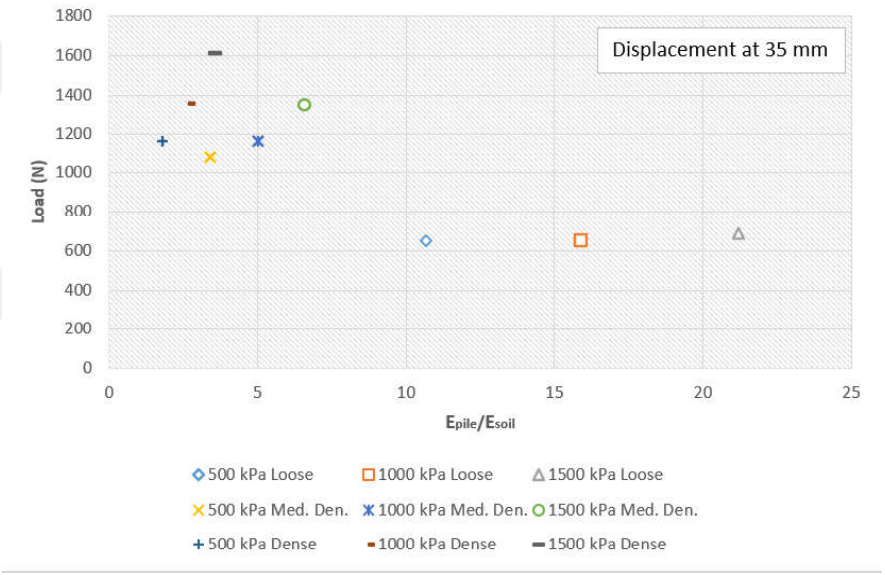


Figure 4.24. Pile-Soil Modulus Ratios and Load Values at Displacement of 35 mm.

5. CONCLUSION

The segmental pile system, which is composed of alternating concrete blocks and rubber sheets tied with an anchor cable, is a non-continuous system, and there is a question of whether it can be treated as a beam. The rigidity can be adjusted by increasing or decreasing the tension on the anchor cable. The working mechanism is through the friction developed at the joints. The primary objective of this study is to compare the load-displacement behavior with the continuous pile with adjustable rigidity. To be able to adjust the rigidity of the continuous pile system, water pressure in a confined rubber cylinder is applied. Three different water pressures are applied to change the pile rigidity. Poorly-graded sand is compacted at loose, medium dense, and dense states. This way, different pile-soil modulus ratios are obtained. A single continuous pile and nine continuous piles with a 3 x 3 configuration are used. The piles are spaced with a distance of 2.4D. The length and outer diameter of piles are 340 mm and 35 mm, respectively. The experiments are conducted on fixed-head piles at large displacements of up to 50 mm (pile diameter, D is equal to 35 mm). Horizontal displacement is applied to the pile group head, and the corresponding lateral capacity values are obtained.

An experimental study is performed to examine the effect of pile-soil rigidities for different soil and pile conditions; afterward, limited to the tests results obtained in the study, the following conclusions are drawn:

- The continuous model pile system is designed to have adjustable rigidity in this study. The rigidity of the continuous pile system was satisfactorily adjusted by using three different water pressures inside the rubber confined cylinder. The material can be resisted up to 50 bar pressure, and connection fittings are accessible and economical. Pile-soil modulus ratios are investigated and tested by changing the pile rigidity by controlling the water pressure inside the piles.
- The test results of the previous studies related to the non-continuous pile system

are verified. It is observed that the non-continuous pile system and the continuous pile system showed similar behavior at the same pile-soil modulus ratios. Although, the mechanisms leading to horizontal capacity development for both pile systems are completely different.

- The effect of pile-soil modulus ratio on laterally loaded pile groups is observed. The applicability of rigidity adjustment for this continuous pile system will simplify and promote studies on model piles tests targeting pile-soil modulus ratio effects.
- For the laterally loaded pile group tests conducted in loose state soil (pile-soil modulus ratio is between 10.7-21.2), it has been observed that the increase in the flexural rigidity of the piles does not affect the lateral capacity of the pile group. On the other hand, for the tests conducted in both medium dense soil (pile-soil modulus ratio is between 3.4-6.6) and dense soil (pile-soil modulus ratio is between 1.8-3.6), adjusting the pile rigidity of the piles has a significant impact on the lateral capacity of pile groups.
- The results of the study suggest that instead of increasing the pile rigidity in loose sand, the densification of the surrounding soil is more important to achieve higher lateral capacity. Pile rigidity dominates the lateral capacity behavior of the pile in the dense state of sand.
- It is observed through the tests conducted in soils with various relative rigidities that the lateral capacity of the pile group increases as pile and soil modulus values get closer to each other.

REFERENCES

1. S. Narasimha Rao; V. G. S. T. Ramakrishna, Z. and M. B. Rao, "Influence of Rigidity on Laterally Loaded Pile Groups in Marine Clay", *Journal of Geotechnical and Geoenvironmental Engineering*, pp. 542–549, 1998.

2. Matlock, H. and L. Reese, "Generalized Solutions for Laterally Loaded Piles", *Journal of the Soil Mechanics and Foundations Division*, Vol. 86, No. 5, pp. 63–92, 1960.

3. Broms, B., "Lateral Resistance of Piles in Cohesionless Soils", *Journal of the Soil Mechanics and Foundations Division*, Vol. 90, No. 3, pp. 123–156, 1964.

4. Poulos, H. G., "Behavior of Laterally Loaded Piles: I-Single Piles", *Journal of the Soil Mechanics and Foundations Division*, Vol. 97, No. 5, pp. 711–731, 1971.

5. Poulos, H. G. and E. H. Davis, "Development of Negative Friction With Time in End-Bearing Piles.", *Australian Geomechanics Journal*, Vol. G2, No. 1, pp. 11–20, 1972.

6. Reese, L., "Handbook on Design of Piles and Drilled Shafts Under Lateral Load", *U.S. Department of Transportation, Federal Highway Administration, Office of Implementation, Washington, D.C.*, Vol. FHWA-IP-84, p. 392, 1984.

7. Reese, L., "Behavior of Piles and Pile Groups Under Lateral Load", *U.S. Department of Transportation, Federal Highway Administration, Office of Engineering and Highway Operations Research and Development, Washington, D.C.*, Vol. FHWA- RD-8, p. 311, 1986.

8. Jai B. Kim and R. J. Brungraber, "Full-Scale Lateral Load Tests of Pile Groups", *Journal of the Geotechnical Engineering Division*, Vol. 102, No. 1, pp. 87–105, 1976.

9. Poulos, H. and E. Davis, *Pile Foundation Analysis and Design*, 1980.

10. Prakash, S. and H. D. Sharma, *Pile Foundations In Engineering Practise*, 1990.

11. Fayyazi, M., M. Taiebat, W. Finn and C. Ventura, "Evaluation of Group Factor Method for Analysis of Pile Groups", *15th World Conference on Earthquake Engineering (15WCEE)*, 2012.

12. Christensen, D. S., "Full Scale Static Lateral Load Test of a 9 Pile Group in Sand", *M.Sc. Thesis Brigham Young University*, 2006.

13. Walsh, J. M., "Full-Scale Lateral Load Test of a 3x5 Pile Group in Sand", *Brigham Young University - Provo*, 2005.

14. Ohi, S. J., "Use of Broms' Charts for Evaluating Lateral Load Capacity of Vertical Piles in a Two Layer Soil System", *1st International Conference on Advances in Civil Engineering 2012 (ICACE 2012)*, Vol. 2012, No. September, pp. 12–14, 2015.

15. Ti, K. S., B. B. Huat, J. Noorzaei, M. S. Jaafar and G. S. Sew, "Modeling of Passive Piles", *Electronic Journal of Geotechnical Engineering*, Vol. 14 P, pp. 1–22, 2009.

16. Ellis, E. A. and S. M. Springman, "Modelling of soil-structure interaction for a piled bridge abutment in plane strain FEM analyses", *Computers and Geotechnics*, Vol. 28, No. 2, pp. 79–98, 2001.

17. Shukla, R. P., "Passive Piles Subjected To Excavation Induced Soil Movement : an Overview Passive Piles Subjected To Excavation Induced Soil", *International Conference on Sustainable Energy and Built Environment*, pp. 494–501, 2015.

18. Phanikanth, V. S., D. Choudhury and G. Rami Reddy, "Response of single pile under lateral loads in cohesionless soils", *Electronic Journal of Geotechnical Engineering*, Vol. 15 H, No. January 2010, pp. 1–18, 2010.

19. Das, B. M., *Principles of Foundation Engineering*, Taylor & Francis, 2004.

20. Gupta, B. K. and D. Basu, "Analysis of laterally Loaded Short and Long Piles in Multilayered Heterogeneous Elastic Soil", *Soils and Foundations*, Vol. 57, No. 1, pp. 92–110, 2017.

21. Ruigrok, J. A. T., "Laterally Loaded Piles: Models and Measurements", p. 360, 2010.

22. Hannigan, P. J., F. Rausche, G. E. Likins, B. R. Robinson and M. Becker, "Design and Construction of Driven Pile Foundations Workshop Manual", Vol. I, No. November, p. 517, 1998.

23. Lymon C. Reese, H. M., "Non-dimensional Solutions for Laterally-loaded Piles with Soil Modulus Assumed Proportional to Depth", *Texas Conference on Soil Mechanics and Foundation Engineering*, 1956.

24. Davisson, M. T. and H. L. Gill, "Laterally Loaded Piles in a Layered Soil System", *Journal of the Soil Mechanics and Foundations Division*, Vol. 89, No. 3, pp. 63–94, 1963.

25. Broms, B., "Design of Laterally Loaded Piles", *Journal of the Soil Mechanics and Foundation Division*, Vol. 91, No. 3, pp. 77–99, 1965.

26. Douglas, D. J. and E. H. Davis, "The Movement of Buried Footings due to Moment and Horizontal Load and the Movement of Anchor Plates", *Geotechnique*, Vol. 14, No. 2, pp. 115–132, 1964.

27. Spillers, W. R. and R. D. Stoll, "Lateral Response of Piles", *Journal of the Soil Mechanics and Foundations Division*, Vol. 90, pp. 1–10, 1964.

28. Blum, H., "Wirtschaftliche Dalbenformen und dereń Berechnung", *Die Bautechnik*, Vol. 5, 1932.

29. Coduto, D. P., "Foundation Design Principles and Practices (2nd Edition)", *Prentice Hall*, p. 484, 1994.

30. Norris, G., "Theoretically based BEF laterally loaded pile analysis.", *Proceedings of the Third International Conference on Numerical Methods in Offshore Piling. Nantes, France.*, pp. 361–386, 1986.

31. Ashour, M., G. Norris and P. Pilling, "Lateral Loading of a Pile in Layered Soil Using the Strain Wedge Model", *Journal of Geotechnical and Geoenvironmental Engineering*, Vol. 124, No. 4, pp. 303–315, 1998.

32. Ashour, M., G. Norris and P. Pilling, "Laterally Loaded Isolated Piles, Drilled Shafts and Pile Groups Using the Strain Wedge Model", *Journal of Bridge Engineering*, Vol. 7, No. August, pp. 800–815, 2002.

33. Brown, B. D. A., C. Morrison and L. C. Reese, "Lateral load behaviour of pile group in sand", *International Journal of Rock Mechanics and Mining Sciences & Geomechanics Abstracts*, Vol. 26, No. 3-4, p. A145, 1988.

34. American Association of State Highway and Transportation Officials, *AASHTO LRFD Bridge Design Specifications, Washington, DC*, 2012.

35. ASTM A572. Standard Specification for High-Strength Low-Alloy Columbium-Vanadium Structural Steel., "ASTM A572 Grade 50 (S 355 GP) HSLA", *Book of ASTM Standards*, Vol. 50, pp. 1–6, 2019.

36. Kim, Y., S. Jeong and J. Won, "Effect of Lateral Rigidity of Offshore Piles Using Proposed p-y Curves in Marine Clay", *Marine Georesources and Geotechnology*, Vol. 27, No. 1, pp. 53–77, 2009.

37. Zhu, B., R.-p. Chen, J.-f. Guo, L.-g. Kong and Y.-m. Chen, "Large-Scale Modeling and Theoretical Investigation of Lateral Collisions on Elevated Piles", *Journal of Geotechnical and Geoenvironmental Engineering*, Vol. 138, No. 4, pp. 461–471,

2012.

38. Kim, B. T. and G. L. Yoon, "Laboratory Modeling of Laterally Loaded Pile Groups in Sand", *KSCE Journal of Civil Engineering*, Vol. 15, No. 1, pp. 65–75, 2011.

39. Mohamedzein, Y. E., F. A. Nour Eldaim and A. B. Abdelwahab, "Laboratory Model Tests on Laterally Loaded Piles in Plastic Clay", *International Journal of Geotechnical Engineering*, Vol. 7, No. 3, pp. 241–250, 2013.

40. Mufty, A., "Effects of Pile Rigidity and Soil Stiffness on the Settlement of Piles Using RSPile for Understanding Pile Behavior", pp. 1–11, 2020.

41. Abbas Al-Shamary, J. M., Z. Chik and M. R. Taha, "Modeling the lateral response of pile groups in cohesionless and cohesive soils", *International Journal of Geo-Engineering*, Vol. 9, No. 1, pp. 1–17, 2018.

42. McVay, M., R. Casper and T. I. Shang, "Lateral Response of Three-row Groups in Loose to Dense Sands at 3D and 5D Pile Spacing", *Journal of Geotechnical Engineering*, Vol. 121, No. 5, pp. 436–441, 1995.

43. Prakash, S., *Behavior of Pile Groups Subjected to Lateral Loads*, University of Illinois at Urbana-Champaign, 1962.

44. Uncuoğlu, E. and M. Laman, "Lateral Resistance of a Short Rigid Pile in a Two-layer Cohesionless Soil", *Acta Geotechnica Slovenica*, Vol. 8, No. 2, pp. 19–43, 2011.

45. Uncuoğlu, E. and M. Laman, "Numerical Modelling of Short Pile Behaviour Subjected to Lateral Load", *European Journal of Environmental and Civil Engineering*, Vol. 16, No. 2, pp. 204–235, 2012.

46. Yahia, Y. I. O., "An Experimental Study on the Behavior of Segmental Pile with Variable Flexural Rigidity", *Ph.D. Thesis Bogazici University*, 2014.

47. Sengez, M., "Lateral Capacity of Segmental Model Piles Under Cyclic Loading", *M.Sc. Thesis Bogazici University*, 2019.

48. Keklik, A., "An Experimental Study on the Behavior of Segmental Piles Subjected to Large Lateral Displacement", *M.Sc. Thesis Bogazici University*, 2020.

49. Öztürk, B., "Stress and Displacement Measurement for Geotechnical Modelling Using Open Platform", *M.Sc. Thesis Bogazici University*, 2020.

50. ASTM, "Standard Practice for Classification of Soils for Engineering Purposes (Unified Soil Classification System)", Vol. D2487-06, 2010.

51. ASTM D6913 / D6913M-17, "Standard Test Methods for Particle-Size Distribution (Gradation) of Soils Using Sieve Analysis", *ASTM International, West Conshohocken; PA*, 2017.

52. ASTM D854-14, "Standard Test Methods for Specific Gravity of Soil Solids by Water Pycnometer", *ASTM International, West Conshohocken, PA*, 2014.

53. ASTM D4253-16e1, "Standard Test Methods for Maximum Index Density and Unit Weight of Soils Using a Vibratory Table", *ASTM International, West Conshohocken, PA*, 2016.

54. ASTM D3080, "Standard Test Method for Direct Shear Test of Soils Under Consolidated Drained Conditions", *ASTM International, West Conshohocken, PA*, 2011.

55. Baykal, G., "Development of Soil-Structure Interface Testing System Using Pneumatic Muscles", *BAP 5580 Project, Bogazici University, Istanbul*, 2015.

56. Baykal, G., "Large Displacement-Constant Contact Area Geosynthetic Soil Interface Direct Shear Test Device", *Eurogeo6, European Geosynthetics Conference, Ljubliana*, 2016.

57. Baykal, G., "Implementation of Pneumatic Muscles in Geotechnical Laboratory Equipment Development", *4th International Conference on New Developments in Soil Mechanics and Geotechnical Engineering, Near East University, Nicosia.*, 2016.

58. Baykal, G., "Large Size-Large Displacement Residual Direct Shear Test Device Development", *Proceedings of the 19th International Conference on Soil Mechanics and Geotechnical Engineering, Seoul*, 2017.

59. ASTM D790-17, "Standard Test Methods for Flexural Properties of Unreinforced and Reinforced Plastics and Electrical Insulating Materials", *ASTM International, West Conshohocken, PA*, pp. 1–12, 2017.

60. ASTM D2435 / D2435M-11 (2020), "Standard Test Methods for One-Dimensional Consolidation Properties of Soils Using Incremental Loading", *ASTM International, West Conshohocken, PA*, pp. 1–10, 2020.

61. ASTM D3966 / D3966M-07 (2013) e1, "Standard Test Methods for Deep Foundations Under Lateral Load", *ASTM International, West Conshohocken, PA*, pp. 1–18, 2013.

62. Chen, L. T. and H. G. Poulos, "Closure to "Piles Subjected to Lateral Soil Movements" by L. T. Chen and H. G. Poulos", *Journal of Geotechnical and Geoenvironmental Engineering*, Vol. 125, No. 6, p. 541, 1997.

63. Hetenyi, M., "Beams on Elastic Foundation: Theory with Applications in the Fields of Civil and Mechanical Engineering", *Ann Arbor, MI: University of Michigan Press*, 1946.

64. Lymon C. Reese, W. R. Cox and F. D. Koop, "Analysis of Laterally Loaded Piles in Sand", *Offshore Technology Conference*, 1974.

APPENDIX A: ADDITIONAL TEST RESULTS

A total of 27 three-point bending tests with three repetitions are conducted, and the results are presented in Figure A.1 - A.9.

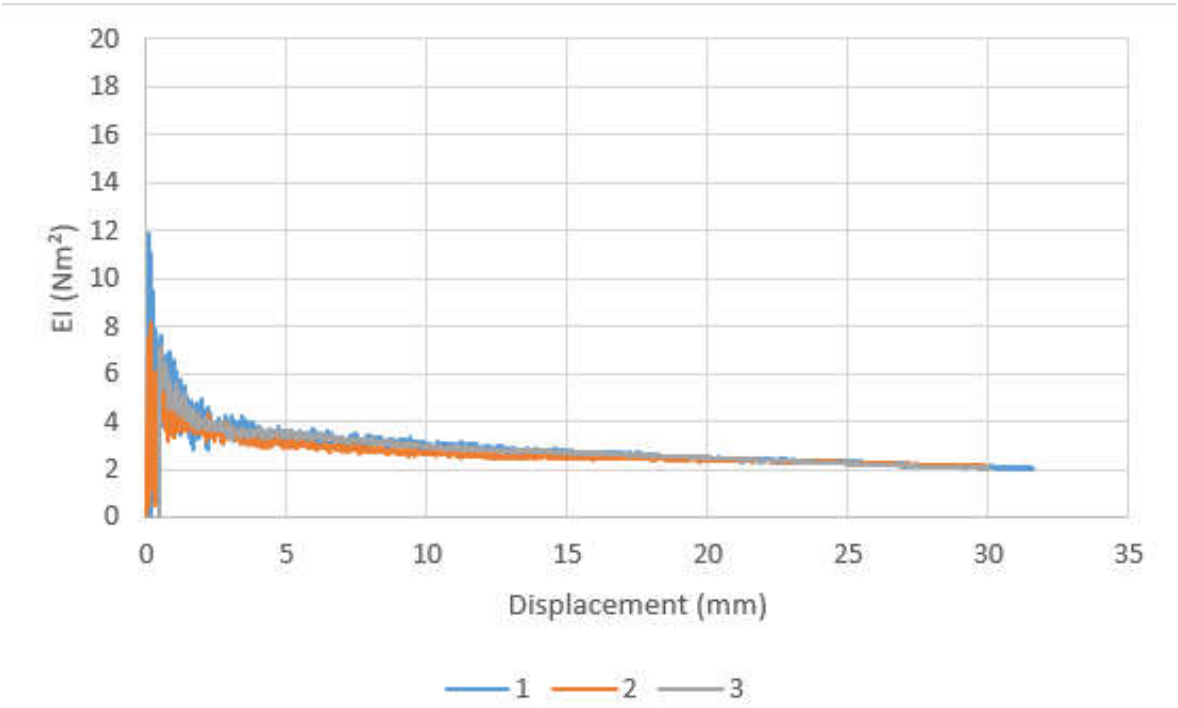


Figure A.1. Flexural Rigidity and Displacement Curves for the Piles (500 kPa without a Wearing Layer).

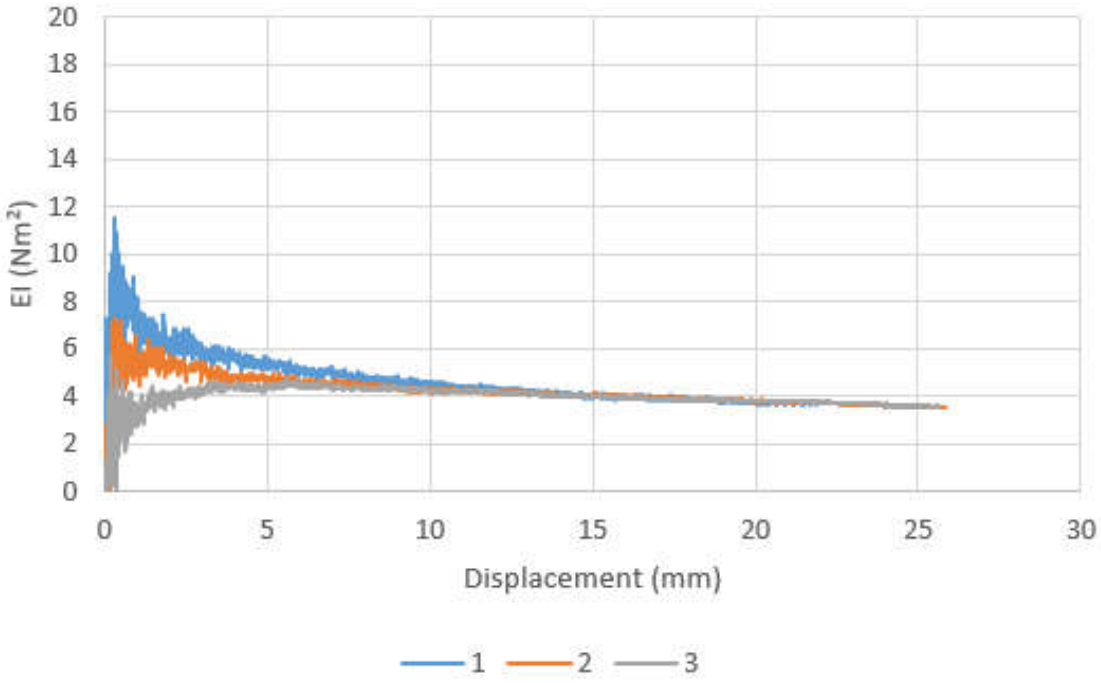


Figure A.2. Flexural Rigidity and Displacement Curves for the Piles (1000 kPa without a Wearing Layer).

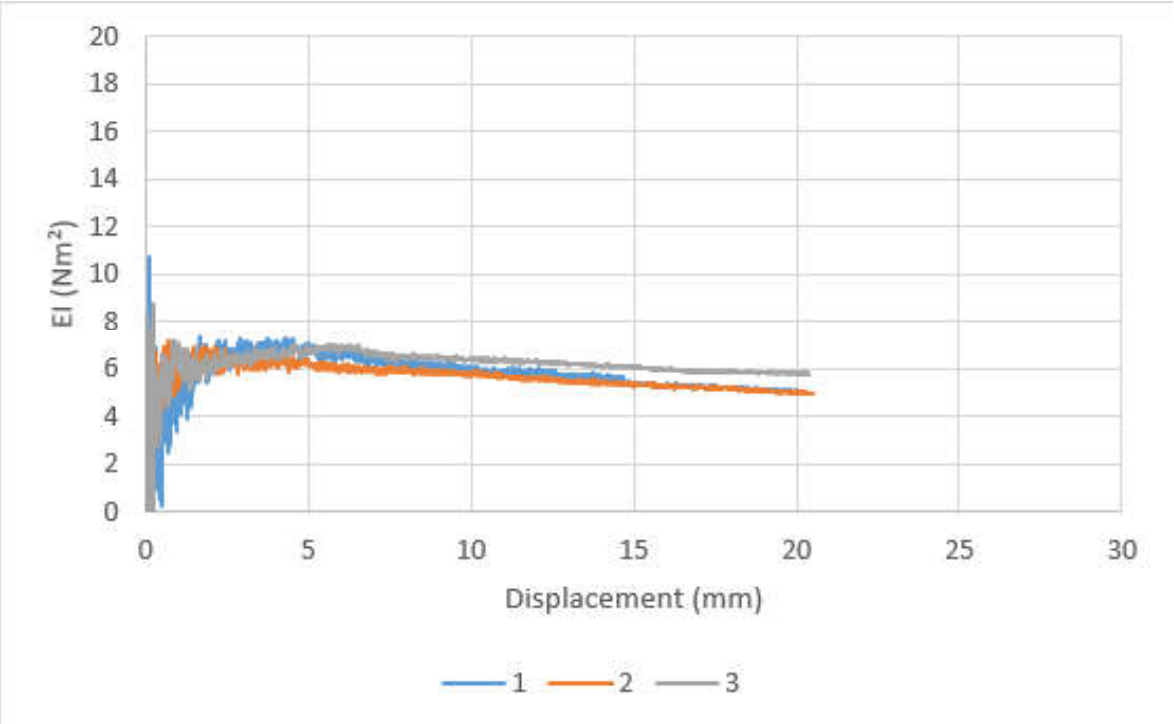


Figure A.3. Flexural Rigidity and Displacement Curves for the Piles (1500 kPa without a Wearing Layer).

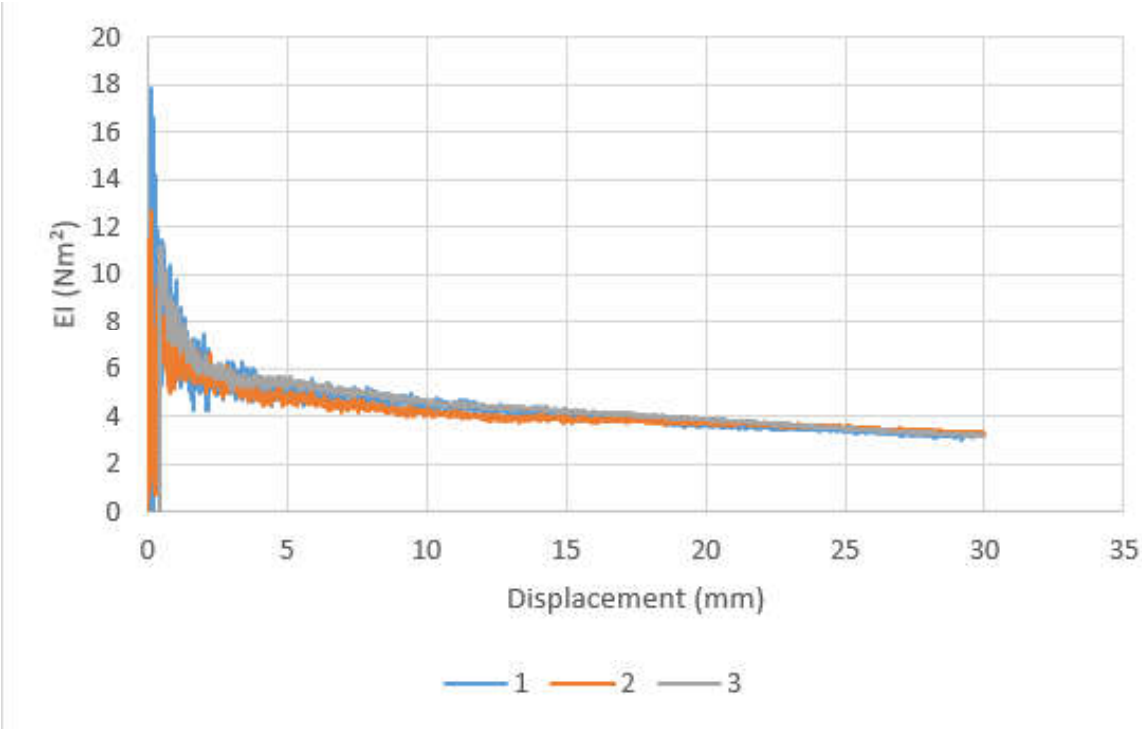


Figure A.4. Flexural Rigidity and Displacement Curves for the Piles (500 kPa with a Single Wearing Layer).

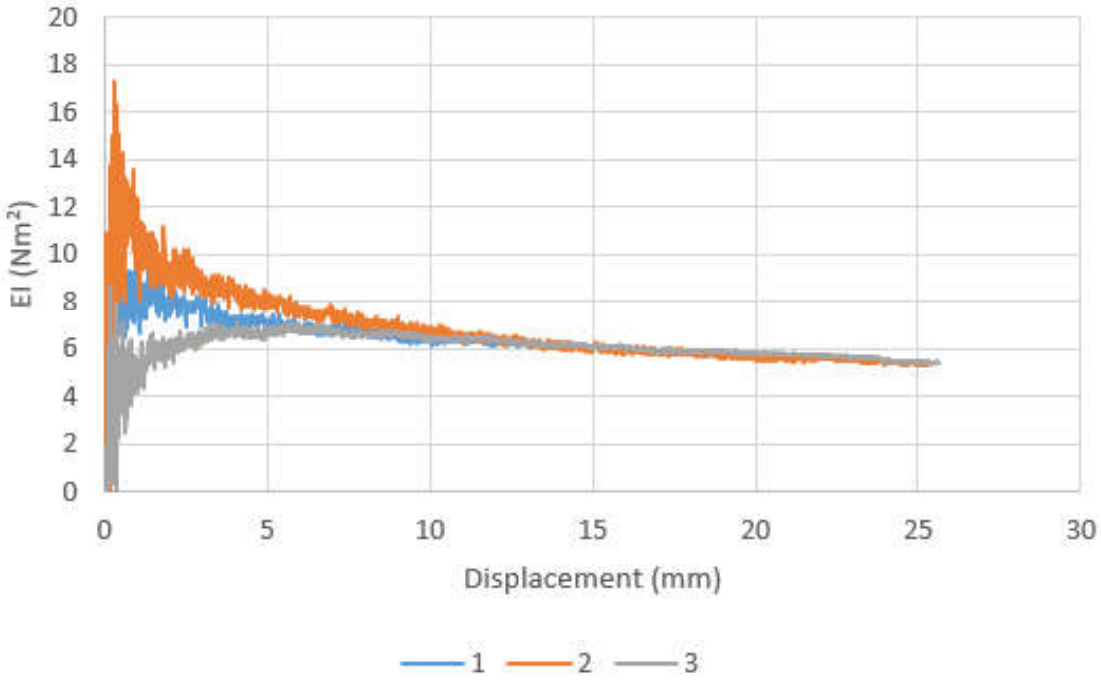


Figure A.5. Flexural Rigidity and Displacement Curves for the Piles (1000 kPa with a Single Wearing Layer).

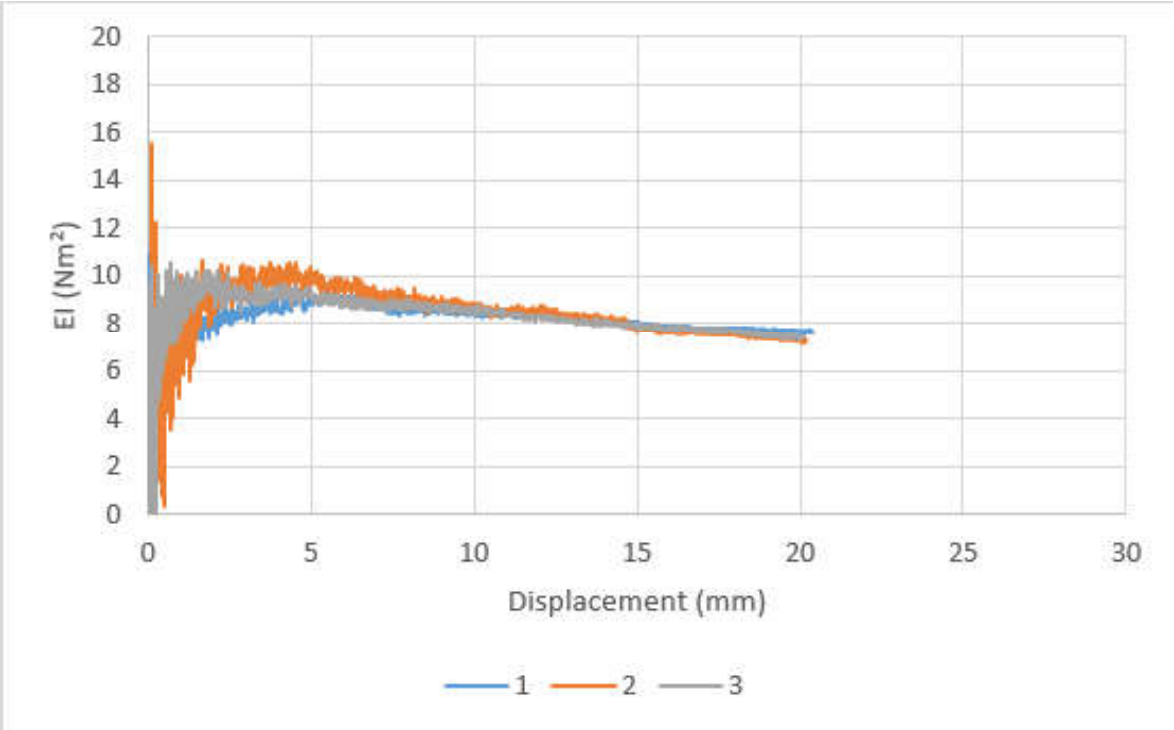


Figure A.6. Flexural Rigidity and Displacement Curves for the Piles (1500 kPa with a Single Wearing Layer).

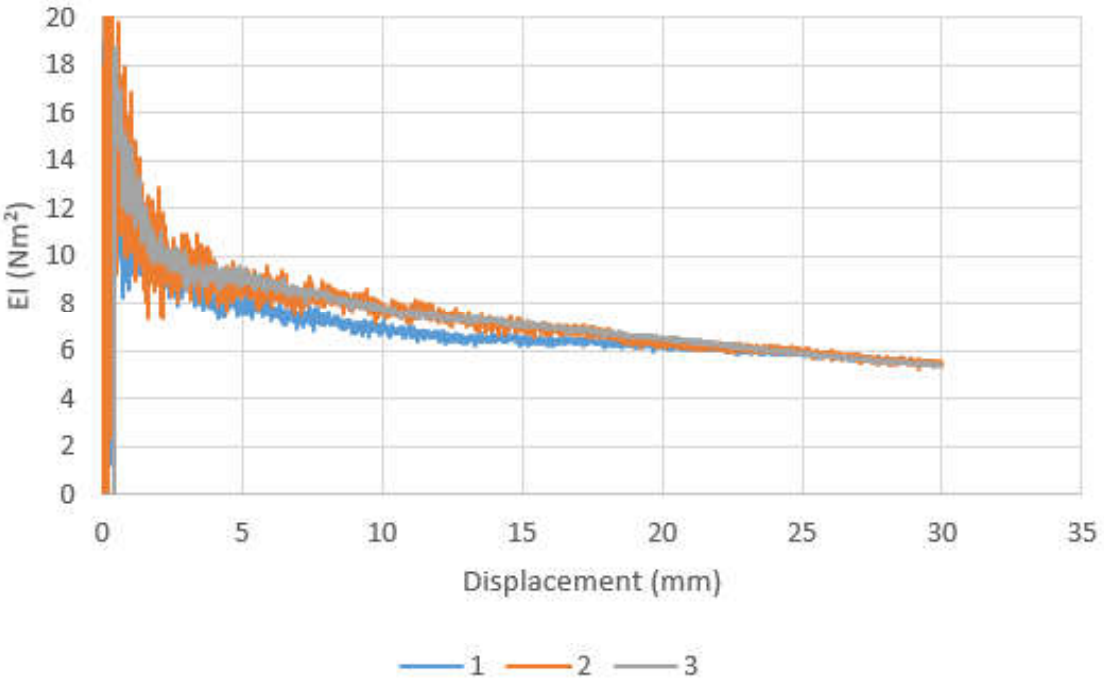


Figure A.7. Flexural Rigidity and Displacement Curves for the Piles (500 kPa with a Double Wearing Layer).

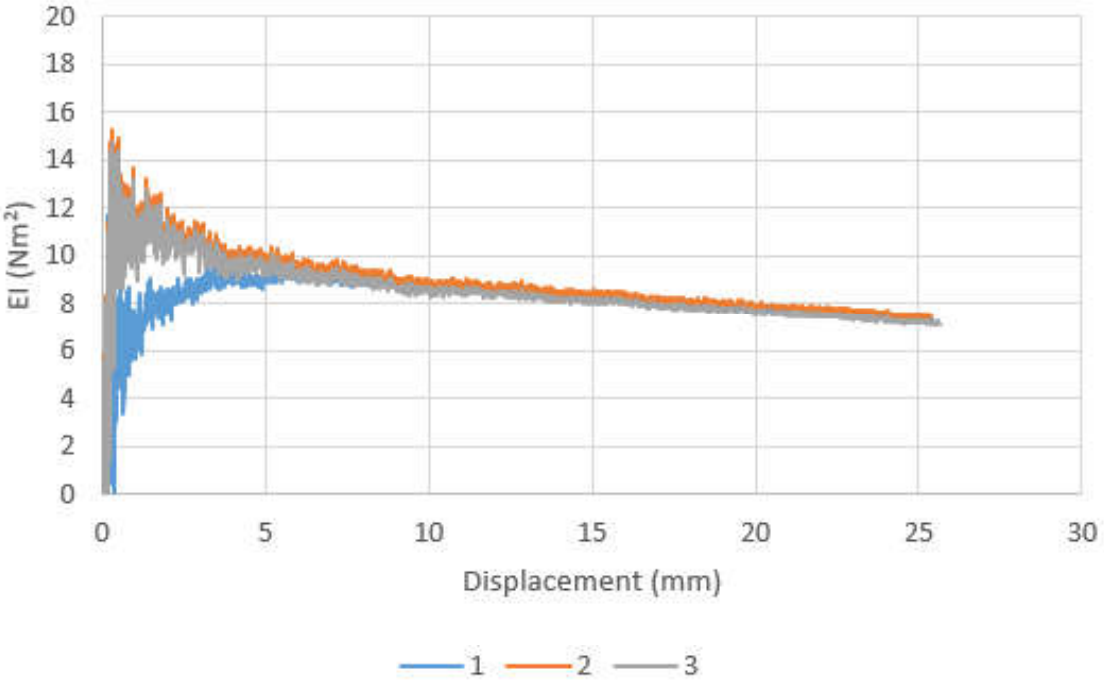


Figure A.8. Flexural Rigidity and Displacement Curves for the Piles (1000 kPa with a Double Wearing Layer).

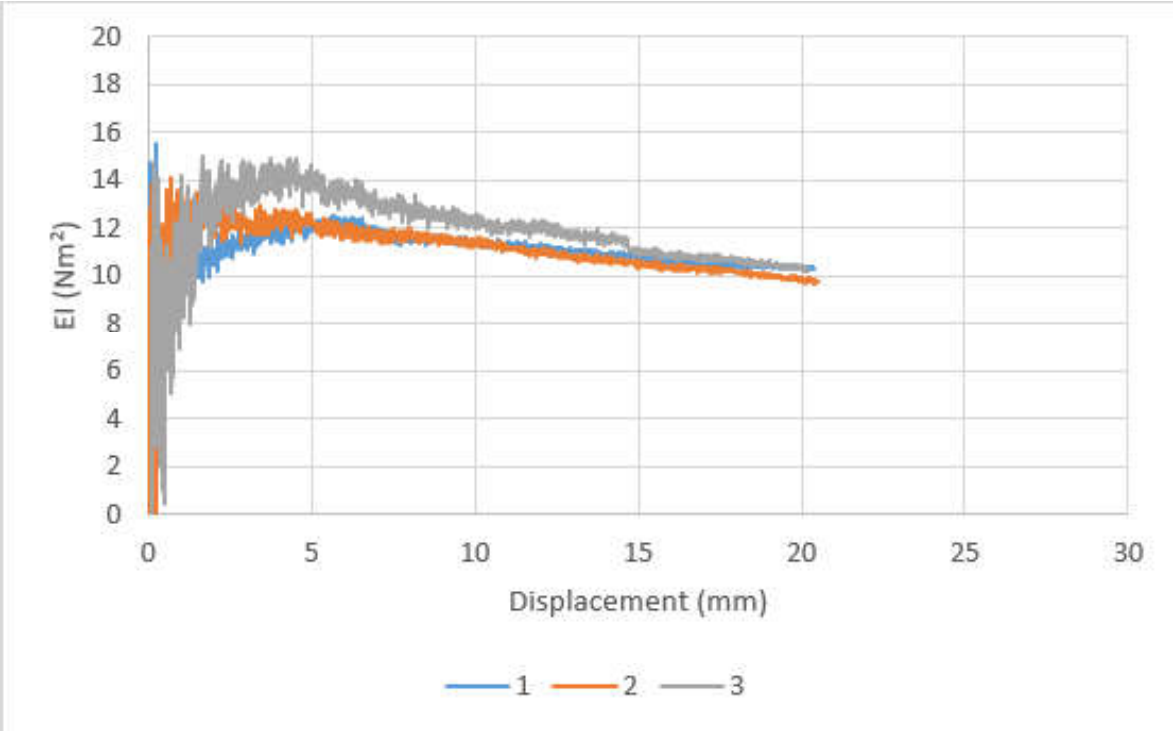


Figure A.9. Flexural Rigidity and Displacement Curves for the Piles (1500 kPa with a Double Wearing Layer).